

①

AFIT/DS/PH/83-3

AD-A159 226

20000727272

FALLOUT FRACTIONATION IN
SILICATE SOILS

DISSERTATION

AFIT/DS/PH/83-3 Charles R. Martin
Capt USAF

Reproduced From
Best Available Copy

DTIC
SELECTED
SEP 18 1985

DTIC FILE COPY

Approved for public release; distribution unlimited.

85 09 17 001

REPORT DOCUMENTATION PAGE		READ INSTRUCTIONS BEFORE COMPLETING FORM
1. REPORT NUMBER AFIY/DS/PH/83-3	2. GOVT ACCESSION NO. AD-A159 226	3. RECIPIENT'S CATALOG NUMBER
4. TITLE (and Subtitle) FALLOUT FRACTIONATION IN SILICATE SOILS		5. TYPE OF REPORT & PERIOD COVERED PhD dissertation Aug 80 - Jul 83
		6. PERFORMING ORG. REPORT NUMBER
7. AUTHOR(s) Charles R. Martin		8. CONTRACT OR GRANT NUMBER(s)
9. PERFORMING ORGANIZATION NAME AND ADDRESS Air Force Institute of Technology (AFIT-EN) Wright-Patterson AFB, Ohio 45433		10. PROGRAM ELEMENT, PROJECT, TASK AREA & WORK UNIT NUMBERS
11. CONTROLLING OFFICE NAME AND ADDRESS Defense Nuclear Agency (DNA/NATA) Washington, DC 20305		12. REPORT DATE December, 1983
		13. NUMBER OF PAGES 163
14. MONITORING AGENCY NAME & ADDRESS (if different from Controlling Office)		15. SECURITY CLASS. (of this report) UNCLASSIFIED
		15a. DECLASSIFICATION/DOWNGRADING SCHEDULE
16. DISTRIBUTION STATEMENT (of this Report) Approved for public release; distribution unlimited		
17. DISTRIBUTION STATEMENT (of the abstract entered in Block 20, if different from Report) APPROVED FOR PUBLIC RELEASE: IAW AFR 150-1 LYNN E. WOLAVER Dean for Research and Professional Development Air Force Institute of Technology (AFIT) Wright-Patterson AFB OH 45433		
18. SUPPLEMENTARY NOTES Approved for public release: IAW AFR 150-1 LYNN E. WOLAVER 14 AUG 83 Dean for Research and Professional Development Air Force Institute of Technology (AFIT) Wright-Patterson AFB OH 45433		
19. KEY WORDS (Continue on reverse side if necessary and identify by block number) Fractionation Fallout		
20. ABSTRACT (Continue on reverse side if necessary and identify by block number) The existing models for treating fractionation in nuclear weapon debris are discussed and compared. A method which extends the existing theory for the case of surface bursts over silicate soils is developed and validated with weapons test data. Fission product uptake is modeled as follows: The weapon debris and some soil is fully vaporized. Some soil is merely melted. As the fireball cools, the refractory fission products are absorbed by this liquid material. After the fireball has cooled below the soil		

CONF

solidification temperature, the remaining fission products can be adsorbed onto any available surfaces. Soil which enters the fireball after the soil solidification time will also adsorb fission products. Test data and other evidence indicate that the distributions of melted and unmelted soil particles have different modes. This model uses diffusion theory to transport the fission products into the particles. In addition, it allows for injection of unmelted material near the time of soil solidification.

The results of the research indicate that in standard DELFIC calculations too much activity is carried in the larger particles. In addition, the distribution of volatile fission product nuclides relative to a refractory reference nuclide is in general better modeled by the new method.

Accession For	
NTIS GRA&I	<input checked="" type="checkbox"/>
DTIC TAB	<input type="checkbox"/>
Unannounced	<input type="checkbox"/>
Justification:	
By _____	
Distribution/	
Availability Codes	
Avail and/or	
Dist	Special
A1	



UNCLASSIFIED

AFIT/DS/PH/83-3

FALLOUT FRACTIONATION IN
SILICATE SOILS

DISSERTATION

Presented to the Faculty of the School of Engineering
of the Air Force Institute of Technology
Air University
in Partial Fulfillment of the
Requirements for the Degree of
Doctor of Philosophy

by

Charles R. Martin, B.S.N.E., M.S.N.E.

Captain

USAF

Approved for public release; distribution unlimited.

85 09 17 021

AFIT/DS/PH/83-3

FALLOUT FRACTIONATION IN
SILICATE SOILS

by

Charles R. Martin, B.S.N.E., M.S.N.E.

Captain

USAF

Approved:

Charles J. Bridgman

Charles J. Bridgman (Chairman)

George John

George John

John Jones Jr.

John Jones, Jr.

John Prince

John Prince

Ernest A. Dorko

Ernest A. Dorko

Accepted:

J. S. Przemieniecki 9 Dec. 1983

J. S. Przemieniecki, Dean, School of Engineering

Preface

I am deeply grateful to Dr. Charles J. Bridgman of the Air Force Institute of Technology, for his guidance and assistance in the development of this research; to Drs. George John, John Prince, and John Jones for their advice on special occasions; and to Dr. Dave Auton of the Defense Nuclear Agency for sponsoring this research project. I would also like to thank Drs. E. C. Freiling, H. G. Hicks, and J. H. Norman for the benefit of their council. Finally, I wish to express my gratitude to my wife, Susann, who helped in preparation of the final draft and gave invaluable moral support all during the project, and my two sons, Ricky and Andy, who provided inspiration. A special thanks goes to Cathryn Reed Poukey who typed the manuscript.

CONTENTS

	<u>Page</u>
Preface	ii
List of Figures	v
List of Tables	ix
Abstract	x
I. Introduction	I-1
Background	I-1
Problem Statement	I-4
Scope	I-4
II. Historical Development	II-1
Introduction	II-1
Miller's Thermodynamic Model	II-1
Radial Power Law	II-15
Modified Radial Power Law Model	II-30
Diffusion Model	II-36
III. The G-X Diffusion ModelIII-1
IntroductionIII-1
Method OverviewIII-6
MethodIII-7
Particle Size DistributionIII-21
Partition of SoilIII-23
Crystal-Glass DistributionsIII-26
Bias in the DataIII-27
Determination of Diffusion CoefficientsIII-30
Determination of Henry's Law ConstantsIII-31
Theoretical ConsiderationsIII-31
IV. Results and Discussion	IV-1
V. Conclusions and Recommendations	V-1
BibliographyBIB-1

CONTENTS (Continued)

	<u>Page</u>
Appendix A: The S-V Model	A-1
Appendix B: $R_{i,j}$ Plots for Small Boy	B-1
Appendix C: $R_{i,j}$ Plots for Johnny Boy	C-1
Appendix D. Specific Activity Plots for Small Boy	D-1

LIST OF FIGURES

<u>Figure</u>		<u>Page</u>
1	Schematic of Early Cloud Near the Time of Soil Solidification	I-3
2	Surface versus Volume Distributed Activity for a 1 Megaton Ground Burst	I-4
3	Surface versus Volume Distributed Activity Size Distributions	I-5
4	Henry's Law of Dilute Solutions	II-4
5	The Square Root of F_R versus the Correlation Slopes for Johnnie Boy Data	II-22
6	F_R versus the Correlation Slopes for Johnnie Boy Data	II-23
7	Plots of Equation (52) for Several Values of the Freiling Ratio	II-26
8	Radiograph of a Fallout Particle with Activity Distributed Uniformly Throughout its Volume (Miller, 1963)	III 3
9	Radiograph of a Fallout Particle with Activity Located Primarily on the Surface (Miller, 1963)	III-4
10	Radiograph of an Irregularly Shaped Crystalline Fallout Particle (Miller, 1963)	III-5
11	Decay Paths in Mass Chain 89 for the the Diffusion Model	III-19
12	Decomposition of the Mass Frequency Distribution into Crystalline and Glassy Components	III-29
13	$R_{89,95}$ versus Particle Size for Each Method	IV 2
14	Total Specific Activity Versus Particle Size for Shot Small Boy	IV 6
15	Dose Size Distributions for Shot Small Boy	IV-7

LIST OF FIGURES (Continued)

<u>Figure</u>		<u>Page</u>
16	Strontium 90 Concentration as a Function of Particle Size for Crystalline Particles, Glassy Particles, and the Weighted Average	IV-8
17	Zirconium 95 Concentration as a Function of Particle Size for Crystalline Particles, Glassy Particles, and the Mass Weighted Average	IV-9
18	Total Specific Activity for Glassy and for Crystalline Particles in Shot Small Boy as Predicted by the G-X Model	IV-11
19	Observed versus Calculated Fractionation Plot Slopes for Shot Small Boy	IV-12
20	Observed versus Calculated Fractionation Plot Slopes for Shot Johnny Boy	IV-13
21	Fractionation Plot Slope Errors for Shot Small Boy: Solid Bars are the G-X Model, Open Bars are the F-T Model	IV-14
22	Fractionation Plot Slope Errors for Shot Johnny Boy: Solid Bars are the G-X Model, Open Bars are the F-T Model	IV-15
23	Small Boy Fractionation Plots: Mass Chain 137 . . .	B-2
24	Small Boy Fractionation Plots: Mass Chain 132 . . .	B-3
25	Small Boy Fractionation Plots: Mass Chain 106 . . .	B-4
26	Small Boy Fractionation Plots: Mass Chain 131 . . .	B-5
27	Small Boy Fractionation Plots: Mass Chain 136 . . .	B-6
28	Small Boy Fractionation Plots: Mass Chain 140 . . .	B-7
29	Small Boy Fractionation Plots: Mass Chain 103 . . .	B-8
30	Small Boy Fractionation Plots: Mass Chain 91 . . .	B-9
31	Small Boy Fractionation Plots: Mass Chain 141 . . .	B-10
32	Small Boy Fractionation Plots: Mass Chain 144 . . .	B-11

LIST OF FIGURES (Continued)

<u>Figure</u>		<u>Page</u>
33	Small Boy Fractionation Plots: Mass Chain 99 . . .	B-12
34	Small Boy Fractionation Plots: Mass Chain 90 . . .	B-13
35	Johnny Boy Fractionation Plots: Mass Chain 137 . . .	C-2
36	Johnny Boy Fractionation Plots: Mass Chain 132 . . .	C-3
37	Johnny Boy Fractionation Plots: Mass Chain 131 . . .	C-4
38	Johnny Boy Fractionation Plots: Mass Chain 90 . . .	C-5
39	Johnny Boy Fractionation Plots: Mass Chain 136 . . .	C-6
40	Johnny Boy Fractionation Plots: Mass Chain 140 . . .	C-7
41	Johnny Boy Fractionation Plots: Mass Chain 91 . . .	C-8
42	Johnny Boy Fractionation Plots: Mass Chain 141 . . .	C-9
43	Johnny Boy Fractionation Plots: Mass Chain 144 . . .	C-10
44	Johnny Boy Fractionation Plots: Mass Chain 99 . . .	C-11
45	Small Boy Specific Activity for Mass Chain 137 . . .	D-2
46	Small Boy Specific Activity for Mass Chain 89 . . .	D-3
47	Small Boy Specific Activity for Mass Chain 132 . . .	D-4
48	Small Boy Specific Activity for Mass Chain 106 . . .	D-5
49	Small Boy Specific Activity for Mass Chain 131 . . .	D-6
50	Small Boy Specific Activity for Mass Chain 136 . . .	D-7
51	Small Boy Specific Activity for Mass Chain 140 . . .	D-8
52	Small Boy Specific Activity for Mass Chain 103 . . .	D-9
53	Small Boy Specific Activity for Mass Chain 91 . . .	D-10
54	Small Boy Specific Activity for Mass Chain 141 . . .	D-11
55	Small Boy Specific Activity for Mass Chain 144 . . .	D-12

LIST OF FIGURES (Continued)

<u>Figure</u>		<u>Page</u>
56.	Small Boy Specific Activity for Mass Chain 99 . . .	D-13
57.	Small Boy Specific Activity for Mass Chain 95 . . .	D-14
58.	Small Boy Specific Activity for Mass Chain 90 . . .	D-15

LIST OF FIGURES (Continued)

<u>Figure</u>		<u>Page</u>
56.	Small Boy Specific Activity for Mass Chain 99 . . .	D-13
57.	Small Boy Specific Activity for Mass Chain 95 . . .	D-14
58.	Small Boy Specific Activity for Mass Chain 90 . . .	D-15

LIST OF TABLES

<u>Table</u>		<u>Page</u>
1.	Raw Data for Mass Size Distribution Decomposition .	III-28
2.	Diffusion Coefficients	III-32
3.	Henry's Law Coefficients	III-33
4.	Logarithmic Correlation Slopes - Small Boy	IV-3
5.	Logarithmic Correlation Slopes - Johnny Boy	IV-4

ABSTRACT

The existing models for treating radiochemical fractionation in nuclear weapon debris are discussed and compared. A method which extends the existing theory for the case of surface bursts over silicate soils is developed and validated with weapons test data.

There is evidence that fission product absorption by soil and weapon debris is diffusion controlled. There is also evidence that there are two superimposed distributions of soil particles. A computational model is developed here based on this evidence. The following is a synopsis of the model: A portion of the soil is fully vaporized along with the weapon debris while some soil is merely melted. As the fireball cools, the refractory fission products will be absorbed by this liquid material. After the fireball has cooled below the soil solidification temperature, the remaining fission products can be adsorbed onto any available surfaces. Any soil which entered the fireball at the soil solidification time or later will also adsorb fission products. Test data and other evidence indicate that the distributions of melted and unmelted soil particles have different modes. This model uses Henry's Law to find surface concentrations. It then uses diffusion theory to transport the fission products into the particles. In addition, it allows for injection of unmelted material near the time of soil solidification.

The results of the research indicate that in standard DELFIC calculations too much activity is carried in the larger particles and

too little in the smaller particles. In addition, the distribution of volatile fission product nuclides relative to a refractory reference nuclide is in general better modeled by the new method. Since many other fallout modeling codes make use of fits to DELFIC activity size distributions, these codes might be modified to reflect these new findings.

FALLOUT FRACTIONATION IN SILICATE SOILS

I. Introduction

Background

In a surface burst of a nuclear weapon, a large amount of soil is broken up, while some is melted and some is even vaporized. Part of this debris is taken into the fireball and is carried with it as the fireball rises. Part of this material will come into intimate contact with the radioactive fission products. As the fireball cools, the soil and debris from the device will condense and scavenge the available fission products. At the time that the soil begins to solidify, most of the condensed fission products will be more or less uniformly distributed throughout the particles. After that time, the soil particles are essentially solid. Those fission products which were still gaseous at the soil solidification temperature will later condense onto the surfaces of the particles still in the cloud.

The above is a very simple picture of the processes which cause fractionation taking place inside of the nuclear cloud. Simply stated, radiochemical fractionation is a distribution of isotopes which is different from that which would be expected if all of the radioactivity were distributed uniformly throughout the fallout particles. An important feature of this process which has always been observed but never treated is the presence of a very large number of irregularly shaped particles which carry radioactivity only on their

surfaces. These particles, because they show no evidence of having been melted, must have been introduced into the active region of the fireball after the gas temperature had dropped to near or below the soil solidification temperature (see Figure 1). One of the objectives of this research was to take this fact into consideration.

The careful treatment of this problem is very important because of the large difference in downwind extent of isodose contours if the radioactivity were all surface distributed as opposed to being all volume distributed. Figure 2 illustrates this point by showing in cross section the dose rates along the hot line for a one Mt yield (50 percent fission) weapon. In this case, the 450 R contour for the purely volume distributed activity extends for about 65 miles past that for the purely surface distributed case. This illustrates that when one is trying to determine the expected number of casualties in a given attack scenario, the effect of fractionation cannot be ignored. In terms of placement of the activity, Figure 3 shows the distribution of radioactivity for these two extremes as a function of particle size for an assumed lognormal particle size distribution.

Historically, the first attempt to develop a theory for fractionation was by Miller with his Thermodynamic Equilibrium Model (Miller, 1960; Miller, 1963; Miller, 1964). The model essentially consisted of distributing the fission products in the cloud among the particles according to the equilibrium distribution. The model used 1400 degrees C as the temperature below which condensing nuclides could not penetrate the fallout particles. The difficulty with the

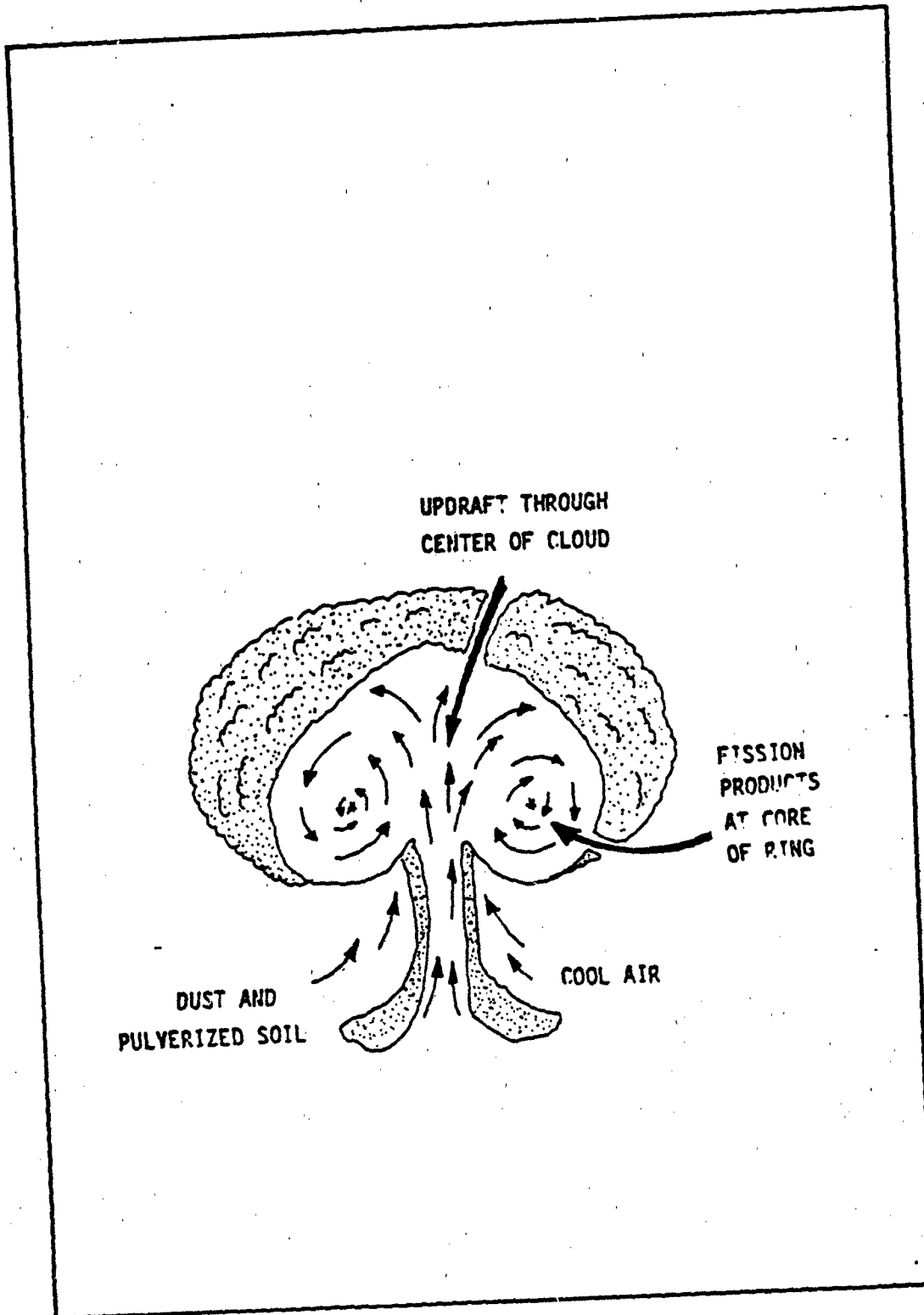


Figure 1. Schematic of Early Cloud Near the Time of Soil Solidification

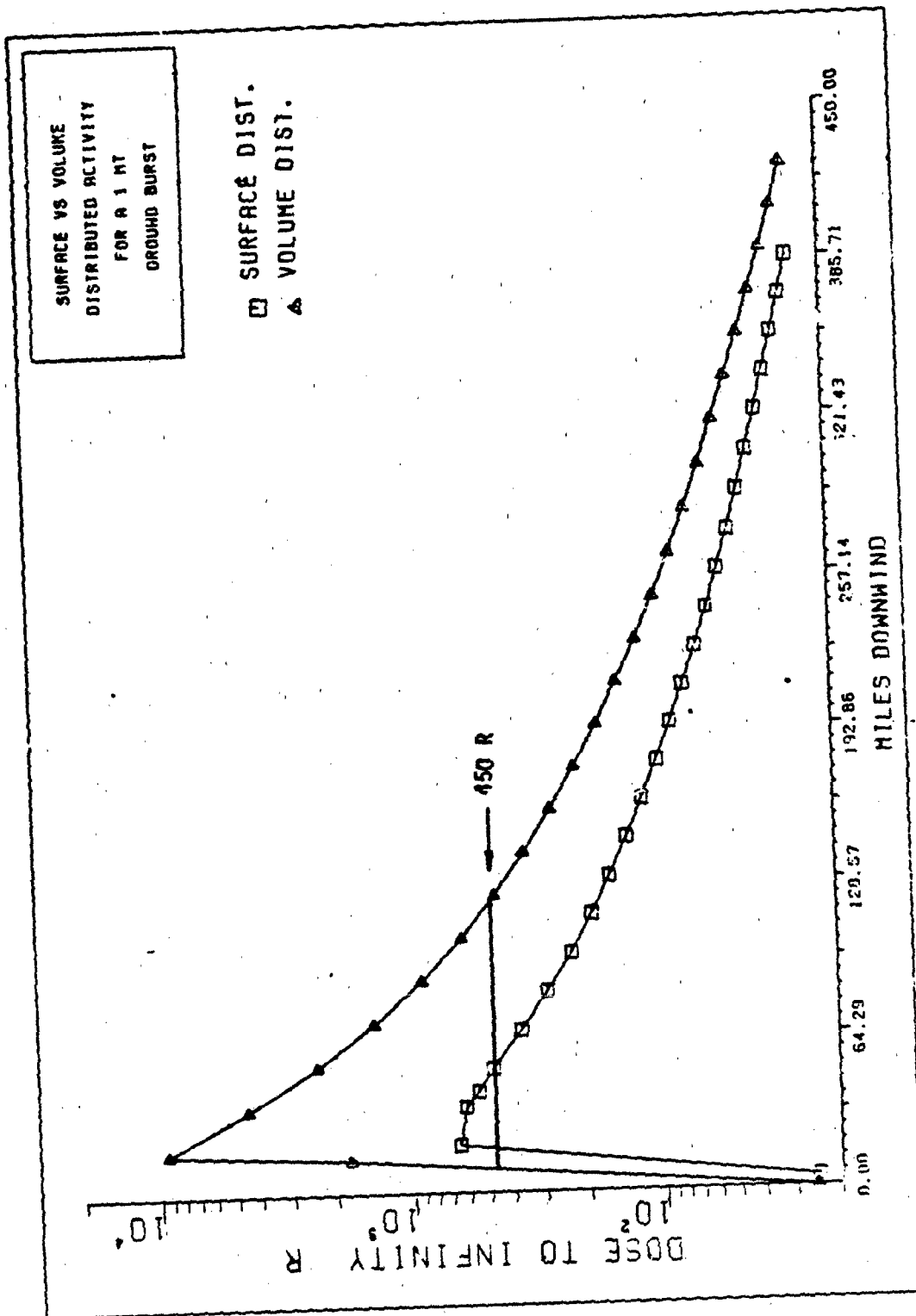


Figure 2. Surface versus Volume Distributed Activity
for a 1 Megaton Ground Burst

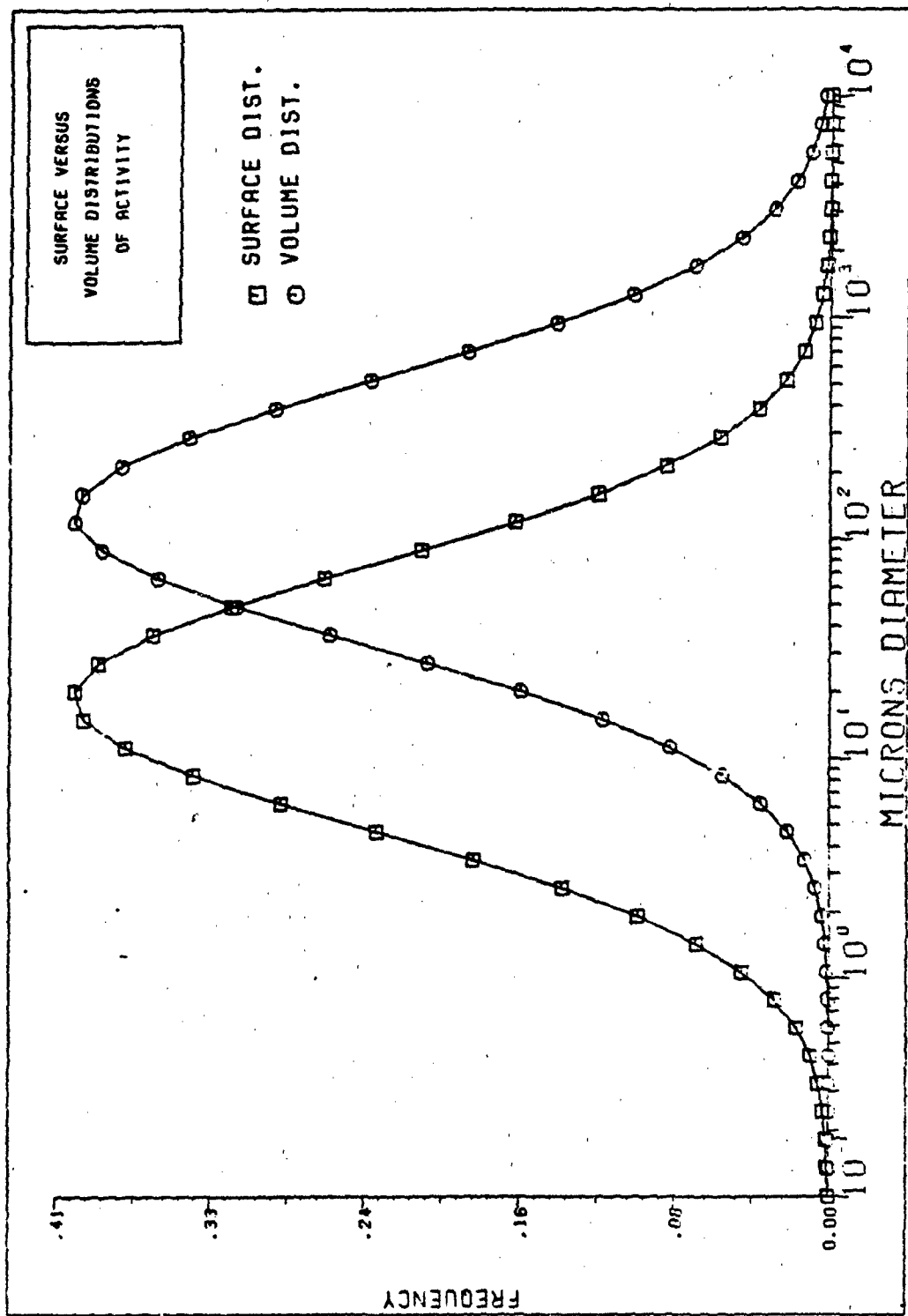


Figure 3. Surface versus Volume Distributed Activity
Size Distributions

model was that adequate thermodynamic data was not available at the time it was developed. Thus, the model could not be properly implemented. The next attempt to treat fractionation came from Freiling with his Radial-power-distribution Model (Freiling, 1961; Freiling, 1963; Freiling, 1963 b; Freiling, 1964). This model assumed that there was a collection of spherical particles and that all mass chains were distributed according to some power of the particle radius. With these assumptions, Freiling found that the model produces logarithmic correlations between radionuclide ratios. Freiling, in his analysis of Pacific weapons test data, observed that radionuclide ratios could be correlated logarithmically as well as they could be linearly. This was taken as evidence that the method had some validity. The correlation parameters formed the basis for a model to predict fractionation effects. The next attempt to treat the problem was by Korts and Norman with their diffusion limited approach (Korts, 1967). In developing this model, a great deal of work was done to measure the thermodynamic properties of fission product oxides and the diffusion properties of various soil types. The essence of the method was a hybrid of the equilibrium treatment of Miller with diffusion of the condensed fission product oxides into the soil particles. This model assumed a distribution of spherical, glassy particles. Attempts were underway in the late 1960's to bring even greater sophistication to the fractionation problem. The skeleton for a more complete kinetic model had been laid out by this time, but because of funding cutbacks and laboratory reorganizations (e.g., the

closing of the U.S. Naval Radiological Defense Laboratory), research on particle formation was largely stalled.

Problem Statement

The objective of this research project was to review the literature on fallout fractionation and, if possible, extend or improve the theory. As a result of the research, a complete computational model was produced even though that was not one of the initial goals. In fact, two distinct models were produced: one is referred to as the G-X model (for glass-crystal), while the other (a hybrid of Miller's model) is referred to hereafter as the S-V model (for surface-volume). The latter model was incidental to the main thrust of the research. For this reason it is presented in Appendix A.

Scope

The problem of fractionation includes many aspects which will not be treated here. No attempt will be made to treat fractionation which occurs because of sampling methods. Nor will fractionation which occurs because of leaching of grounded particles prior to collection be treated. The treatment here is of the process termed "primary fractionation" by Freiling (Freiling, 1961: 1991). The problem is further limited to surface bursts over silicate soil. This restriction to silicate soils is made since no effort has ever been made to accurately identify the particle size distributions for the different types of particles found in surface bursts over calcium

based soils. The restriction to surface bursts is made because the fractionation process is fundamentally different for each type of burst condition. Surface bursts are of particular interest because they present the greatest fallout hazards. They are also interesting because of the complicated mixing of unmelted material with fission products, melted soil and weapon debris.

II. Historical Development

Introduction

The early attempts to model fractionation were made difficult by a general lack of data. The collection of weapons test data which would be of use to fallout researchers was a low priority. In addition, early investigators were not sure what types of data were needed. Data collection for fallout studies was often an afterthought. Even when it was carefully planned, equipment was often unreliable. High radiation in some areas would frequently delay sample recovery allowing contamination of samples by non-radioactive debris carried by winds (Freiling, 1965 b).

On top of these difficulties, nuclear, thermodynamic, and chemical data for the fission products and their oxides were limited or non-existent. In spite of these problems, several investigators managed to develop workable models for predicting the effects of fractionation as well as a theoretical framework for understanding it. The most notable of these were E. C. Freiling, J. H. Norman, and C. F. Miller. In the following sections, their models will be surveyed in order to provide a foundation for understanding the G-X model developed in the next chapter.

Miller's Thermodynamic Model

Introduction. Miller's theory of fractionation was developed about the same time as Freiling's treatment (Miller, 1963). Since

Miller's model required rather a great deal to be known about the thermodynamics of the cooling fireball, and since the thermodynamic data for the fission products were not available, it was of limited value as a computational model. It did in its original form, however, treat many of the important phenomena in a qualitative way and pointed the way for the collection of the data that would be necessary to implement a more complete theoretical model at some later date. It was because of the lack of data for Miller's model that Freiling's semi-empirical Radial Power Law was adopted as a stop-gap device for predicting fractionation effects (Freiling, 1965). But even as a purely theoretical model, Miller's treatment leaves room for improvement as it neglects some important phenomena.

It should be noted in the following discussion that Miller treats the melt of carrier material as a single mass rather than as a distribution of particles of varying sizes. This poses no particular problem, although it ignores the effect of particle size on the condensation mathematics.

Miller divides the condensation process into two more or less distinct time periods. The major feature of the first period is the existence of vapor-liquid phase equilibria. This period of condensation ends when the carrier material solidifies, with the fission products either fixed in a solid solution matrix or compounded with the carrier material.

The major feature of the second period of condensation is the existence of vapor-solid phase equilibria in which the remaining

fission product elements condense at lower temperatures on the surfaces of solid particles. The second period of condensation never ends completely except for those particles which leave the volume of space containing the residual gases. In fact, the process can reverse for a fission product element that later decays to a more volatile element. For example, elements like iodine and the rare gases could sublime as fast as they form from non-volatile precursors which condensed on the surfaces of fallout particles. This process is unlikely, however, when the fission products are trapped within a glassy matrix. The vapor pressures due to the low concentration of dissolved fission products would be extremely low, and diffusion through the solid glass would be very slow.

The essential problem in the theory for the process during the first period of condensation is to establish the vapor-liquid phase equilibria of each fission product element at the time that the carrier material solidifies; that is to determine the fraction of each element present which has condensed and migrated into the carrier melt at the time of solidification.

When one of the two phases in contact is a gas, simple kinetic theory can be used to show that condensation - vaporization equilibrium can be established very quickly at temperatures above 2000 degrees Kelvin (Miller, 1960). Thus, those gaseous species of each fission product element that do not react with the liquid carrier but dissolve into it should obey Henry's Law of dilute solutions (see Figure 4). In fact, the solutions should be sufficiently dilute as to

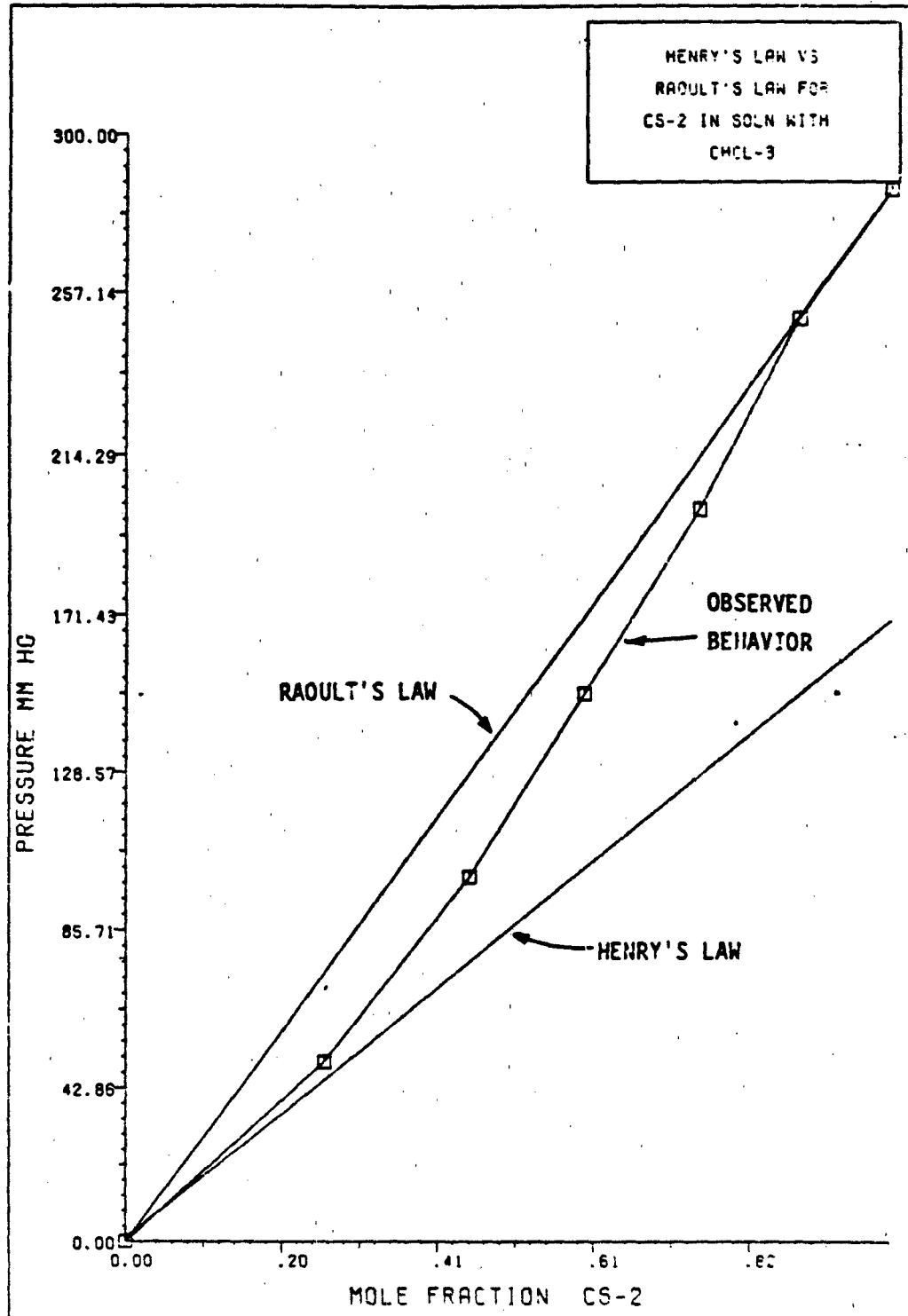


Figure 4. Henry's Law of Dilute Solutions

result in no appreciable change in the Gibbs free energy of the liquid carrier. Thus, the free energy of each element in the solution should be independent of any other. It is possible, then, to consider the solubility of each element by treating each as a binary system with the carrier. Further, there should be no appreciable surface loading (large excess surface concentrations of fission product elements/compounds) during the condensation process if the temperature range over which the liquid carrier exists exceeds 200 or 300 degrees C. Miller allows, however, that a concentration gradient should exist for the larger particles of which some may not be melted in the center when the air or gas temperature about the particle falls below the melting point of the bulk carrier (Miller, 1963: 99-101).

Development of Equations for Miller's Model. When considering the thermodynamics of a multicomponent system, the various thermodynamic functions must include the amount of each component as a variable. The chemical potential, μ_i , is a useful quantity for treating equilibrium or near equilibrium systems. It represents the change in the Gibbs free energy of a system per mole of added component i , with temperature, pressure, and the other molar quantities kept constant. Adamson gives the total derivative of the chemical potential as (Adamson, 1973: 355):

$$d\mu_i = RT d(\ln f_i) \quad (1)$$

where f_i is the fugacity of component i . Fugacity is an effective pressure for the component. It accounts for deviations from ideal behavior. The defining equation for fugacity for state $i = 1$ going to state $i = 2$ is (Andrews, 1970: 204):

$$\ln f_2 \stackrel{\Delta}{=} \frac{G_2}{RT} + \lim_{P_1 \rightarrow 0} \left(\ln P_1 - \frac{G_1}{RT} \right) \quad (2)$$

where G_i is the Gibbs free energy for state i . When dX_i moles of element i condense from a gaseous mixture to a liquid solution leaving X_i moles in the gas and X_i moles in the liquid, the change in the chemical potential in the gas is found as follows: First we expand the derivative given in Equation (1) to obtain

$$d\mu_i^\circ = \left(\frac{\partial \mu_i^\circ}{\partial P} \right)_{T, X_i^\circ} dP + \left(\frac{\partial \mu_i^\circ}{\partial T} \right)_{P, X_i^\circ} dT + \left(\frac{\partial \mu_i^\circ}{\partial X_i^\circ} \right)_{T, P} dX_i^\circ \quad (3)$$

or equivalently

$$d\mu_i^\circ = RT \left(\frac{\partial \ln f_i}{\partial P} \right)_{T, X_i^\circ} dP + RT \left(\frac{\partial \ln f_i}{\partial T} \right)_{P, X_i^\circ} dT + RT \left(\frac{\partial \ln f_i}{\partial X_i^\circ} \right)_{T, P} dX_i^\circ \quad (4)$$

The corresponding change in the chemical potential, μ_i , in the solution is

$$du_1 = RT \left(\frac{\partial \ln f_1}{\partial P} \right)_{T, X_1} dP + RT \left(\frac{\partial \ln f_1}{\partial T} \right)_{P, X_1} dT + RT \left(\frac{\partial \ln f_1}{\partial X_1} \right)_{T, P} dX_1 \quad (5)$$

where P is the total pressure, T is the temperature, X_1° is the mole fraction of element 1 in the gas mixture, X_1 is its mole fraction in the liquid, f_1° is its fugacity in the gas phase, and f_1 is its fugacity in the liquid phase. At moderate and low pressures, the fugacity of the element in the gas phase is by definition given by

$$f_1^{\circ} = X_1^{\circ} f_1^* \quad (6)$$

in which f_1^* is the fugacity of the gas at the total pressure of the mixture and therefore

$$\left(\frac{\partial \ln f_1^{\circ}}{\partial X_1^{\circ}} \right)_{P, T} = \frac{1}{X_1^{\circ}} \quad (7)$$

The fugacity of the element in the liquid phase, according to Henry's Law of dilute solutions, is given by

$$f_1 = X_1 k_1 \quad (8)$$

in which k_i is the Henry's Law constant at a given temperature and total pressure; hence

$$\left(\frac{\partial \ln f_i}{\partial X_i}\right)_{P,T} = \frac{1}{X_i} \quad (9)$$

Adams gives the change in the chemical potential with respect to pressure and temperature as

$$\left(\frac{\partial \mu_i}{\partial P}\right)_{T,X_i} = \frac{RT}{P} = V_i \quad (10)$$

and

$$\left(\frac{\partial \mu_i}{\partial T}\right)_{P,X_i} = -S_i \quad (11)$$

so that Equation (4) becomes

$$d\mu_i = V_i^{\circ} dP - S_i^{\circ} dT + RT \frac{dX_i^{\circ}}{X_i^{\circ}} \quad (12)$$

and Equation (5) becomes

$$d\mu_1 = \bar{V}_1 dP - \bar{S}_1 dT + RT \frac{dX_1}{X_1} \quad (13)$$

The two changes in the chemical potential for the transfer of dX_1 moles from the gas mixture to the liquid solution are equal in an equilibrium process. Dividing Equations (12) and (13) by RT while noting that

$$\bar{S} = \frac{\bar{Q}}{T} \quad (14)$$

and then equating Equation (1) and Equation (2), after substituting for the indicated partial differentials, gives

$$\frac{\bar{V}_1^0}{RT} dP - \frac{\bar{Q}_1^0}{RT^2} dT + d \ln X^0 = \frac{\bar{V}_1}{RT} dP - \frac{\bar{Q}_1}{RT^2} dT + d \ln X_1 \quad (15)$$

in which \bar{V}_1^0 is the partial molar volume of element i in the gas mixture, \bar{Q}_1^0 is its relative partial molar heat content in the gas mixture, \bar{V}_1 is its partial molar volume in the liquid solution, \bar{Q}_1 is its relative partial molar heat content in the liquid solution, R is the molar gas constant, P is total pressure, and

T is the temperature in degrees Kelvin. In the case of dilute solutions (Miller, 1960: 10)

$$\bar{U}_i^* - \bar{U}_i = \Delta H_v \quad (16)$$

where ΔH_v is the heat of vaporization of the condensing element i. Miller points out that ΔH_v is the heat of reaction for the vaporization of the gas from solution. If it exists as a different compound in solution, the heat of formation of this compound is included in the value of ΔH_v . For an ideal solution, ΔH_v is just the heat of vaporization. Since

$$V_i^* \gg V \text{ then } \left(\frac{V_i}{RT}\right) \quad (17)$$

can be neglected. Thus, Equation (15) becomes

$$\frac{V_i^*}{RT} dP + d(\ln X_i^*) = \frac{\Delta H_v}{RT^2} dT + d(\ln X_i) \quad (18)$$

but by Equation (10) this reduces to

$$\frac{dP}{P} + d(\ln X_i^*) = \frac{\Delta H_v}{RT^2} dT + d(\ln X_i) \quad (19)$$

Upon integration, this becomes

$$\ln P + \ln X_i^{\circ} = \frac{-\Delta H_v}{RT} + \ln X_i + \ln k_i' \quad (20)$$

or

$$\ln \left(\frac{P X_i^{\circ}}{k_i' X_i} \right) = - \frac{\Delta H_v}{RT} \quad (21)$$

and finally

$$\frac{P X_i^{\circ}}{X_i} = k_i' e^{-\Delta H_v/RT} \quad (22)$$

in which k_i is an integration constant and where the term

$$k_i \triangleq k_i' e^{-\Delta H_v/RT} \quad (23)$$

can be identified from Equation (6) and Equation (8) where ($f_i^{\circ} = f_i = p_i$, the partial pressure of element i ; and $f_i = P$) as the Henry's Law constant. Now substituting from the definitions of X_i

$$X_i^{\circ} \triangleq \frac{n_i^{\circ}}{n_i^{\circ} + n_{air}} \approx \frac{n_i^{\circ}}{n_{air}} \quad (24)$$

and

$$X_i \approx \frac{n_i}{n_i + n_{\text{soil}}} \approx \frac{n_i}{n_{\text{soil}}} \quad (25)$$

and using the ideal gas law for n_{air}

$$n_{\text{air}} = \frac{Pv}{RT} \quad (26)$$

then Equation (22) becomes

$$\frac{n_i/n_{\text{air}}}{n_i/n_{\text{soil}}} = \frac{k_i}{P} \quad (27)$$

where n_{soil} is the number of moles of liquid soil. Finally (from Equation 27), the number of moles of the i th element, n_i , in the liquid is related to the total number of moles Y_i in both phases by the relation

$$n_i = \frac{Y_i R T}{RT + (k_i v/n_{\text{soil}})} \quad (28)$$

In the second period of condensation under the Miller model, the soil carrier has solidified. Fission product uptake then continues by surface adsorption. The adsorption condensation can be considered as one in which the relative amount of each element condensed is related to its sublimation pressure (Miller, 1960: 109-110). The

computational values from such a process will reflect the relative volatility of the constituent molecules at all temperatures at which this kind of condensation can occur. If an excess of solid surface area is present, the number of moles condensed by the process (assuming that the process of reversible) at any time after solidification of the carrier is given by

$$n_i^s = n_i^o - n_i^r \quad (29)$$

in which n_i^s is the residual amount of element i condensed on the surface of the solid particles, n_i^o is the amount of the element in the gas phase at the start of the second period, and n_i^r is the residual amount in the vapor phase. All three quantities depend on time because the radionuclides continue to decay. In the case of a perfect gas

$$n_i^r = \frac{p_i^s v}{RT} \quad (30)$$

where v is the volume enclosing the n_i moles of the gaseous species and P_i is the sublimation pressure and is given by

$$p_i^s = e^{\Delta S_s/R} e^{-\Delta H_s/RT} \quad (31)$$

in which ΔS_s is the entropy of sublimation and ΔH_s is the heat of sublimation at the temperature, T. If mixing in the fireball volume is assumed to be uniform for the particles and gaseous fission products, then v is the fireball volume. The material balance for element i is

$$Y_i = n_i + n_i^S + n_i^R \quad (32)$$

so that, Equation (29), with Equations (27), (28), (30), and (32), becomes

$$n_i^S = \frac{\left\{ \frac{k_i v}{n_{\text{sof}} RT} \right\} Y_i}{1 + \left\{ \frac{k_i v}{n_{\text{sof}} RT} \right\}} - \frac{v P_i^S}{RT} \quad (33)$$

In Equations (28) and (33), the quantities n_{sof} and v are estimated from the thermal data and empirical scaling equations.

Miller's work was notable in that it treats the essence of the problem in a physically meaningful way. The method developed by Freiling presented in the next section is largely empirical. While none of the necessary Henry's Law constants were available when Miller wrote his report, many are now. In those cases where data is still not available, Raoult's Law, which is an idealization of Henry's Law, may be used. In Appendix A, a variation of the Miller method is developed which has an especially attractive feature: viz., it could

be easily modified for use with fast running "smear codes" such as that developed by Bridgman and Bigelow (Bridgman, 1982).

The next section provides an overview of the Radial Power Law developed by Freiling. While it is not as elegant theoretically as Miller's equilibrium treatment, it has the advantage of being less difficult computationally.

RADIAL POWER LAW

Introduction. Freiling's Radial Power Law is a semi-empirical fractionation model which is presently used in modified form in the official Department of Defense fallout modeling computer code, DELFIC. The discussion here is restricted to the pure form of the Radial Power Law rather than the modification used in DELFIC. Discussion of the Tompkins implementation of the Radial Power Law in DELFIC form is presented in the following section. The Radial Power Law has some limitations, which will be discussed after the model has been presented.

The model itself is simple and does to a degree incorporate the radiochemistry of the cooling radioactive elements. First, the principal compound (usually but not always an oxide) of each element which would exist in the hot fireball must be identified. The boiling point of this compound is then taken as the boiling point of that element for computational purposes. Next, a melting point is determined for the soil which will be the carrier of the

radioactivity. Without the presence of a large mass of this carrier material, there is essentially no local fallout from a nuclear weapon (Miller, 1963: 3). A rough rule of thumb is that particles larger than 10-20 μm will be deposited locally, or within a few hundred miles of the detonation point (Glasstone, 1967: 36-37). In the Freiling model, the user must supply the yield, height of burst, soil type, fuel, fission yield, the particle size distribution, and the fission yields of each radionuclide for each of several fuel types and neutron energy spectra. In addition, the model needs all of the decay chain data necessary to follow the decay of the fission products.

Thermodynamic characteristics of the fireball must be computed as well. These include how much soil is vaporized or melted and carried aloft, as well as the time at which the fireball reaches the solidification temperature of the soil. The number of fission product atoms which are in a refractory form at that point in time is determined for each mass chain by solving rigorously the Bateman equations which describe radioactive decay. The fraction of atoms in each chain which are in a refractory form at this time is used as a parameter in distributing the nuclides of each chain in the soil particles.

Discussion. There are two essential points in the following discussion: First, Freiling's conclusions from his analysis of Pacific weapons test data are not well supported by data from ground bursts over silicate soil. Second, Freiling's theoretical explanation

of his empirical correlations is likewise not well supported by later data. The data from continental United States tests suggest that simple empirical correlations are not sufficient to predict fractionation behavior in the case of ground bursts over silicate soils.

Freiling makes the following analysis: In a sample of fallout, the apparent number of fissions which yielded a given nuclide is

$$f_i = a_i/Y_i \quad (34)$$

where a_i is the number of atoms of nuclide i in the sample and Y_i is the number of atoms of nuclide i per fission. The ratio $r_{i,j}$ is defined by

$$r_{i,j} = f_i/f_j \quad (35)$$

This ratio is useful for the following reason: Let nuclide j be a nuclide which is volatile and whose precursors were also volatile. This nuclide would tend to be surface distributed since both it and its parents would have lower boiling points than the soil carrier. Now let nuclide i first be another similarly behaving nuclide. Then $r_{i,j}$ would be approximately equal to 1. Now, if j was a nuclide which was refractory and had refractory parents, then the corresponding boiling points would be higher than the soil solidification temperature. So the tendency would be for this nuclide

to be volume distributed. The ratio $r_{i,j}$ would then have an extremum since we are measuring the greatest possible difference in behavior of two nuclides. Now we take $r_{v_{ref}, s_{ref}}$ to be our reference $r_{i,j}$ where v_{ref} is the reference volume distributed, refractory nuclide and s_{ref} is the reference surface distributed, volatile nuclide. This ratio will be abbreviated $r_{v,s}$ (an alternate notation is $r_{r,v}$ where the subscript r indicates a refractorily behaving nuclide and v represents a volatilyly behaving nuclide). Then form the ratio $r_{i,s}$ between f_i where i is arbitrary and f_s where s represents our reference surface distributed nuclide. Next, consider plotting the relationship between these ratios for various actual fallout samples. That is, given a sample of fallout material, analyze the characteristic end products of each mass chain (^{90}Sr for $i = 90$, ^{99}Mo for $i = 99$, ^{137}Cs for $i = 137$, etc.). Then form the ratios $r_{i,s}$ and $r_{v,s}$ (we will take $s = 89$ for ^{89}Sr and $v = 95$ for ^{95}Zr for our reference nuclides). These ratios can best be correlated logarithmically for the high yield coral and water surface bursts analyzed by Freiling (Freiling, 1961: 1994, Heft, 1970: 256-257). Freiling considered two types of relationships between fractionation ratios:

$$(a) \quad r_{i,89} = k_1 r_{95,89} + k_2 \quad (36)$$

$$(b) \quad \ln(r_{i,89}) = k_3 \ln(r_{95,89}) + k_4 \quad (37)$$

where the k's are constants to be determined. Of these two, the latter had the smaller variance in the data fit (Note: $r_{i,89}$ and $r_{95,89}$ are functions of particle size). Note further the following: If i is a refractorily behaving nuclide, then $r_{i,89}$ will mimic $r_{95,89}$ so that Equation (37) reduces to

$$k_3 = (\ln(r_{v,s}) - k_4) / \ln(r_{v,s}) \quad (38)$$

If k_4 was zero, then we see that $k_3 = 1$. Similarly, if i is volatile, then Equation (37) reduces to

$$\ln r_{s,s} = k_3 \ln r_{v,s} + k_4 \quad (39)$$

but $r_{s,s} = 1$ so we have

$$0 = k_3 \ln r_{v,s} + k_4 \quad (40)$$

or

$$k_3 = -k_4 / \ln(r_{v,s}) \quad (41)$$

and again if $k_4 = 0$, then $k_3 = 0$. As it turns out, Freiling found in his plots that k_4 is approximately zero and k_3 is approximately unity when i is a nuclide whose chain is all refractory, and k_3 is approximately zero when i is a nuclide whose chain is all volatile.

In summary, logarithmic correlations seem to work well for high yield coral surface bursts. They do not, however, for low yield silicate surface bursts. Later investigators found evidence for linear relationships in the latter case (Heft, 1970: 256, Bridgman, 1983).

To establish a theoretical basis for his semi-empirical model, Freiling postulated first that the particle size distribution was lognormal. He then further postulated that the distribution of a given mass chain goes as some power of the radius of the fallout particles, where the exponent lies between 2 and 3 (Tompkins, 1968: 11-16). If the chain is all refractory, then its long-lived members will be refractory and will be distributed as the third moment of the particle size distribution. But if the chain is all volatile, then the members observed in analysis will be volatile and will be distributed as the second moment of the final particle size distribution. When Freiling used this type of analysis, he found that the data for coral and water high yield surface bursts best fit Equation (37) with $k_4 = 0$ and k_3 equal to the square root of the fraction of the decay chain i which exists in refractory form at the time of soil solidification (Freiling, 1961: 1995). This conclusion violates the intuitive hypothesis that volatile nuclides are surface distributed and refractory nuclides are volume distributed. If it were true that a single mass chain contained some nuclides which were purely volume distributed and some nuclides which were purely surface distributed, then the superposition of these two distributions would not be a simple fractional moment between 2 and 3 of the lognormal

particle size distribution (which was itself a lognormal distribution). It rather is the sum of two different lognormal distributions, which is not lognormal.

To help resolve the apparent conflict between Freiling's theory and the data, consider the following points: First, the data used by Freiling was limited to high-yield surface bursts over coral and water. There is evidence that for silicate soil surface bursts of lower yield the slope should be equal to the fraction of the chain which exists in refractory form at the time of soil solidification, rather than the square root of the refractory fraction, $\sqrt{F_R}$, as Freiling's Pacific Test Site data suggested (Bridgman, 1983: b) (see Figures 5 and 6). So Freiling's square-root relationship may only apply in an approximate sense to high yield coral or water surface bursts.

Second, when the soil carrier is in the liquid phase, the degree to which the radioactive nuclides collect on and diffuse into the soil droplets is a function of the vapor pressure of those nuclides. As noted in the previous section, Miller asserts that the essence of the fractionation problem lies in vapor-liquid phase equilibria established for each fission product element (or compound) at the time just prior to solidification of the carrier material. That is, one needs to find what fraction of each fission product could be found in the liquid phase and determine to what degree it had diffused into the carrier melt when solidification occurred. Those gaseous species of each fission product element that do not react with the liquid carrier

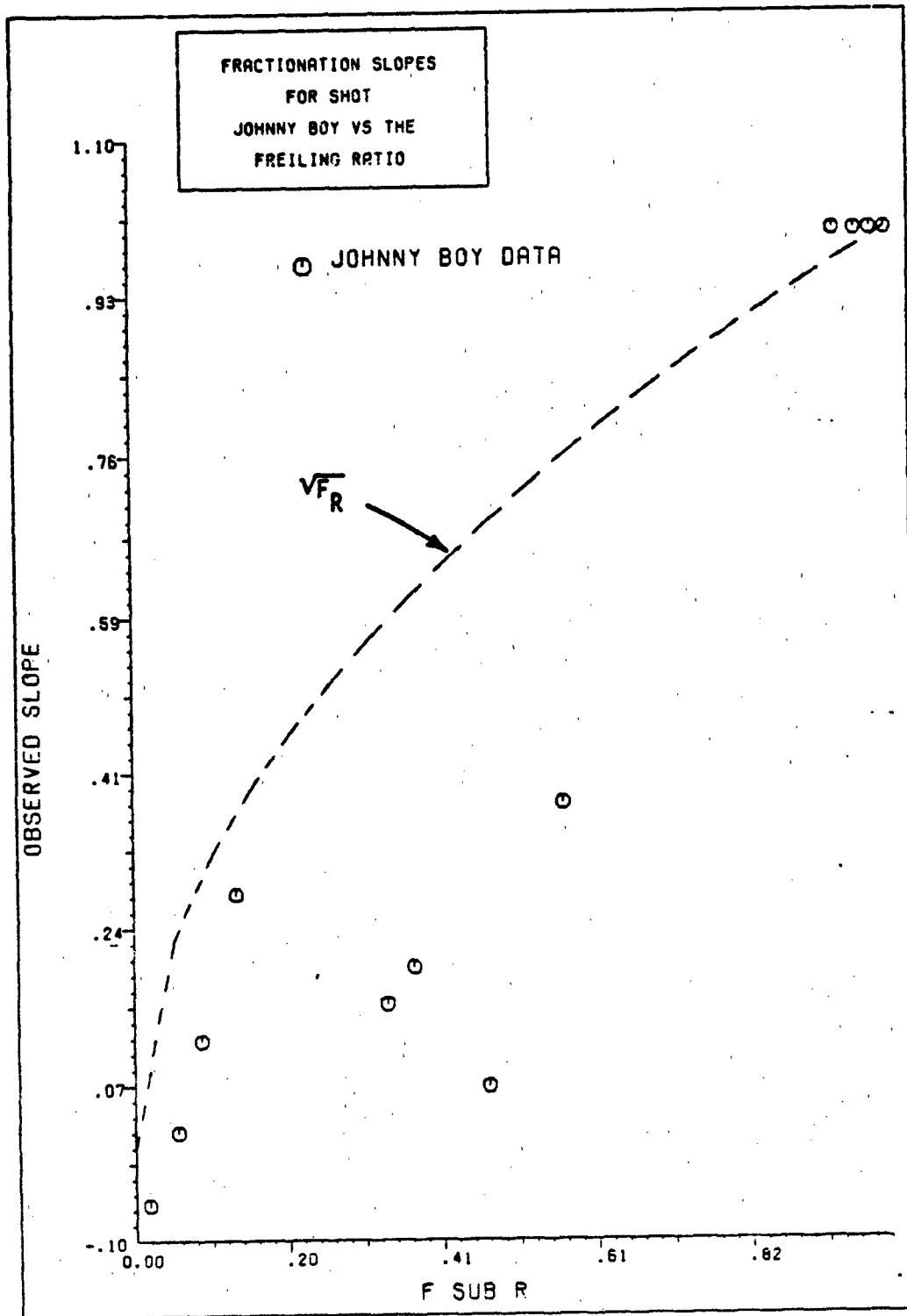


Figure 5. The Square Root of F_R versus the Correlation Slopes for Johnnie Boy Data

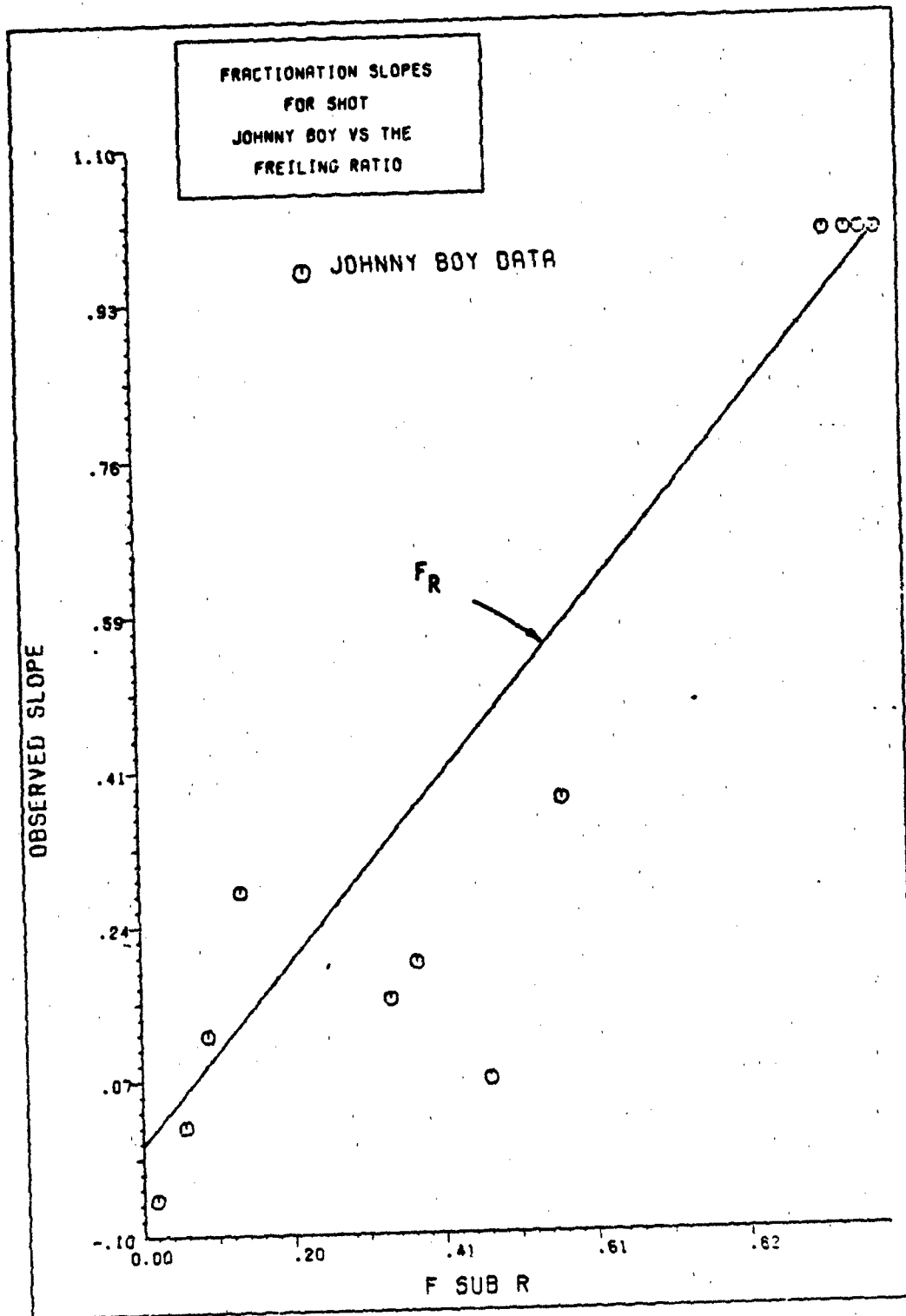


Figure 6. F_R versus the Correlation Slopes
for Johnnie Boy Data

but dissolve into it should obey Henry's Law of dilute solutions. A concentration gradient, however, should exist in many particles, especially for the larger particles of which some may not have been completely melted.

In other words, one should not expect to find all refractory nuclides distributed uniformly throughout the volume of the soil particles. Similarly, volatile nuclides will not necessarily be restricted to the surfaces of the soil particles. On the other hand, there exists the possibility for desorption of nuclides which have condensed on the surfaces of particles, especially after they have left the cloud. Some nuclides will have especially small sticking coefficients and thus exhibit poor surface adsorption. The lack of treatment of these phenomena is a weakness of the Radial Power Law model.

Now consider the following analysis. First, define

d = particle diameter

$N(d)$ = particle size distribution

F_T = total number of equivalent fissions in all particles

Y_i = fission yield of i -th mass class

$F_i(d)$ = distribution of equivalent fissions for particles of diameter d for mass chain i

(r_i, r) = fractionation ratio = $F_i(d)/F_r(d)$ where r is index for a refractory behaving chain

f_r = fraction of the decay chain i which exists in refractory form at the time of soil solidification

While Freiling used a volatile chain for his reference chain, a refractory chain is the more natural choice since it will be more or less uniformly distributed throughout the fallout. The following analysis will therefore use a refractory chain for the reference nuclide. Now if it's true that the refractory nuclides will be distributed as the third moment of the particle size distribution and volatile nuclides will be distributed as the second moment, then for an arbitrary chain f we can write

$$F_f(d) = \frac{F_T \{K_r f_r d^3 + K_v (1-f_r^2) d\} N(d)}{\int_0^{\infty} \{N(\bar{d}) \{f_r \bar{d}^3 + (1-f_r) \bar{d}^2\} d \bar{d}} \quad (42)$$

where K_r and K_v are normalization constants. For a refractorily behaving chain we get

$$F_r(d) = \frac{F_T N(d) d^3}{\int_0^{\infty} N(\bar{d}) \bar{d}^3 d \bar{d}} \quad (43)$$

Now the fractionation ratio is

$$(r_{f,r})(d) = \frac{\frac{F_T N(d) (f_r d^3 + (1-f_r) d^2)}{\int_0^{\infty} N(\bar{d}) (f_r \bar{d}^3 + (1-f_r) \bar{d}^2) d \bar{d}}}{\frac{F_T N(d) d^3}{\int_0^{\infty} N(\bar{d}) \bar{d}^3 d \bar{d}}} \quad (44)$$

or

$$(r_{i,r})(d) = \frac{(f_r + (1-f_r)d^{-1}) \int_0^{\infty} N(\bar{d}) \bar{d}^3 d \bar{d}}{\int_0^{\infty} N(\bar{d}) (f_r \bar{d}^3 + (1-f_r) \bar{d}^2) d \bar{d}} \quad (45)$$

And the mass distribution is given by

$$f_m(d) = \frac{N(d) d^3}{\int_0^{\infty} N(\bar{d}) \bar{d}^3 d \bar{d}} \quad (46)$$

Multiply Equation (46) by $f_r + (1-f_r)/d$ and integrate over all size groups to get

$$\int_0^{\infty} f_m(\bar{d}) (f_r + (1-f_r)/\bar{d}) d \bar{d} = \frac{\int_0^{\infty} N(\bar{d}) (f_r \bar{d}^3 + (1-f_r) \bar{d}^2) d \bar{d}}{\int_0^{\infty} N(\bar{d}) \bar{d}^3 d \bar{d}} \quad (47)$$

Comparing this result with Equation (45) we find

$$(r_{i,r})(d) = \frac{1}{\int_0^{\infty} f_m(\bar{d}) (f_r + (1-f_r)/\bar{d}) d \bar{d}} (f_r + (1-f_r)/d) \quad (48)$$

Now notice in Equation (48) the expression

$$C_i = \frac{1}{\int_0^{\bar{d}} f_m(\bar{d}) \{ f_r + (1-f_r)/\bar{d} \} d \bar{d}} \quad (49)$$

is a normalization constant for mass chain i . For a chain which consists only of volatile species, Equation (48) becomes then

$$(r_{v,r})(d) = C_v \frac{1}{d} \quad (50)$$

since $f_r = 0$ in this case. While for a general chain

$$(r_{i,r})(d) = C_i \{ f_r + (1-f_r)/d \} \quad (51)$$

Solving Equation (50) for d and substituting into Equation (51) yields

$$(r_{i,r})(d) = C_i f_r + \frac{C_i}{C_v} (1-f_r) (r_{v,r})(d) \quad (52)$$

This is a simple linear relation between $(r_{i,r})(d)$ and $(r_{v,r})(d)$. Now Freiling suggests that instead of separating the surface and volume fractions, that a given mass chain will have its activity distributed as a simple power of the diameter of the particles. The equations equivalent to Equation (50) and Equation (51) under Freiling's assumption (the Radial Power Law) are

$$(r_{v,r})(d) = C_v \frac{1}{d} \quad (53)$$

and

$$(r_{i,r})(d) = C_i d^{\sqrt{f_r}-1} \quad (54)$$

Eliminating d between these last two, and taking the logarithm of both sides of the result, gives

$$\begin{aligned} \ln(r_{i,r})(d) &= (1 - \sqrt{f_r}) \ln(r_{v,r})(d) \\ &+ \{(\sqrt{f_r}-1) \ln C_v + \ln C_i\} \end{aligned} \quad (55)$$

This is a logarithmic relation with slope $(1 - \sqrt{f_r})$. Freiling has observed this logarithmic relationship in fallout sample data, and indeed the $1 - \sqrt{f_r}$ expression in the slope above is a best fit of the observed correlation slopes to the fraction of the chain existing in refractory form at the time of soil solidification (Freiling, 1961: 11-16).

Note that if Equation (52) is plotted on log-log paper the limits ($f_r = 0$, $f_r = 1$) agree with observations in the data, but for intermediate chains ($0 < f_r < 1$), Equation (52) predicts a distinct curvature to the data (see Figure 7). This doesn't seem to agree very well with the data cited by Freiling. On the other hand, the expression in Equation (55) agrees very well with the Pacific weapons

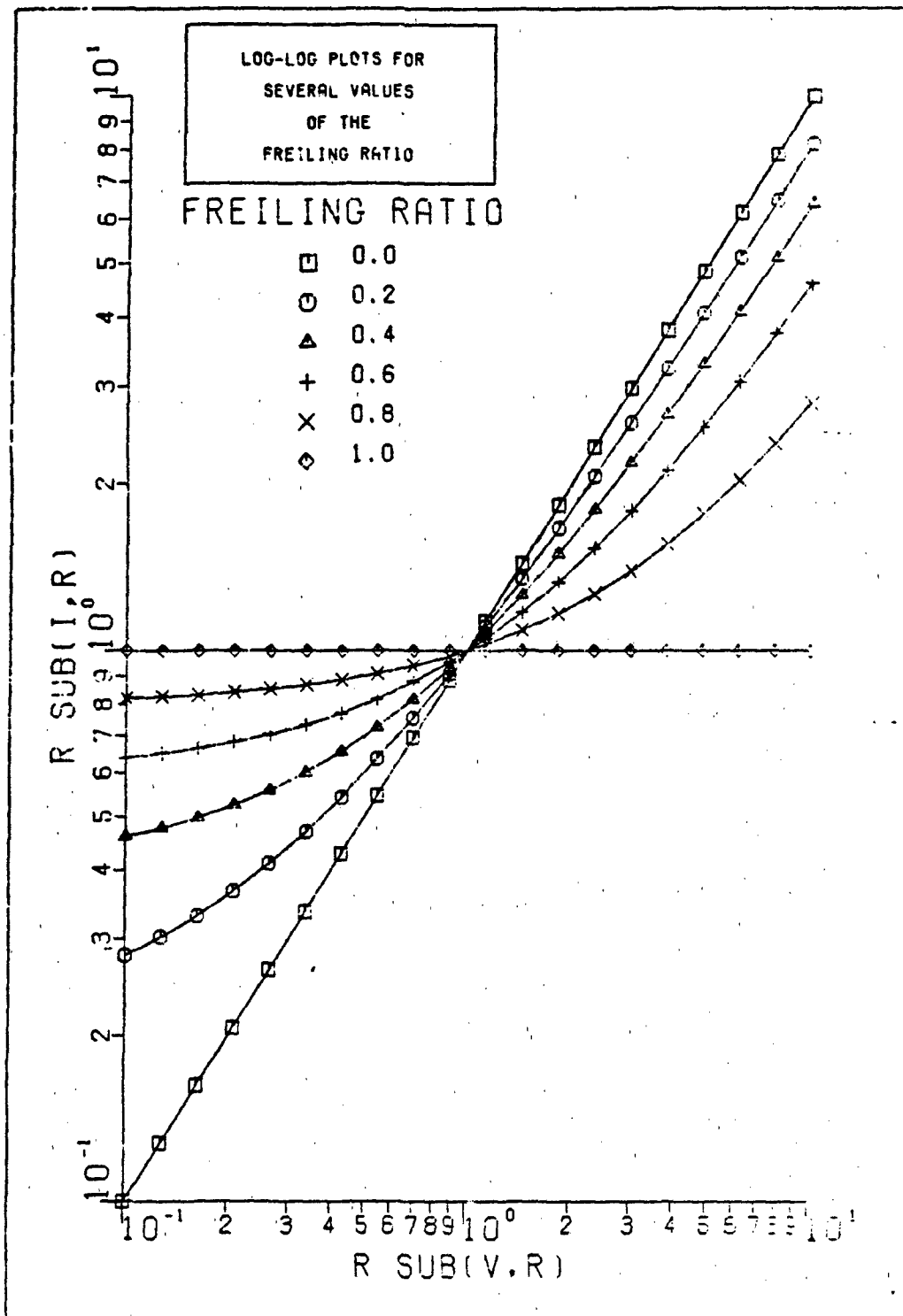


Figure 7. Plots of Equation (52) for Several Values of the Freiling Ratio

test data. Russell and Heft (Heft, 1970: 256-257, Bridgman, 1983 c) have shown, however, that in the case of silicate soil surface bursts, that we do see curvature in the plots of Equation (52).

It is clear, then, that there are limitations to the Freiling model. Freiling himself offered several caveats on the method (Freiling, 1961: 1908, Radionuclides, 1970: 336). The correlations that Freiling has observed should depend on weapon yield, and the type of carrier which constitutes most of the particles. Yet his correlations involved only high yield data for coral and water surface bursts. Since Freiling made his correlations irrespective of yield or carrier material, the Radial Power Law disregards these effects. His approach is primarily a graphical device which is useful for drawing general trends in behavior. A single set of correlations cannot be expected to cover all burst conditions. Care should be exercised in applying the Radial Power Law to low yield events or to events over silicate soils.

In the next section, the Tompkins modification to the Radial Power Law will be discussed. It was developed to bring the results of the Radial Power Law into better agreement with specific activity observations.

MODIFIED RADIAL POWER LAW

Introduction. When the Radial Power Law was considered by Defense Atomic Support Agency (DASA) for the DELFIC code, Tompkins

made the observation that there is a tendency for specific activity data to level out as particle size increases regardless of the volatility of the species being investigated. The transition point in the curves appeared to Tompkins to be about 100 to 200 microns for surface bursts (Tompkins, 1968: 15). In order to account for this, Tompkins required all fission products, regardless of volatility considerations, to be volume distributed above 100 microns. The model neglects to account for the fact that the specific activity begins to fall off again for very large particle sizes (Tompkins, 1970: 382). The resulting activity size distribution will be biased with the very large particles carrying too much activity while the smaller particles will carry too little.

Model Description. In Freiling 's Radial Power Law model, the particle size distribution was assumed to be log-normal. Tompkins' modification generalized the particle size distribution to allow for arbitrary distributions to be entered in tabular form. Let

d_k = geometric mean diameter of kth particle-size class,

$b_i = \sqrt{f_{r_i}}$, where f_{r_i} is the refractory fraction for mass chain i ,

N_k = number of particles in class k ,

F_T = total number of fissions in all size classes,

N_i = number of atoms in mass chain i in size class k ,

Y_i = fission yield of i th mass chain,

and

r = index for a refractory chain.

The number of atoms of mass chain i in size class k is

$$\bar{N}_i(d_k) = F_T Y_i f_i(d_k) \quad (56)$$

where

$$f_i(d_k) = N_k d_k^{b_i+2} / \sum_{k=1}^n N_k d_k^{b_i+2} \quad (57)$$

For a refractory chain, ($b_i = 1$), Equation (56) becomes

$$\bar{N}_r(d_k) = F_T Y_r f_M(d_k) \quad (58)$$

where

$$f_M(d_k) = N_k d_k^3 / \sum_{k=1}^n N_k d_k^3 \quad (59)$$

is the mass fraction in the k th size class. The fractionation ratio is then

$$(r_{i,r})_k = \frac{Y_i f_i(d_k)}{Y_r f_M(d_k)} \quad (60)$$

or

$$(r_{i,r})_k = \frac{Y_i d_k^{i-1} \sum_{k=1}^n N_k d_k^3}{Y_r \sum_{k=1}^n N_k d_k^{b_i+2}} \quad (61)$$

Then noting that

$$\frac{\sum_{k=1}^n N_k d_k^{b_i+2}}{\sum_{k=1}^n N_k d_k} = \sum_{k=1}^n (f_M(d_k^3) d_k^{b_i-1}) \quad (62)$$

and defining

$$E_i = 1 / \sum_{k=1}^n (f_M(d_k^3) d_k^{b_i-1}) \quad (63)$$

Equation (61) becomes

$$(r_{i,r})_k = \frac{Y_i}{Y_r} d_k^{b_i-1} (E_i) \quad (64)$$

It then follows from Equations (56), (60), and (64) that

$$\bar{N}_i(d_k) = F_T Y_i E_i d_k^{b_i-1} f_M(d_k) \quad (65)$$

Now Tompkins' modification assumes a two-component system. One part obeys the Radial Power Law, but the other part has a constant specific activity. Let

R_i = fraction of atoms in i th mass chain that obeys the Radial Power Law, and

S_i = fraction of atoms in i th mass chain that exhibits a constant specific activity

Equation (65) then can be written

$$\bar{N}_i(d_k) = F_T Y_i (R_i E_i d_k^{b_i-1} + S_i) f_M(d_k) \quad (66)$$

The crossover point between the Radial Power Law and the constant distribution yields

$$R_i E_i d_{\text{cross}}^{b_i-1} = S_i \quad (67)$$

but since

$$R_i + S_i = 1 \quad (68)$$

or

$$R_i (1 + E_i D_{\text{cross}}^{b_{i-1}}) = 1 \quad (69)$$

then

$$R_i = \frac{1}{1 + E_i D_{\text{cross}}^{b_{i-1}}} \quad (70)$$

and

$$S_i = \frac{E_i D_{\text{cross}}^{b_{i-1}}}{1 + E_i D_{\text{cross}}^{b_{i-1}}} \quad (71)$$

Then finally we have

$$\bar{N}_i(d_k) = \frac{F_{T_i} Y_i E_i}{1 + E_i D_{\text{cross}}^{b_{i-1}}} (d_k^{b_{i-1}} + D^{b_{i-1}}) f_m(d_k) \quad (72)$$

The model described above is termed the F-T model for purposes of comparison with the G-X model to be developed in the next chapter. The F-T model is considered to be the state of the art in fallout modeling by present researchers in this area. It was for this reason that it was selected for comparison with the G-X model. The next section will describe the most recent effort to model fractionation before the present research.

Diffusion Model

In 1966, Korts and Norman at General atomic reconsidered Miller's fractionation model to include the glassy nature of fallout particles from a general land surface detonation. The occurrence of glass formation suggested the use of temperature variable condensed state diffusion coefficients in place of the temperature switched equilibrium model proposed by Miller.

When describing fission product sorption according to a diffusivity-condensation model, fallout formation is assumed to be governed by equilibria established at the gas-surface interfaces, the rate of cooling of the cloud, and the rate of diffusion of adsorbed fission products into the central portions of the fallout particles (Norman, 1966: 12-54).

The assumption that soil solidification takes place at a fixed temperature, as is done in the Miller model, is inadequate for silicate soil fallout both above and below any reasonable "freezing temperature" (Norman, 1966). First, "molten" silicates in the region

just above their "freezing temperatures" are generally viscous liquids which have low mobilities (diffusivities) of their component species. Therefore, above the "freezing temperature," liquid silicate fallout particles won't be uniformly loaded with fission products but will show a considerable radial concentration gradient. Additionally, molten silicates tend to form glasses on cooling. A glass is just a supercooled liquid whose viscosity has become so high that the tendency toward crystallization has become essentially negligible. Norman and Winchell suggest that diffusivity in a glass can, as a first order approximation, be treated as an extension of diffusivity in the corresponding molten silicate (Norman, 1966). The system behaves, then, as if no phase transition has occurred. Thus not only is the assumption of homogeneity above a "freezing temperature" inadequate, but the assumption of strictly surface adsorption occurring after the "freezing temperature" has been reached is also questionable. In fact, the very smallest fallout particles will probably absorb fission product oxides essentially homogeneously at temperatures lower than the "freezing temperature" (Norman, 1966). Using temperature-dependent diffusivities instead of the "freezing temperature" model is a logical extension of the Miller model. Sorption of fission products occurs in this model by allowing a homogeneous gas phase to equilibrate with the surfaces of all fallout particles. The adsorbed fission products are then allowed to diffuse into the fallout particles. All of this occurs in the time-temperature field associated with a nuclear detonation (Norman, 1966).

Concentration-independent diffusion in spherical particles as presented by Carslaw and Jaeger (Carslaw, 1959) is assumed to govern the diffusion of the condensed fission products into the carrier material. The diffusion coefficient, D , is related to the average concentration, \bar{C} , and the surface concentration, C_0 , through the following equation:

$$\frac{C_0 - \bar{C}}{C_0} = \frac{6}{\pi^2} \sum_{n=1}^{\infty} \frac{1}{n^2} e^{-(\pi^2 n^2 D t / R^2)} \quad (73)$$

where R is the radius of the spherical particle and t is the diffusion time. Both the Henry's Law constant and the diffusion coefficient are assumed to follow Arrhenius and Clausius-Clapeyron temperature dependencies, respectively (Norman, 1966: 15).

The cooling rate as a function of yield is given by the following cooling rate scaling equation given by Freiling (Freiling, 1965):

$$-\frac{dT}{dt} \approx 3 \times 10^{11} W^{-0.3} T^4 \quad (74)$$

where $-dT/dt$ is the cooling rate (degrees Kelvin/sec) and W is the energy yield (Kt).

The mathematical model involves time-temperature stepping, Henry's Law constants, diffusion coefficients, a detonation model, and

a mass balance equation relating the total amount of a nuclide in the cloud to the amounts of this nuclide in the gas phase and in the particles of various sizes through an analytically determinable surface concentration of the nuclide. By stepping the temperature and allowing the nuclides to decay, a similar but more complicated determination of an increment to the surface concentration can be made. This process is then repeated until the diffusion process essentially ceases. This process can be carried out through each nuclide chain in order to account for transmutation effects. In this way, it is possible to make calculations describing the chemistry of fallout formation according to a condensation-diffusion mode (Norman, 1966: 21).

Norman achieved some promising results with this model (Norman, 1968). According to Norman, the method was going to be tested for use in the official DoD fallout code, DELFIC, but apparently this was never done (Norman, 1983). It was because of the very encouraging results that Norman reported that a condensation-diffusion approach was chosen as a basis for the G-X model developed in the next chapter.

III. The G-X Diffusion Model

Introduction

There is a considerable amount of data to suggest that the following description of the fallout formation process applies to a surface burst: Soil particles are entrained by the rising fireball and a small percentage of the total is completely vaporized. As condensation begins, very small particles with fission products fused within them are created. Many of these coalesce with other larger melted and unmelted particles along with the vapors of the more volatile fission products. Those soil particles which are not vaporized generally remain in the fireball for a shorter period of time. In addition, they constitute the larger fallout particles. The unmelted particles enter the fireball at later times and leave the cloud at earlier times. Thus they receive only a limited amount of heating and consequently the fission products they contain are fused into the outer layer or attached to the surfaces only (Miller, 1967: 3, Heft, 1970: 255-256, Tompkins, 1970: 388, Norment, 1966: 23-28).

There are several sources of information to validate this picture of the early fireball: First is the separation of the fallout samples into two distinct types of particles: glassy and crystalline (hence the name G-X model). The glassy particles are those which were exposed to high temperatures and either fully melted or vaporized. The crystalline particles are those which never vaporized or melted or at most only slightly melted. Second, the two types of particles

exhibit very distinct behavior with respect to specific activity. The glassy particles which were exposed to higher temperatures and present in the cloud earlier both absorb refractory fission products and adsorb volatile fission products. The crystalline particles were not present in the active region of the cloud at early time and so absorb the more refractory fission products to a much smaller extent. This effect is offset some by the tendency of the smaller particles to agglomerate, but this will be neglected. This model of behavior is supported by specific activity data. Glassy particles in general show much higher specific activity than crystalline particles of the same size (Pascual, 1967: 8, Mackin, 1958: 17, Crocker, 1965: 5).

In addition to this evidence for two separate types of fractionation behavior, there is evidence that the simple temperature switch used by Freiling and Miller is not correct. This was the premise for the diffusion studies by Norman in his treatment of fractionation (Norman, 1966-1971). Since the spherical particles are glasses which by definition are supercooled liquids, they exhibit no well-defined melting point. In defense of his diffusion hypothesis, Norman took thin sections of glassy fallout particles and obtained concentration profiles in agreement with his model (Norman, 1967: 219). Figures 8, 9, and 10 from a report by Miller show additional radiographic evidence for diffusion of radioactivity into fallout particles (Miller, 1964: 22-31). Additional evidence for the diffusion approach from specific activity measurements on ground bursts is given by Nathans (Nathans, 1970).

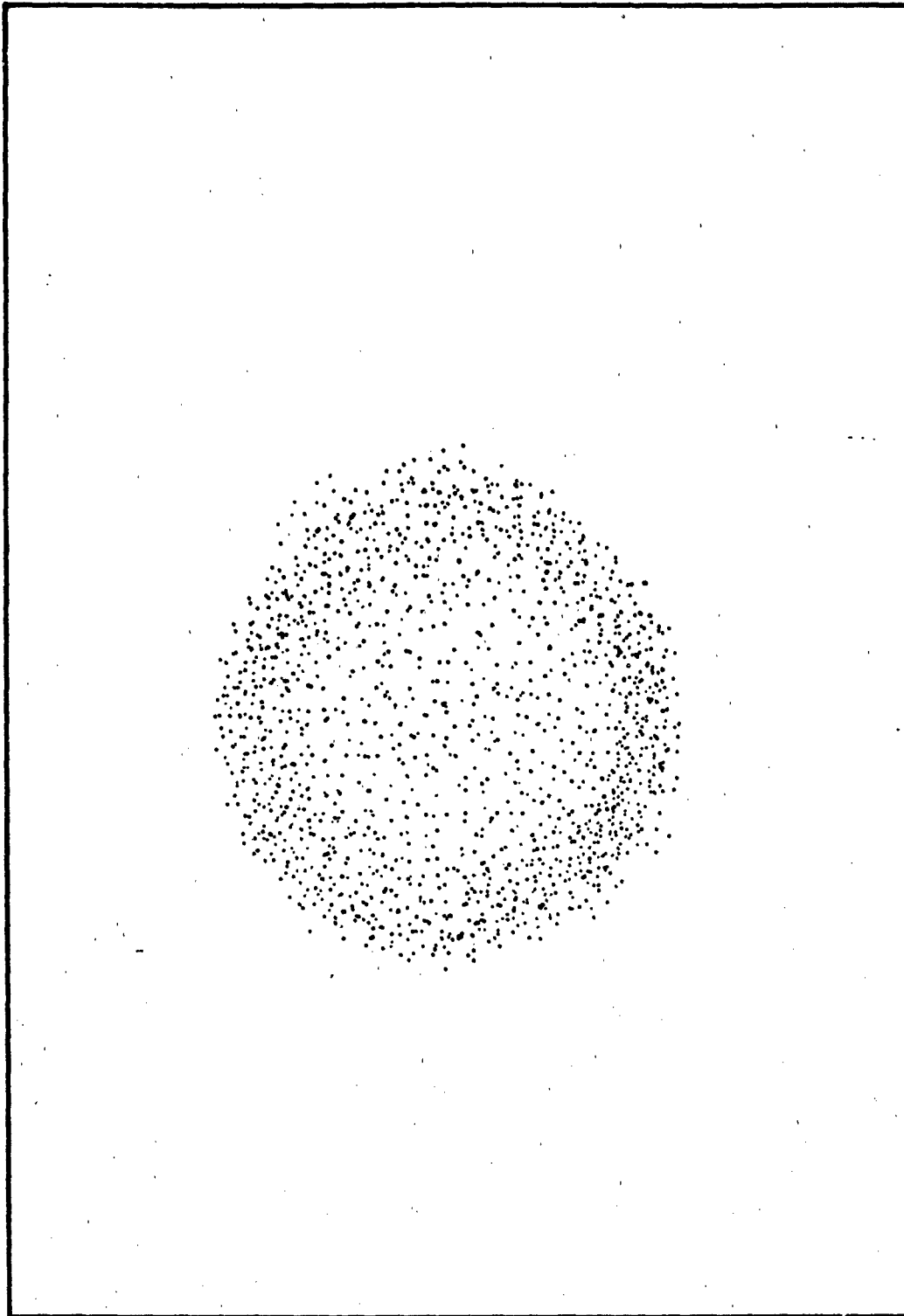


Figure 8. Radiograph of a Fallout Particle with
Activity Distributed Uniformly Throughout
its Volume (Miller, 1963)

III-3



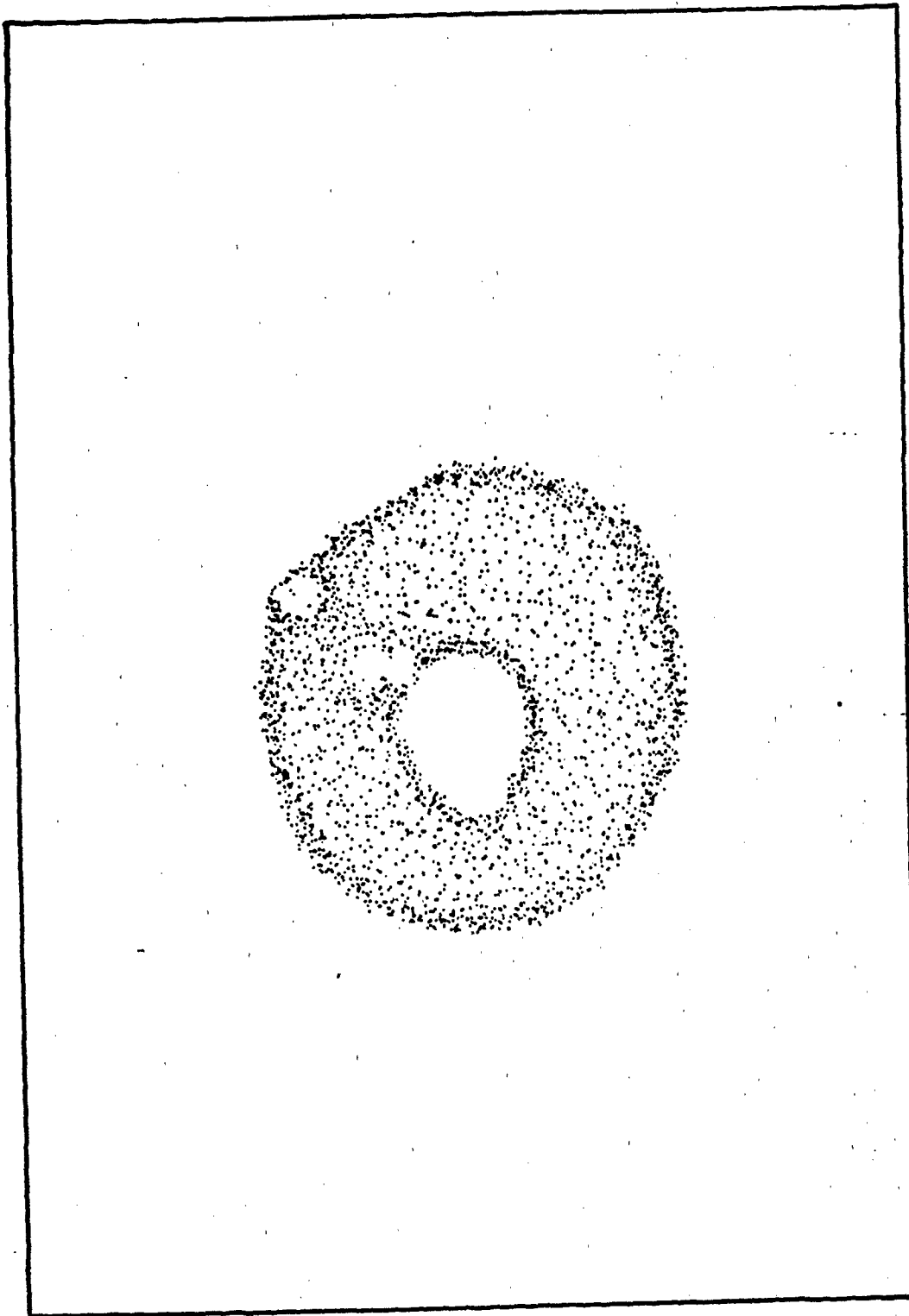


Figure 9. Radiograph of a Fallout Particle with
Activity Located Primarily on the Surface
(Miller, 1963)

III-4

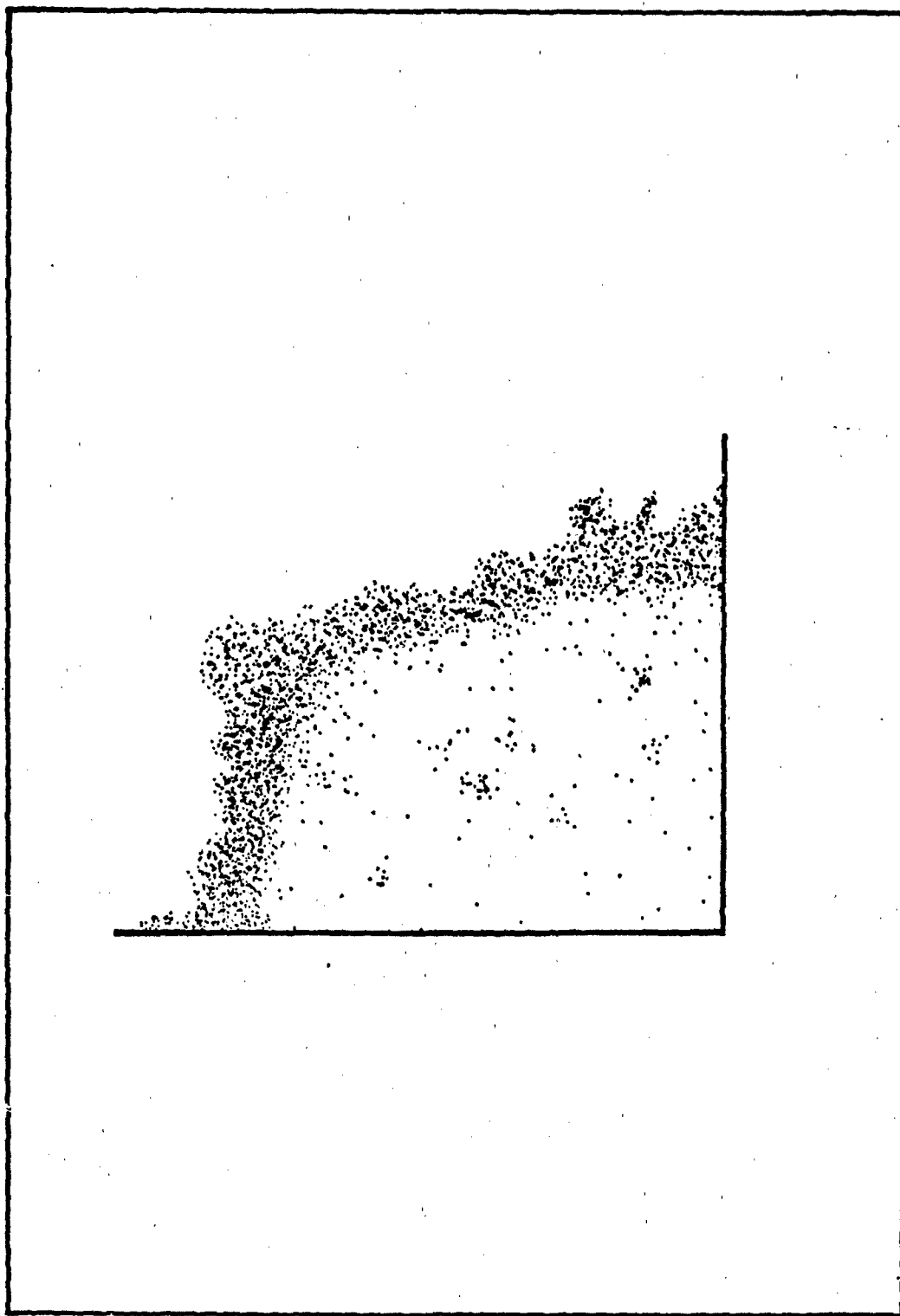


Figure 10. Radiograph of an Irregularly Shaped
Crystalline Fallout Particle (Miller, 1963)

III-5



One important question in developing the diffusion model is whether gas-phase diffusion of fission products to the surfaces of particles, surface attachment coefficients, or diffusion within the particles is the rate controlling mechanism. In a working group at the April 1966 Fallout Phenomena Symposium (Proceedings, 1966: 456), Freiling reported that work done by U.S. Naval Radiological Defense Laboratory (NRDL) on calcium ferrite, $\text{CaO-Al}_2\text{O}_3\text{-SiO}_2$, clay, and sodium oxide-silica indicated that condensed state diffusion was the rate determining mechanism for all but the calcium ferrite samples where gas-phase diffusion was found to be rate determining.

Method Overview

For the G-X model, the particles are assumed to be non-agglomerating, non-convecting, spherical silicate glassy particles of various sizes which are distributed uniformly throughout a cloud which is at a uniform temperature and has a uniform concentration of fission products and air. Calculations proceed on one decay chain at a time beginning at the highest temperature at which diffusion is considered to be rate determining. At this point the isotopes are assumed to surface condense according to Henry's Law and then to diffuse into the fallout particles. Then, the isotopes are allowed to decay, and the time and temperature are incremented. The process is repeated until the temperature is close to the solidification temperature for the glass. At this point, the distribution of glassy particles is augmented with the distribution of crystalline

particles. The process is continued until the diffusion process has essentially terminated. The techniques applied in the particle activity module here were influenced by the work of Korts and Norman. The program is on file at the Air Force Institute of Technology and is fully commented. It is designed to be run with 250,000 60-bit words of memory in three overlays on a CDC Cyber 750.

Method

An overview of the method has been presented. This section presents a derivation of the important equations used in the G-X model.

For an assumed ideal solution, the vapor pressure of fission product i in the gas around a liquid soil particle is given by Raoult's Law as

$$P_i = X_i P_i^* \quad (75)$$

where

X_i = the mole fraction of i

P_i^* = vapor pressure if $X_i = 1$, that is the

vapor pressure which would be found above pure fission product i at the given conditions.

In real solutions, there are often departures from this ideal behavior. Henry's Law of dilute solutions replaces the vapor

pressure of the substance in pure form, P_i (the proportionality constant), with a different constant. This is called the Henry's Law constant. The Henry's Law constant is the slope of a line tangent to the observed behavior of the partial pressure of fission product i as a function of X_i at very low concentrations of substance i (see Figure 4).

$$P_i = X_i k_i \quad (76)$$

Substituting for P_i from the ideal gas law we have

$$n_i \frac{RT}{V} = X_i k_i \quad (77)$$

where

R = gas constant

T = absolute temperature

V = volume

or

$$m_i = n_i M_i = \frac{M_i V}{RT} X_i k_i \quad (78)$$

where

m_i = mass of fission product i in the gas phase

M_i = molecular weight of i

Now the mole fraction of fission product i is

$$X_i = \frac{m_i/M_i}{m_{\text{soil}}/M_s + m_i/M_i} \quad (79)$$

where

m_{soil} = the soil mass

m_i = the mass of i in solution

M_s = the molecular weight of the soil

Because of the very low concentration of fission product i in the soil, the mole fraction is given approximately by

$$X_i = \frac{m_i}{m_s} \frac{M_s}{M_i} \approx C_i \frac{M_s}{M_i} \quad (80)$$

where C_i is the concentration of i in the particles.

As a matter of convenience, the Henry's Law constants were measured in concentration units rather than in molar units. That is

$$\tilde{k}_i = k_i \frac{M_i}{M_s} \quad (81)$$

Thus the amount of fission product i in the gas phase at equilibrium is

$$m_i = \frac{C_i \bar{k}_i V M_i}{RT} \quad (82)$$

In the actual situation, diffusion of fission product atoms to the surfaces of the particles is generally much faster than diffusion into the bulk phase of the particles. In this case, the rates of uptake of fission products are controlled by the diffusion rates in the bulk phase. For this reason, diffusion through the gas is taken to be infinitely fast. In addition, because the cloud is cooling and because the fission products are decaying, equilibrium cannot be established completely. Instead, the gaseous fission products are assumed to be in equilibrium with an infinitesimally thin surface layer on the particles. The amount of fission product i in the gas and liquid phases is determined by a mass balance as follows: At the highest temperature at which fission product sorption by bulk diffusion is determined to be rate determining, the surface concentration of fission product i is found from

$$Y_i = \frac{C_{i1} \bar{k}_{i1} V_i M_i}{RT_1} + m_{i1} \quad (83)$$

where

C_{i1} = surface layer concentration of i in the soil
at the 1st time and temperature

k_{i1} = Henry's Law constant i at 1st time and
temperature

V_1 = volume of active region at the first time

T_1 = temperature at the 1st time

m_{i1} = mass of fp which has diffused into the soil
particles

Y_{i1} = yield of fission product i at the 1st time

The first term on the right of Equation (83) is the amount of fission product i in the gas phase. The second term on the right must be computed by solving the diffusion equation for each particle size class considered, weighting the result by the mass of soil in the size class and summing over all size classes:

$$m_{i1} = \sum_{s=1}^P \bar{C}_{i1}^{(s)} w_s \quad (84)$$

where \bar{C}_{i1} is the average concentration in the particles during time period one. The diffusion equation for spheres with only radial diffusion is

$$\frac{\partial C_i}{\partial t} = D_i \left(\frac{\partial^2 C_i}{\partial r^2} + \frac{2}{r} \frac{\partial C_i}{\partial r} \right) \quad (85)$$

On letting

$$u = C_1 r \quad (86)$$

Equation (85) becomes

$$\frac{\partial u}{\partial t} = D_1 \left(\frac{\partial^2 u}{\partial r^2} \right) \quad (87)$$

with boundary conditions

$$\begin{aligned} u &= 0, r = 0, t > 0 \\ u &= e^{-\delta(t)}, r = a, t > 0 \\ u &= 0, t = 0, 0 < r < a \end{aligned}$$

Crank gives the solution in this case as (Crank, 1975)

$$C_1(r,t) = \frac{-2D_1}{ra} \sum_{k=1}^{\infty} (-1)^k \exp(-D_1 k^2 \pi^2 t/a^2) \quad (88)$$

$$k \pi \sin\left(\frac{k \pi r}{a}\right) \int_{\lambda=0}^t \exp(D_1 k^2 \pi^2 \lambda/a^2) \phi(\lambda) d\lambda$$

which is a Volterra integral equation of the second kind. Since $\phi(t)$ is not known in advance, an iterative technique would be required to solve this equation. For this reason, the solution of the diffusion equation is determined by a superposition technique. For the first

time period, the surface concentration is held constant, and the amount of fission product i which has diffused into a particle of size s during the time period is determined by solving

$$\frac{\partial u}{\partial t} = D_i \left(\frac{\partial^2 u}{\partial r^2} \right) \quad (89)$$

$$u = 0, r = 0, t > 0$$

$$u = a C_{i1}, r = a, t > 0$$

$$u = 0, t = 0, 0 < r < a$$

The solution to this equation is

$$C(r,t) = C_{i1} \left\{ \frac{-2a}{\pi r} \sum_{k=1}^{\infty} \frac{(-1)^k \sin\left(\frac{k\pi r}{a}\right) \exp\left(-\frac{D_i k^2 \pi^2 t}{a^2}\right)}{k} \right\} \quad (90)$$

or

$$C(r,t) \stackrel{\Delta}{=} C_{i1} A_{i1}$$

and the average concentration is given by

$$\bar{C}_{i1}(t) = C_{i1} \left\{ 1 - \frac{6}{\pi^2} \sum_{k=1}^{\infty} \frac{1}{k^2} \exp\left(-\frac{D_i k^2 \pi^2 t}{a^2}\right) \right\} \quad (91)$$

Later time periods are treated independently, and the results are superimposed to give the final result. Returning to the first time period, we have the following mass balance:

$$Y_i = \frac{C_{i1} \bar{k}_{i1} V_1 M_i}{RT_1} + C_{i1} \sum_{s=1}^p \Delta_{i1}^{(s)} m_s \quad (92)$$

where m_s is the mass of soil in particle size class s and p is the number of particle size classes. The surface concentration is assumed to be independent of particle size and type. At this point, time and temperature are incremented. To find the surface concentration at the second temperature, the mass balance is given by

$$Y_{i2} = \frac{C_{i2} V_2 M_i \bar{k}_{i2}}{RT_2} + C_{i1} \exp(-\lambda_i \Delta t_1) \sum_{s=1}^p \Delta_{i1,2}^{(s)} w_s$$

$$+ C_{(i-1)1} [1 - \exp(-\lambda_{(i-1)} \Delta t_1)] \sum_{s=1}^p \Delta_{(i-1),1,1;i,2,2}^{(s)} w_s \quad (93)$$

$$+ \{C_{i2} - C_{i1} \exp(-\lambda_i \Delta t_1) - C_{(i-1)1} [1 - \exp(-\lambda_{(i-1)} \Delta t_1)]\} \sum_{s=1}^p \Delta_{i,2,2}^{(s)} w_s$$

The first term on the right side is the amount of fission product i which is still in the gas phase at t_2 . The second term is the amount of i which had condensed at t_1 after being allowed to decay for Δt_1 and to diffuse during periods Δt_1 and Δt_2 (the diffusion

coefficients will differ for the two periods). The third term is the amount of the immediate precursor of isotope i which decayed into i and was diffusing as isotope $i-1$ during time interval Δt_1 and as isotope i during Δt_2 . The fourth term is the amount of isotope i which has diffused during the second period as a result of the surface concentration perturbation caused by the time-temperature-volume perturbation.

Since the equations at succeeding times become rather involved, further analysis will be restricted to the instance of a mass chain containing only a single isotope. Further, the discussion will be limited to the case of a single particle size class with $w_1 = 1$. These restrictions will make the general case more tractable. In this case, Equation (92) becomes

$$Y = C_1 G_1 + C_1 \Delta_{11} \quad (94)$$

and Equation (93) becomes

$$Y = C_2 G_2 + C_1 \Delta_{12} + (C_2 - C_1) \Delta_{22} \quad (95)$$

or

$$Y = C_2 G_2 + C_2 \Delta_{22} + C_1 (\Delta_{12} - \Delta_{22}) \quad (96)$$

where

$$G_N = \frac{V_N M \bar{k}_N}{RT_N}$$

At the third time period, the mass balance is

$$Y = C_3 G_3 + C_1 \Delta_{13} + (C_2 - C_1) \Delta_{23} + [C_3 - (C_2 - C_1) - C_1] \Delta_{33} \quad (97)$$

or

$$Y = C_3 G_3 + C_1 \Delta_{13} + (C_2 - C_1) \Delta_{23} + (C_3 - C_2) \Delta_{33} \quad (98)$$

At the fourth time, the expression becomes

$$Y = C_4 G_4 + C_1 \Delta_{14} + (C_2 - C_1) \Delta_{24} + (C_3 - C_2) \Delta_{34} + (C_4 - C_3) \Delta_{44} \quad (99)$$

At the Nth step, the expression is

$$Y = C_N G_N + C_1 \Delta_{1N} + \sum_{k=2}^N (C_k - C_{k-1}) \Delta_{kN} \quad (100)$$

or

$$Y = C_N (G_N + \Delta_{NN}) + \sum_{k=1}^{N-1} C_k (\Delta_{kN} - \Delta_{k+1,N}) \quad (101)$$

In order to show the effect of adding crystal particles at late time, the situation must be made slightly more complex. Before the crystalline particles are introduced, the expression for the Nth time step is

$$Y = C_N(G_N + \sum_{s_{\text{glass}}} \Delta_{NH}^{(s)} w_s) + \sum_{k=1}^{N-1} C_k \left\{ \sum_{s_{\text{glass}}} (\Delta_{kN}^{(s)} - \Delta_{k+1,N}^{(s)}) w_s \right\} \quad (102)$$

The mass balance at the time step in which crystal particles are introduced is

$$Y = C_x G_x + C_x \sum_{s_{\text{glass}}} \Delta_{xx}^{(s)} w_s + \sum_{k=1}^{x-1} C_k \left\{ \sum_{s_{\text{glass}}} (\Delta_{kx}^{(s)} - \Delta_{k+1,x}^{(s)}) w_s \right\} \quad (103)$$

$$+ C_x \sum_{s_{\text{xtal}}} \Delta_{xx}^{(s)} w_s$$

$$Y = C_x(G_x + C_x \sum_{\text{all } s} \Delta_{xx}^{(s)} w_s + \sum_{k=1}^{x-1} C_k \left\{ \sum_{s_{\text{glass}}} (\Delta_{kx}^{(s)} - \Delta_{k+1,x}^{(s)}) w_s \right\} \quad (104)$$

For later time steps (after crystal particle entry), the expression becomes

$$\begin{aligned}
Y &= C_M G_M + C_M \sum_{\text{all } s} \Delta_{MM}^{(s)} w_s \\
&+ \sum_{k=1}^{M-1} C_k \left\{ \sum_{s_{\text{glass}}} (\Delta_{kM}^{(s)} - \Delta_{k+1,M}^{(s)}) w_s \right\} \\
&+ \sum_{k=X}^{M-1} C_k \left\{ \sum_{s_{\text{xtal}}} (\Delta_{kM}^{(s)} - \Delta_{k+1,M}^{(s)}) w_s \right\}
\end{aligned} \tag{105}$$

or upon rearrangement

$$\begin{aligned}
Y &= C_M G_M + C_M \sum_{\text{all } s} \Delta_{MM}^{(s)} w_s \\
&+ \sum_{k=1}^{n-1} C_k \left\{ \sum_{s_{\text{glass}}} (\Delta_{kM}^{(s)} - \Delta_{k+1,M}^{(s)}) w_s \right\} \\
&+ \sum_{k=X}^{M-1} C_k \left\{ \sum_{\text{all } s} (\Delta_{kM}^{(s)} - \Delta_{k+1,M}^{(s)}) w_s \right\}
\end{aligned} \tag{106}$$

Each term in the last two sums in Equation (106) contains a surface concentration expression times the difference of two diffusion terms. Each of these must be modified by a decay term. In order to illustrate how decay is handled, take the case of an isotope with three precursors at the j th time step. Figure 11 shows the ways in which growth and decay can occur in the instance of mass chain 89. In the case of ^{89}Kr , there are three possible paths for it to contribute to production of ^{89}Rb after three time increments. The decay coefficients for these three paths are

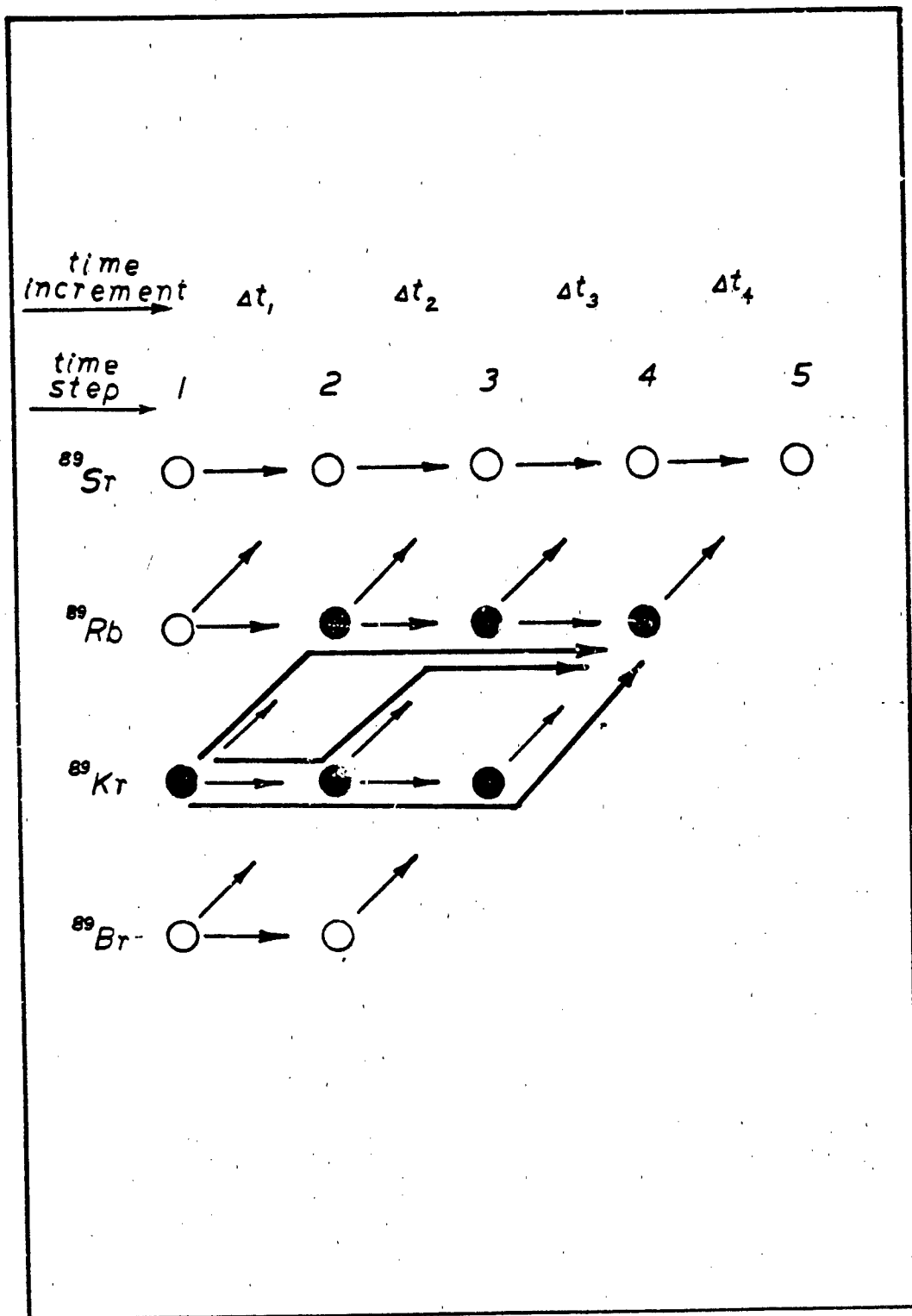


Figure 11. Decay Paths in Mass Chain 89 for the Diffusion Model

$$\{1 - \exp(-\lambda_{Kr}\Delta t_1)\} \exp(-\lambda_{Rb}(\Delta t_2 + \Delta t_3)) \quad (107)$$

$$\{\exp(-\lambda_{Kr}\Delta t_1)\} \{1 - \exp(-\lambda_{Kr}\Delta t_2)\} \{\exp(-\lambda_{Rb}\Delta t_3)\} \quad (108)$$

$$\exp[-\lambda_{Kr}(\Delta t_1 + \Delta t_2)] \{1 - \exp(-\lambda_{Kr}\Delta t_3)\} \quad (109)$$

Recall that each decay expression is associated with the difference of two diffusion terms (see Equation (102)). The first diffusion term represents diffusion from t_k to the current step. The second term represents diffusion from t_{k+1} to the current time step. It is seen, then, that the first diffusion term corresponding to the decay expression in equation (107) is for diffusion as Kr during time step 1 and as Rb from t_2 to t_4 . The second diffusion term is for diffusion as Rb from t_2 to t_4 . Similarly, the first diffusion term associated with Equation (108) is for diffusion as Kr from t_1 to t_2 and as Rb from t_3 to t_4 . The second term is then for diffusion as Kr during Δt_2 and as Rb from t_3 to t_4 . And, finally, the first diffusion term associated with Equation (109) is for diffusion as Kr from t_1 to t_3 and as Rb during Δt_4 , while the second is for diffusion as Kr from t_2 to t_3 and as Rb during Δt_4 . Each of these diffusion terms is just the solution of the diffusion equation using the appropriate argument. For example, the first diffusion term associated with Equation (107) was for diffusion

as Kr during time step 1 and as Rb from t_2 to t_4 . The appropriate argument for the diffusion equation would be

$$\delta t = D_{Kr,1}\Delta t_1 + D_{Rb,2}\Delta t_2 + D_{Rb,3}\Delta t_3 + D_{Rb,4}\Delta t_4 \quad (110)$$

Equation (91) gives the relationships between the average concentration and the surface concentration. The derivation of the general case for the Nth time step is analogous to the derivative for Equation (102). For times prior to the introduction of crystal soil particles, the average concentration is

$$\bar{C}_N = C_{II} \sum_{s_{\text{glass}}} \Delta_{NI}^{(s)} w_s + \sum_{k=1}^{N-1} C_k \left\{ \sum_{s_{\text{glass}}} (\Delta_{kN}^{(s)} - \Delta_{k+1,N}^{(s)}) w_s \right\} \quad (111)$$

Expressions analogous to Equations (103) and (104) can also be similarly derived.

Particle Size Distribution

The lognormal distribution given by

$$F_m(d) = k \int_{-\infty}^d \frac{1}{2\pi Bx} \exp\left(-\frac{1}{2} \left(\frac{\ln x - a}{B}\right)^2\right) dx \quad (112)$$

where

- F_m = cumulative mass fraction
- K = a normalization constant
- σ = \ln (median diameter)
- s = logarithmic standard deviation of the distribution
- d = particle diameter

has been traditionally employed in fallout calculations. The experimental basis for such a choice is found in the analysis of cloud and fallout samples obtained several hours after burst (Heft, 1970, Norment, 1966: 28-29). Based on an analysis of data from the Small Boy event in 1962, a lognormal distribution of particle size with median diameter of .407 microns and a standard deviation of $\ln(4.0)$ was selected as the default distribution for the DELFIC code (McDonald, 1974: 60, Malonel, 1974). In this distribution, 50 percent of the mass is associated with particles smaller than 130 microns in diameter. Later studies of the soil and debris ejected from the craters of various tests where particle sizes ranged from millimeters to meters indicated a power law behavior (Layson, undated):

$$M(d) = k' d^{-p} \quad (113)$$

where p is approximately 0.5 for various soils and rock. In 1966, russell suggested a truncated power law based on evidence that a true power law was unrealistic (Bridgman, 1983 d). A year later, Freiling published a study which concluded that the differences between the

lognormal distribution and the truncated power law were insignificant. He further concluded "that the lognormal distribution had the esthetic advantage of an observationally confirmed theoretical basis" (Freiling, 1966). It seems, however, that requiring the active particles which obtained their activity from the fireball (as opposed to activation products) to fit the distribution of very large particles ejected from the crater is erroneous. At any rate, one can attempt to bridge the gap between these two positions in spite of Freiling's findings by using a hybrid distribution as suggested by McGahan (McGahan, 1974: 61). McGahan has done calculations with lognormal, pure (not truncated) power law, and a hybrid distribution and discovered some differences in predicted dose rates. But if one substitutes the more reasonable truncated power law distribution, there is little difference. As a result, for the purpose of this study, the preferred particle size distribution is the lognormal. This is especially so in view of the fact that this research is compared primarily with shots Small Boy and Johnny Boy which were of similar yield and shot conditions and since a lognormal was deemed to best fit the Small Boy data.

Partition of Soil

The next important question to consider is that of the partition of the soil burden of the cloud into the various phases at early time. This is a question which would best be answered by a combined theoretical and computational effort that would start from first

principles and follow the numerous complex processes from shot time to early cloud development. Because of the enormous complexities involved, however, no such calculation has been attempted, and it remains an important area for further research. On the other hand, bounds can be placed on the problem. The total soil burden of the cloud can be estimated from a number of sources: (1) energy partition, (2) hydrodynamics calculations, (3) cloud buoyancy, (4) back extrapolation, (5) specific activity, (6) crater volume, and (7) fireball volume. Normant and others studied and evaluated all of these and chose methods 4-7. The scaling functions they developed were calibrated with data from the Teapot Ess shot which was a 1 kt underground burst (-67 feet) at the Nevada Test Site in 1955 (Hawthorne, 1979: 201).

The specific partition of the soil into vaporized, melted, and unmelted material is more difficult. First of all, the cloud is anything but uniform at early time. It is extremely hot in the region of the toroidal ring about which dust and debris are being circulated. The temperature falls off rapidly with increasing distance from the center of this region. It is reasonable to expect that the fission products and device debris would be found in the hottest regions of the toroid. Similarly, one would expect to find any soil which had been initially vaporized located here. As the fireball rises, it expands and thus heats and contaminates additional soil. After an initial pseudohydrostatic cloud rise phase (the second temperature maximum occurs in this phase) the fireball begins to rise

rapidly. A strong updraft is produced in the wake of the cloud, and soil dust suspended in the air is sucked upward in the stem toward the cloud cap (Figure 1).

The next thing to consider is the soil itself. For continental United States soils, the characteristic soil types are the common sandy and clay soils. In the case of sand, the chemical composition is nearly 100 percent silicon dioxide (SiO_2). For the more abundant clay soils, the major component is still silicon dioxide, but there is a mixture of Al_2O_3 , CaO , Na_2O , Fe_2O_3 , FeO , MgO , K_2O , and Sb_2O_3 as well. In studies of thermodynamic properties and diffusivities of soils, Norman and others concentrated on a mixture of 62 percent SiO_2 , 15 percent Al_2O_3 and 23 percent CaO , although other mixes were studied too (Norman, 1970, Norman, 1966, Norman, 1967, Winchell, 1967). Since it was determined that this mix was appropriate for Small Boy calculations (Norman, 1968: 1), this is the soil mix which was selected for this study. The major constituents of this soil are silicon dioxide and calcium oxide. The $\text{CaO-Al}_2\text{O}_3\text{-SiO}_2$ soil "solidifies" at about 1620 K. To estimate the amount of soil material which is in the vapor phase, the following observations are made: (1) High temperatures are localized to the inside of the vortex toroid. (2) This region contains most of the fission products. (3) In surface bursts, much of the fallout is composed of unvaporized soil onto which active material condenses. From these it follows that the amount of soil vapor in the cloud will be less than the mass of active fallout. In shots Johnny Boy and

Small Boy, about 38 percent of the gross fallout mass is associated with active material. Therefore, it follows that at least for these shots, less than 38 percent of the total soil burden is vaporized (Norment, 1966). Norment et al. made estimates of the energy available for heating soil by differencing the thermal energies radiated by air and surface bursts and found that 1.5 percent of the soil burden is vaporized per 100 degree excess of the temperature over the soil boiling point at a time shortly after the second temperature maximum (Norment, 1966: 28). Tompkins, et al. have inferred from the magnitude of specific activity of fallout from ground bursts that only about a tenth of the soil is vaporized (Tompkins, 1968).

Crystal-Glass Distributions

In examining samples of Small Boy fallout which were not sieved, Pascual noted bimodality in the sample collected at 9200 feet from ground zero (Pascual, 1967). Besides this and other qualitative remarks made above by various investigators, there are a number of reports which provide some quantitative information on the partition of the particle size distribution between glassy particles and crystalline particles. Two reports which looked specifically into this are Pascual, 1967, and Mackin, 1958. Pascual provides the most relevant data since it uses Small Boy data. Unfortunately, only the larger particle size classes were investigated in the report. Information on the smaller classes had to be inferred from knowledge of the overall particle size distribution and other information.

Table 1 gives the raw data used to determine the fraction of each size class which is composed of glassy particles as opposed to crystalline particles. The two distributions were unfolded by first assuming an overall lognormal particle size distribution of median .407 microns diameter and standard deviation of $\ln(4.0)$. Then using the information in Table 1, qualitative remarks such as that spheres dominate in the smaller particle size classes (Nathans, 1970: 367), and specific activity data, the two distributions were determined using a non-linear search technique for the parameters of two lognormal distributions which when superimposed would yield the closest fit to the observed combined distribution. The resulting distributions are shown in Figure 12.

Bias in the Data

There was some concern that measurements on the particle size distribution for shot Small Boy were in error due to the sieving technique used. The concern was that in the process of separating the fractions using sieves of different mesh sizes that small particles adhering to the surfaces of the larger particles would be shaken loose and thus bias the analysis. Also the larger particles in some cases were fragile and could be broken during size separation. Pascual looked into this source of potential error and concluded that while there was measurable loss of activity from the larger size fractions, the gamma ray spectra were not noticeably altered (Pascual, 1967).

Table 1.

Raw Data for Mass Size Distribution Decomposition			
Particle Size	Particle Type	Percent in Class	Specific Activity CPM/mg
1400 μ	Spheres	35.7	3617
	Crystals	64.2	1657
700-1400 μ	Spheres	38.4	5677
	Crystals	61.6	2780
350-700 μ	Spheres	46.1	6700
	Crystals	53.9	3240

(Pascual, 1967)

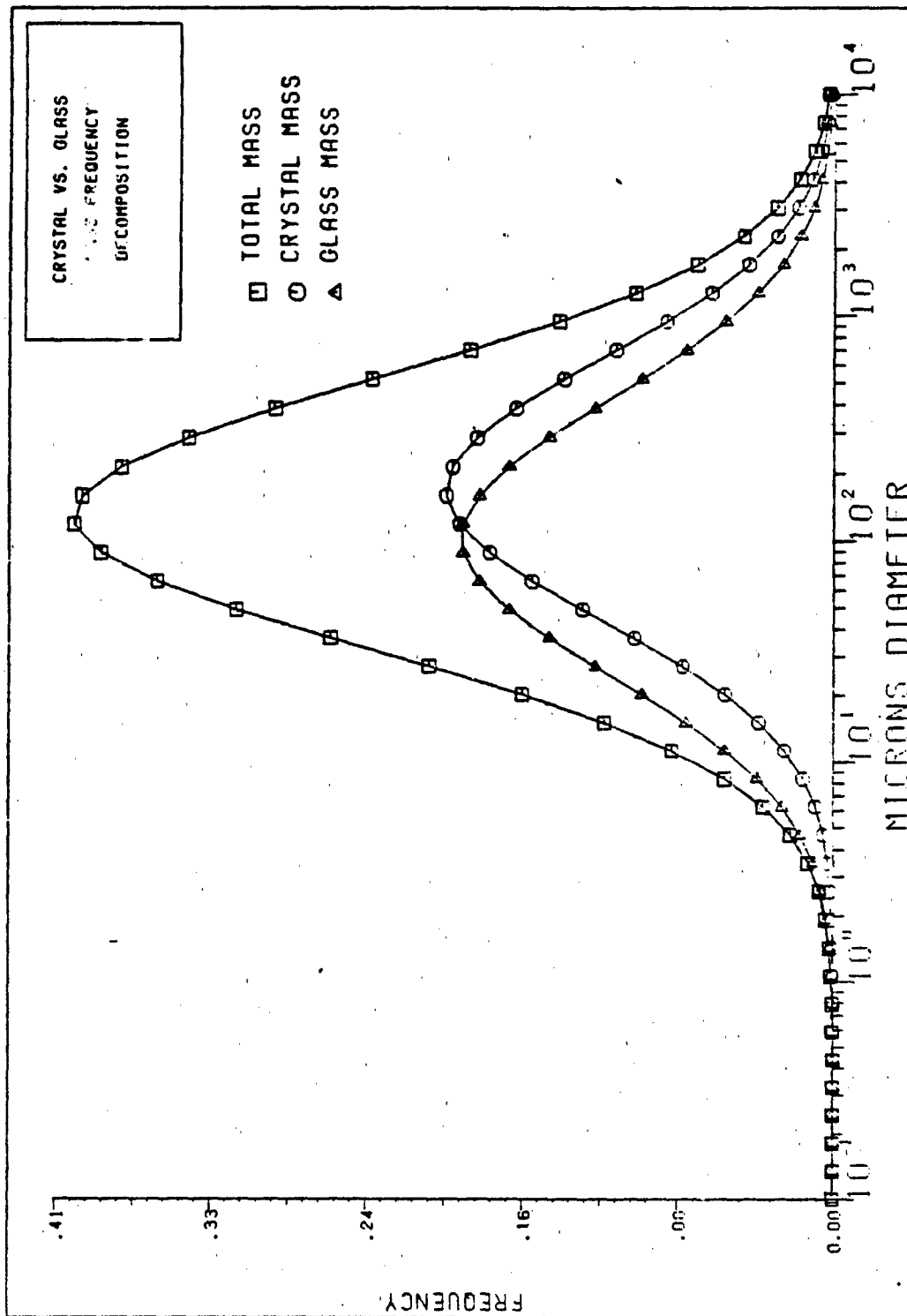


Figure 12. Decomposition of the Mass Frequency Distribution into Crystalline and Glassy Components

Miller and Yu accounted for this effect when determining the total specific activity as a function of particle size (Miller, 1967).

Determination of Diffusion Coefficients

Norman and others spent considerable effort in determining diffusion constants for various soil types (Norman, 1966-1971). The soil type of interest here is the $\text{CaO-Al}_2\text{O}_3\text{-SiO}_2$ soil which is chosen as representative of common soils.

The Arrhenius temperature dependence for diffusion coefficient may be written as

$$D = D_0 e^{-E^*/RT} \quad (114)$$

where D_0 and E^* (activation energy kcal/mole) are found empirically. Data collected by Winchell and Norman indicated a close correlation between E^* and D_0 so that if one is able to make an independent determination of one, one can compute the other with

$$\log_{10} D_0 = -5.79 + 1.23 \times 10^{-4} E^* \quad (115)$$

This relationship is known as the compensation law (Winchell, 1967: 487). As a means of estimating D_0 , one very successful method is to use the ionic radius, r , of the diffusing ionic species. This applies strictly only in the case of monovalent ionic species, but Winchell and Norman suggest using

$$\rho = 1.59 r$$

(116)

where r is the ionic radius for the most probable oxidation state in the silicate at high temperature. Table 2 lists the constants as determined using these procedures for all of the significant diffusing species. The data on ionic radii are taken from Weast (Weast, 1974).

Determination of Henry's Law Constants

Norman et al. have made numerous studies in order to determine Henry's Law constants for those atomic species of interest in fallout research (Norman, 1966-1971). The values used in this research are listed in Table 3. In several cases, no data was available. These few cases were for less important species but for completeness, estimates of the Arrhenius coefficients were made for these by comparing them with those species which demonstrated similar volatility. These cases are indicated in the table.

Theoretical Considerations

While many phenomena remain to be incorporated into any fractionation model, one which should be given attention is the apparent decrease in mixing efficiency between the hot gases in the fireball and the soil as yield increases. A hydrodynamic calculation would be required to determine the extent of this effect. Fractional condensation does not appear to be nearly as important in ground surface bursts as it is in air or tower bursts.

Table 2. Diffusion Coefficients.

Atomic No.	DC1	DC2
27	2.54	14800
28	-4.43	2400
29	2.19	14200
30	-3.3	4400
31	.65	11400
32	-1.44	7700
33	-.0237	9900
34	-2.13	6500
35	8.64	25600
36	2.01	13900
37	4.27	18200
38	2.01	13900
39	-.618	9200
40	3.16	15900
41	3.77	17000
42	.94	12500
43	.46	11100
44	-4.93	1500
45	-4.68	1900
46	3.23	16000
47	6.56	21900
48	4.83	18900
49	3.57	18300
50	2.49	15700
51	2.1	14100
52	3.3	15600
53	7.29	22500
54	3.51	16500
55	5.57	20500
56	6.91	22600
57	5.2	19500
58	4.42	18100
59	4.25	17800
60	.712	11500
61	.522	11200
62	.338	10900
63	4.68	18600
64	.005	10300
65	4.47	18200
66	-.403	9600

See text for reference citations.

Table 3. Henry's Law Coefficients.

Atomic No.	Boiling Point	HC1	HC2
27	3173	9.2	33500
28	3173	(9.2)	(33500)
29	2907	(9.7)	(33500)
30	3000	11.8	23000
31	2976	9.7	35200
32	1764	12.5	23600
33	1010	10.4	17800
34	1026	7.0	4200
35	331.8	4.0	5200
36	120.1	4.0	500
37	1656	7.0	18100
38	3497	4.4	26700
39	4695	9.4	50500
40	4808	6.7	38200
41	3300	8.5	44800
42	1351	7.6	20400
43	583	4.1	7100
44	4505	1.2	2600
45	4149	7.2	18400
46	3436	8.7	24700
47	2451	6.2	14300
48	1831	9.0	19200
49	2123	9.1	30600
50	2247	13.1	32100
51	1832	11.1	29500
52	1534	9.2	11800
53	457.4	3.8	1000
54	165.9	4.1	700
55	1555	6.6	17300
56	3003	4.8	22500
57	4608	7.3	41800
58	4367	7.0	35400
59	4252	5.7	33800
60	4464	7.6	35700
61	4348	7.3	37400
62	4300	6.7	41400
63	4300	(6.7)	(41400)
64	4300	(6.7)	(41400)
65	4300	(6.7)	(41400)
66	4300	(6.7)	(41400)

See text for references. Numbers in parentheses are estimated.

IV. Results and Discussion

Calculations were made with the standard DELFIC computer program and with the G-X Model. In addition to these, computations to generate more detailed data on mass chains 89 and 95 were made with a modification of the G-X code. The output data at the time of interest included number densities for the nuclides of interest as a function of particle size, specific activities for those nuclides as a function of particle size, total yield of those nuclides, the activity size distribution, and the dose size distribution. These raw data were then taken and $R_{1,95}$ values as a function of particle size were determined for each method. Log-log plots of $R_{1,95}$ versus $R_{89,95}$ values were then prepared and fit with linear least squares to determine the correlation slopes (Bevington, 1969:99-102).

In the plots of $R_{89,95}$ as a function of particle size (Figure 13), it is immediately obvious that the G-X method is superior to the pure Freiling method up to about 100 microns, but below about 30 microns, the Freiling-Jompkins (standard DELFIC) Model more closely matches Small Boy data. Also at large particle sizes, the G-X method is far superior to both methods. In terms of the logarithmic correlations which are popular in fractionation analysis, Tables 4 and 5 list the correlation slopes for each of the methods and compares them to Small Boy and Johnny Boy data respectively (Freiling, 1968, Crocker, 1965: 78)). In most cases the agreement between the G-X Method and the data is as good as the other methods. In the case of

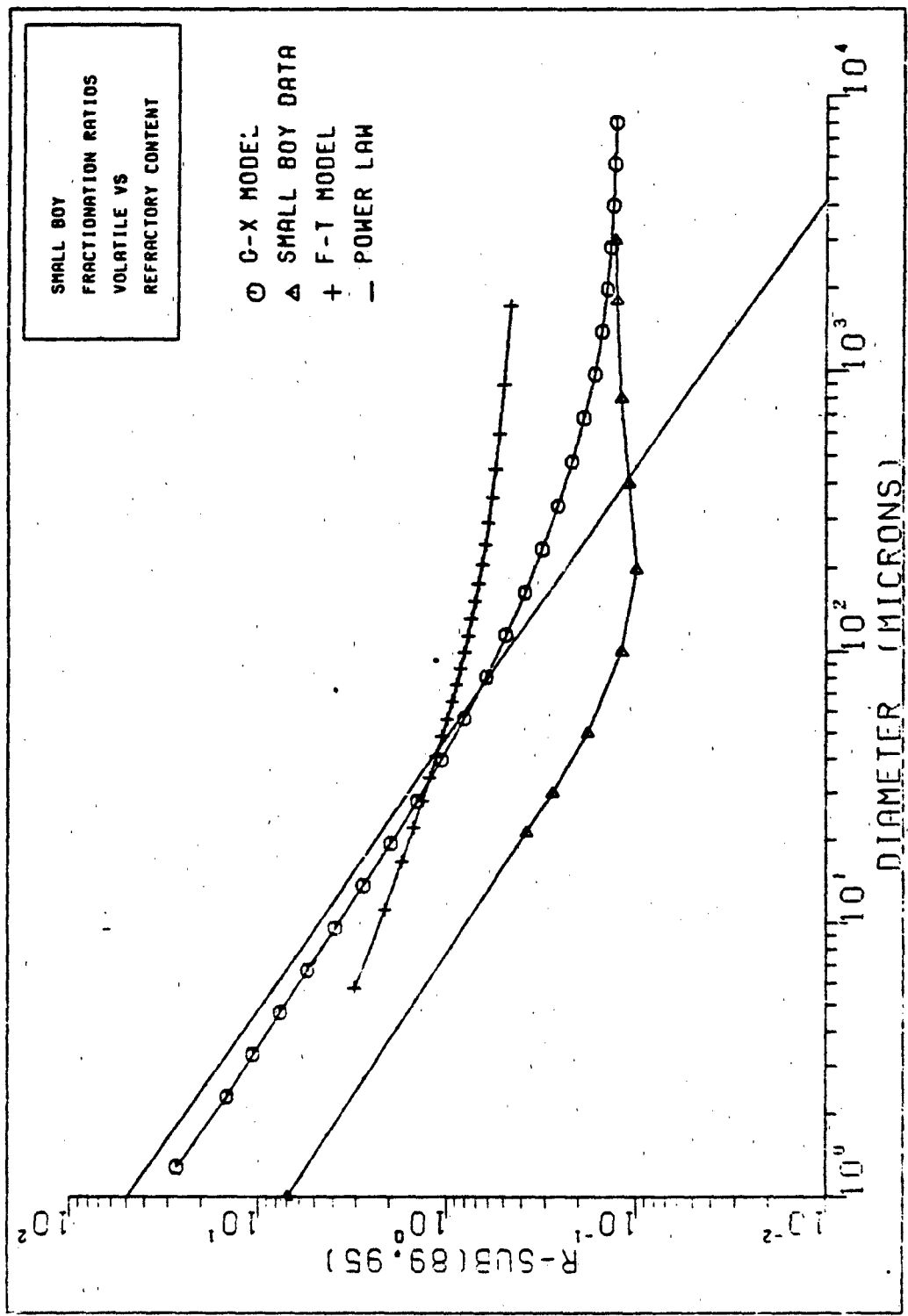


Figure 13. $R_{89,95}$ versus Particle Size for Each Method

Table 4. Logarithmic Correlation Slopes - Small Boy

Mass Chain	Small Boy	G-X	Freiling-Tomp.
89	1	1	1
90	.73	.83	-
91	.51	.64	.40
95	.0	.0	.0
99	.04	-.07	.0
131	.84	.58	.17
132	.90	.61	.31
136	.65	1.39	1.49
137	1.19	.91	1.45
140	.57	.34	.73
144	.03	-.14	.01

Table 5. Logarithmic Correlation Slopes - Johnny Boy

Mass Chain	Small Boy	G-X	Freiling-Tomp.
89	1	1	1
90	-	-	-
91	.54	.576	.422
95	.0	.0	.0
99	.017	-.028	.006
131	1.10	.459	.169
132	1.08	.491	.313
136	.83	.491	1.48
137	1.11	.916	1.45
140	.61	.304	.736
144	-.003	-.052	.022

chains 131 and 132 there is considerable improvement over the Freiling-Tompkins model. The log-log plots for both Small Boy and Johnny Boy are included in Appendices B and C, respectively. Figure 14 shows the total specific activity for the various methods along with the measured specific activity data for shot Small Boy (Miller, 1967:33). Only the G-X Model follows the drop in specific activity for the larger particle sizes. All methods predict an increase in specific activity with decreasing particle size for the smaller particles. This fact has been observed by many investigators, but accurate specific activity for the smaller particle sizes is not available, only the tendency in the data. Figure 15 shows the dose size distributions for the different methods. The comparisons indicate that the Freiling-Tompkins model underpredicts the down field dose rate while overpredicting the close in dose rate. As mentioned in the introductory chapter, this fact will have important consequences for lethality calculations.

Plots of specific activity for specified chains are also included, in Appendix D. They show clearly the effect of treating the crystalline particles separately from the glassy particles. Perhaps more striking are the plots of the concentration of ^{89}Sr and ^{95}Zr for each type of particle as a function of particle size, Figures 16 and 17. Since ^{89}Sr is a volatile species, its distribution on the crystalline particles is very similar to the distribution in the glassy particles. For ^{95}Zr , on the other hand, there is a marked drop in the concentration in the crystalline particles for the larger

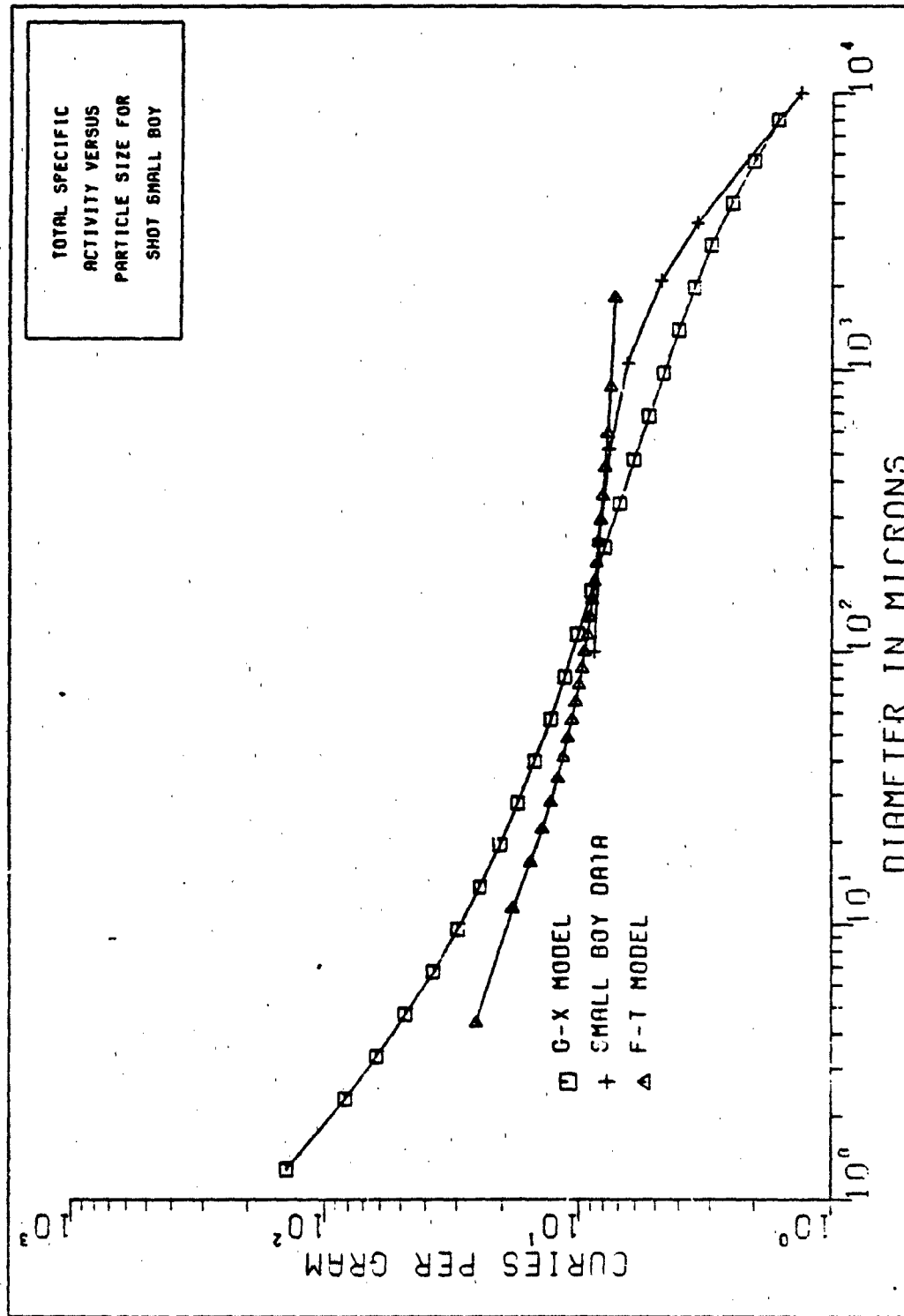


Figure 1A. Total Specific Activity Versus Particle Size for Shot Small Boy

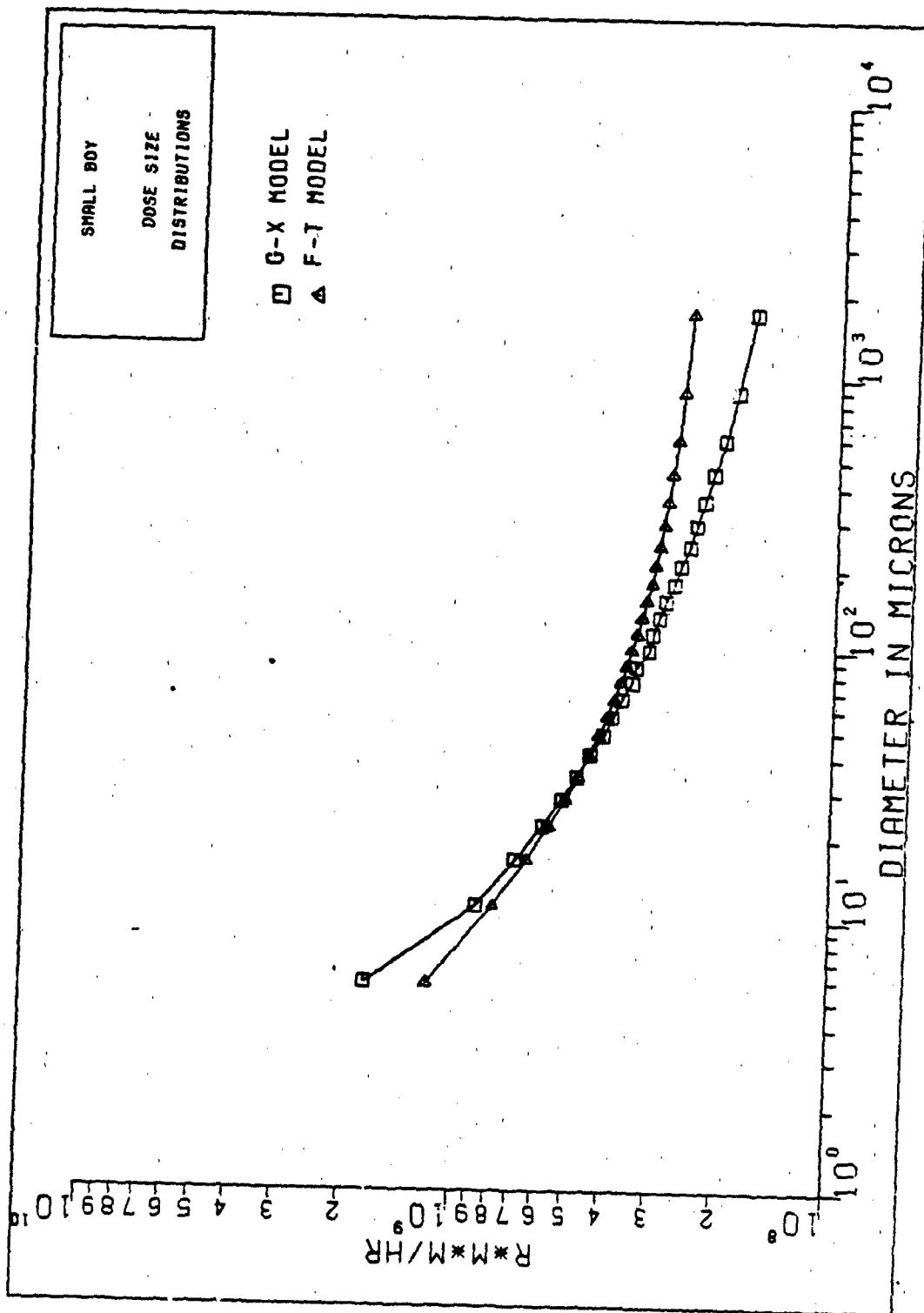


Figure 15. Dose Size Distributions for Shot Small Boy

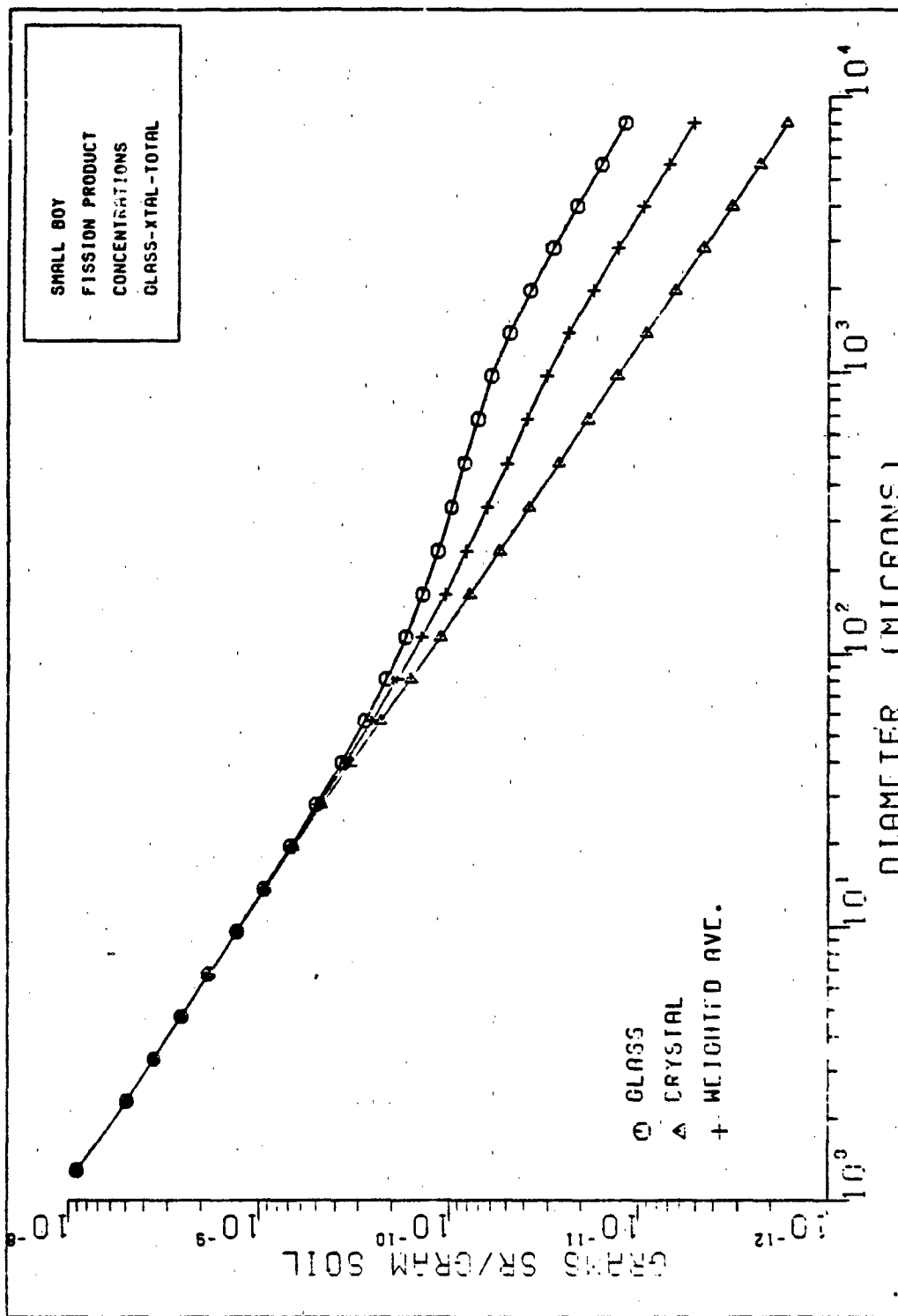


Figure 16. Strontium 90 Concentration as a Function of Particle Size for Crystalline Particles, Glassy Particles, and the Weighted Average

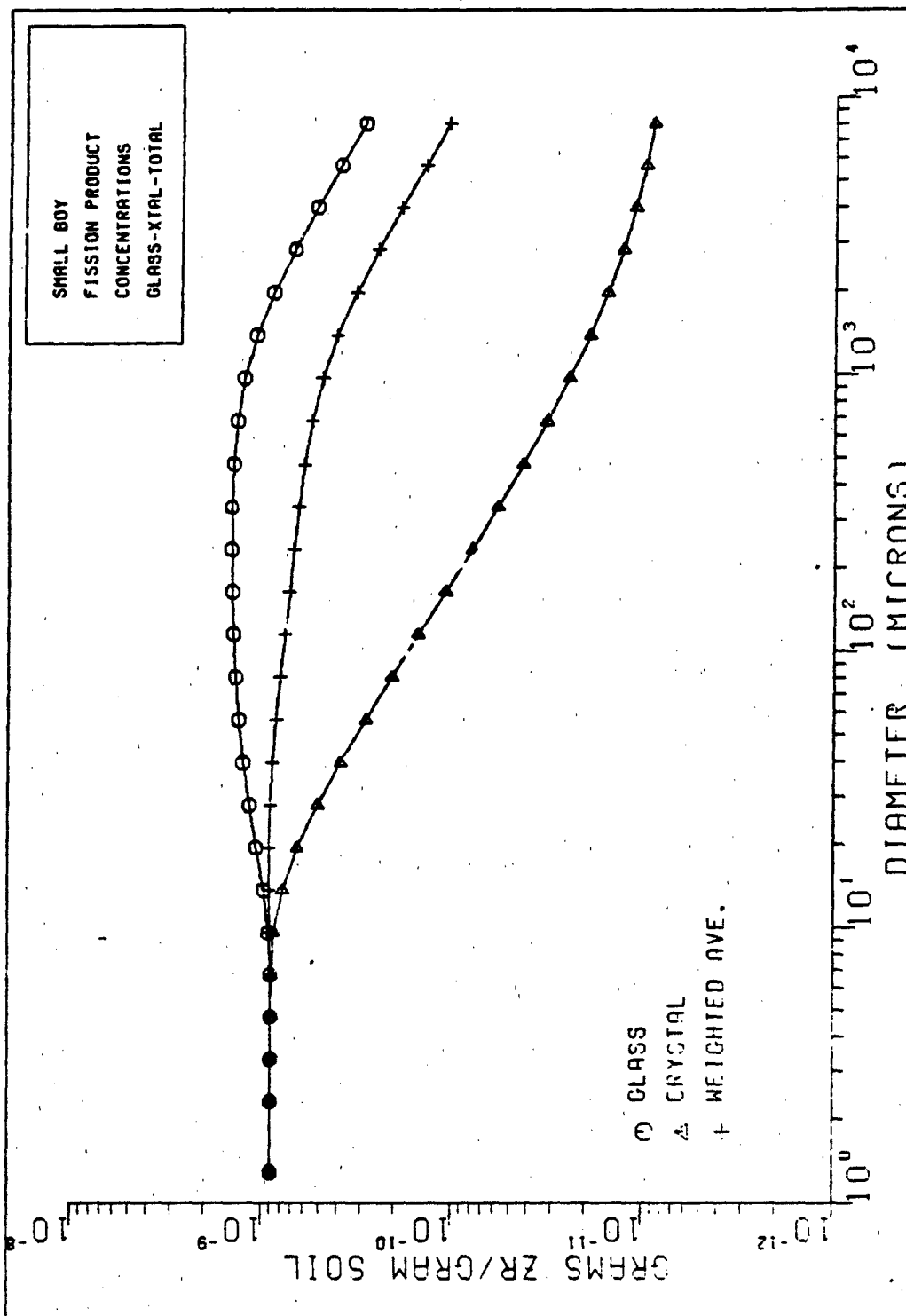


Figure 17. Zirconium 95 Concentration as a Function of Particle Size for Crystalline Particles, Glassy Particles, and the Mass Weighted Average

particle sizes. The effects of diffusion are evident at both ends of the size spectrum. For small particles, even crystalline particles permit volume loading. For large particles, diffusion into the particle interiors is time consuming and these particles cannot load uniformly with ^{95}Zr even for the glassy particles.

Figure 18 shows the total specific activity for each of the particle types. The crystalline particles show a clear surface distribution (decrease in specific activity with increasing particle size), while the glassy particles are surface distributed for small particles and very large particles and are volume distributed (constant specific activity) in the intermediate size range. The drop in specific activity for the large glass particles is probably due to the slow uptake of refractory nuclides by the spheres due to large particle size.

Figures 19 and 20 show a comparison of the observed slopes to the calculated slopes for Small Boy and Johnny Boy respectively. The error magnitudes are plotted as histogram data in Figures 21 and 22. For shot Small Boy the average error for the G-X method was .245 versus .265 for the F-T method. For shot Johnny Boy the average error was .276 for the G-X method versus .341 for the F-T method. Thus in both shots the G-X method gave better results.

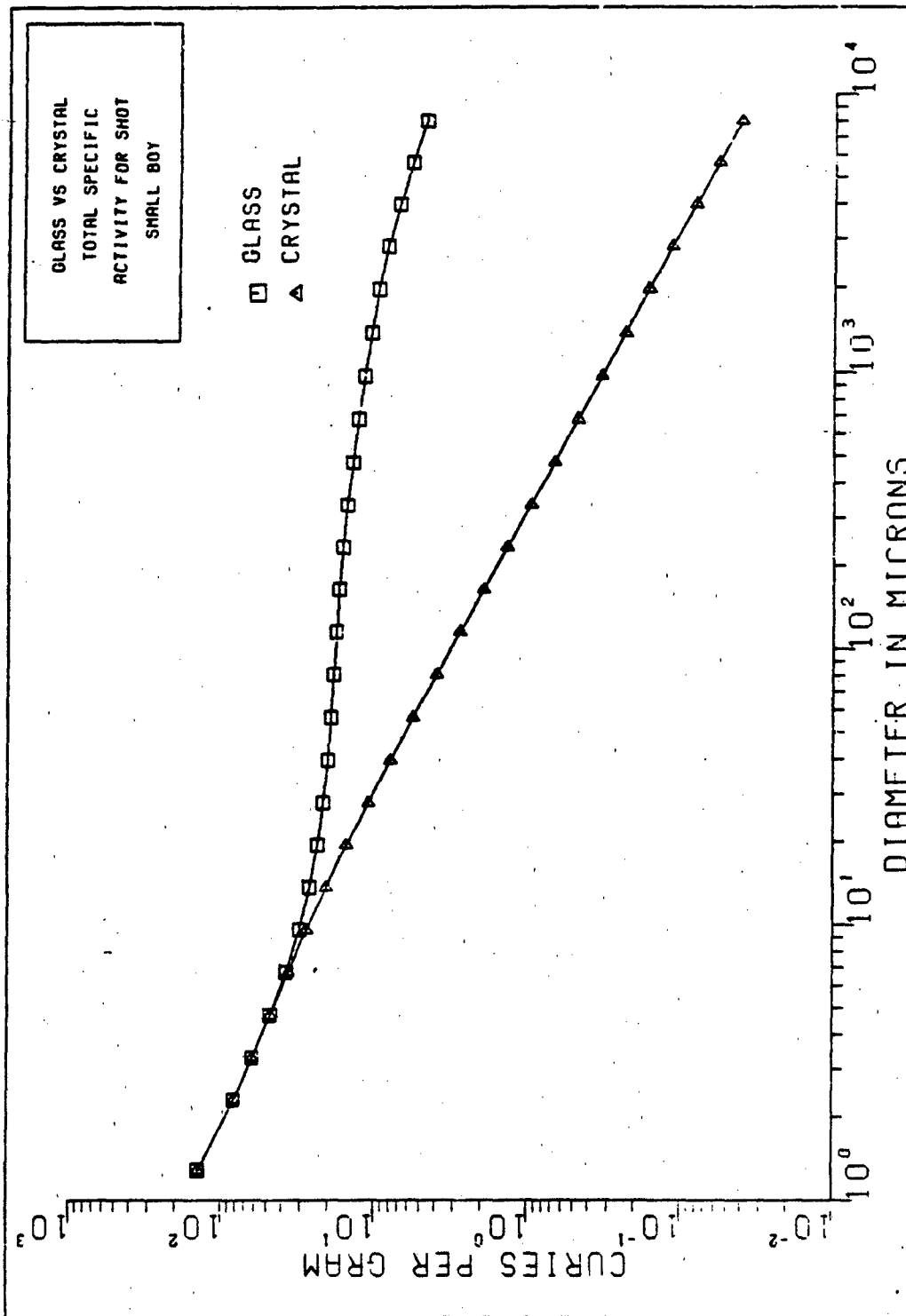


Figure 18. Total Specific Activity for Glassy and for Crystalline Particles in Shot Small Boy as Predicted by the G-X Model

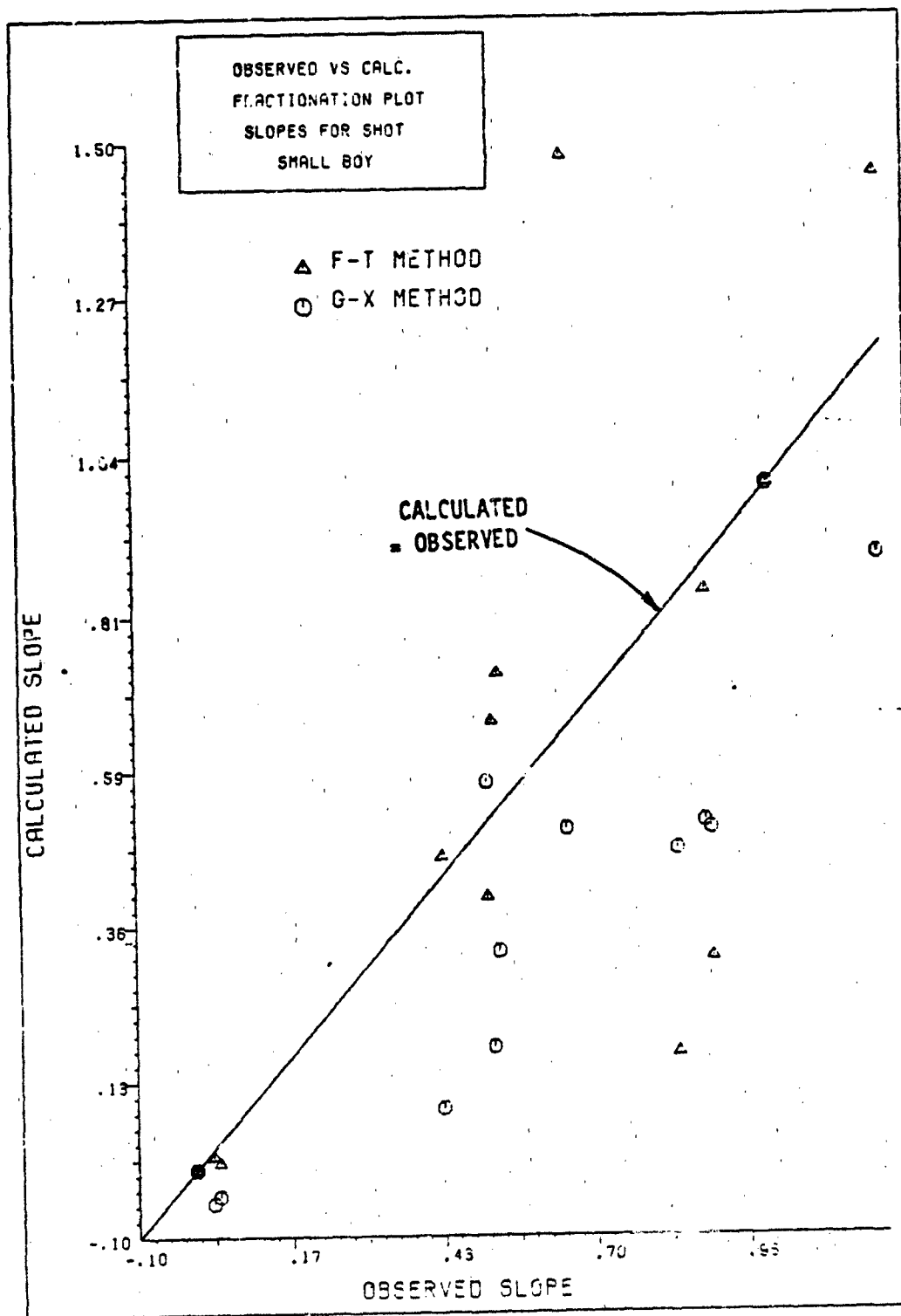


Figure 19. Observed versus Calculated Fractionation Plot.
Slopes for Shot Small Boy

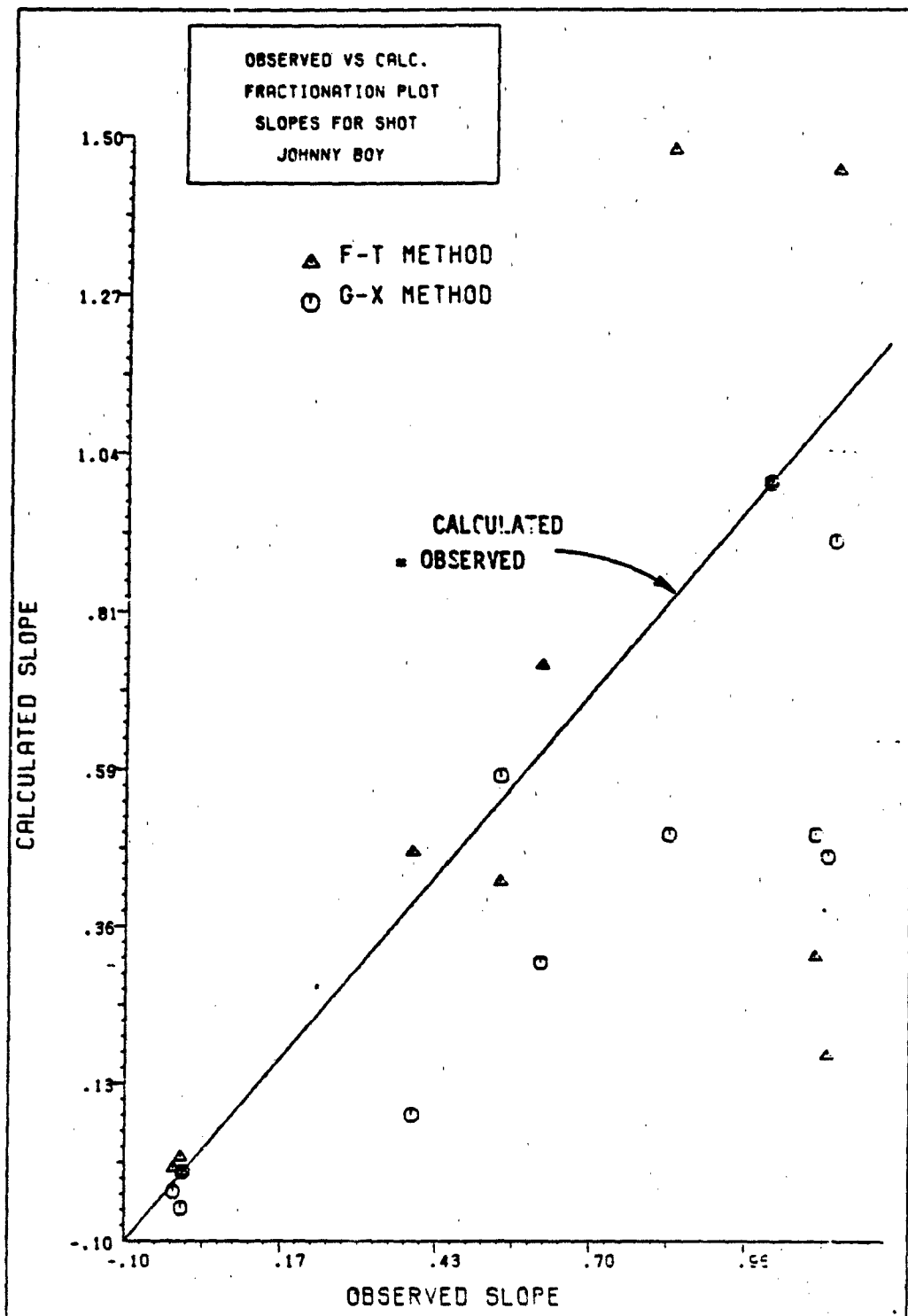


Figure 20. Observed versus Calculated Fractionation Plot
Slopes for Shot Johnny Boy

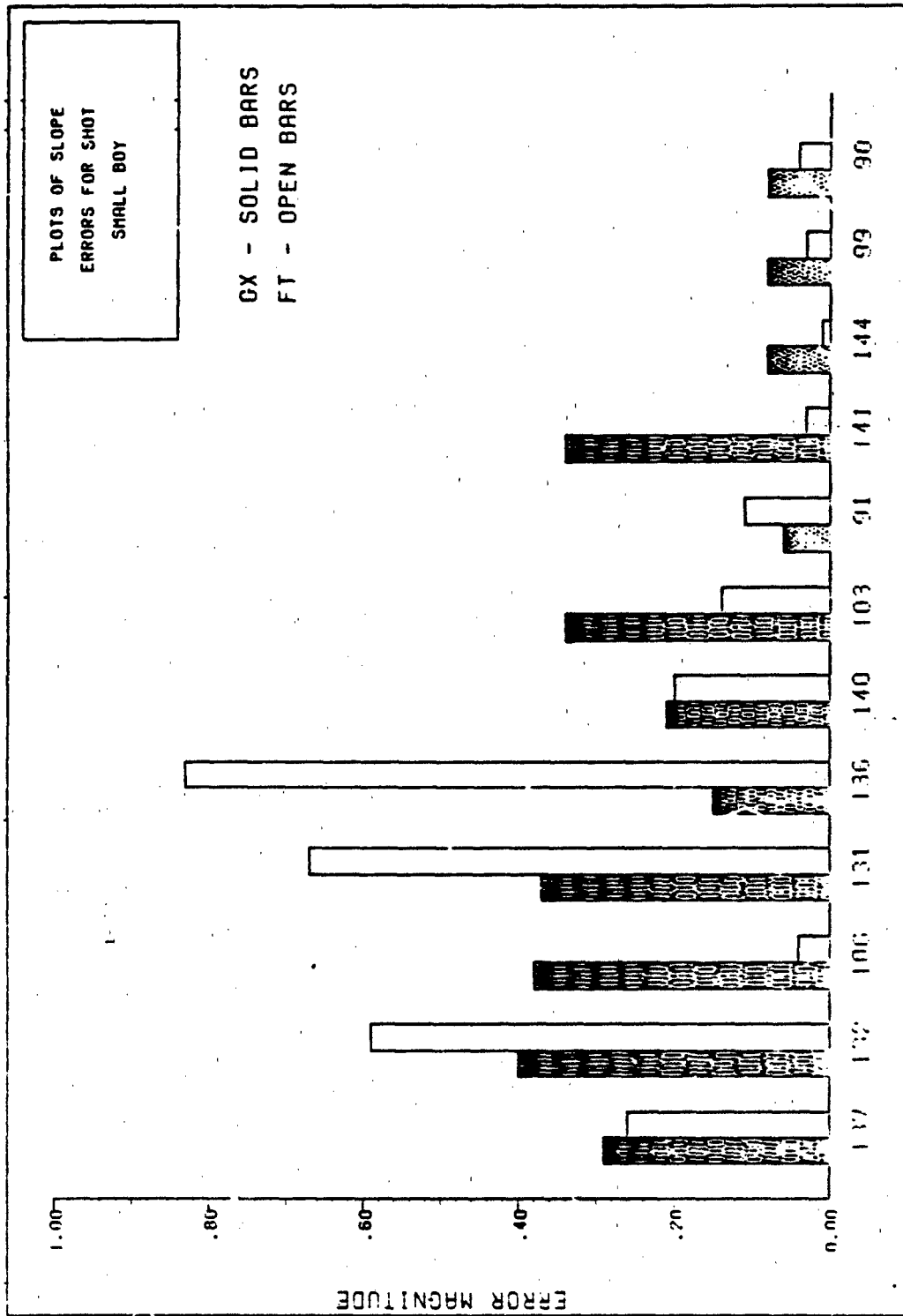


Figure 21. Fractionation Plot Slope Errors for Shot Small Boy:
Solid Bars are the G-X Model, Open Bars are the F-T Model.

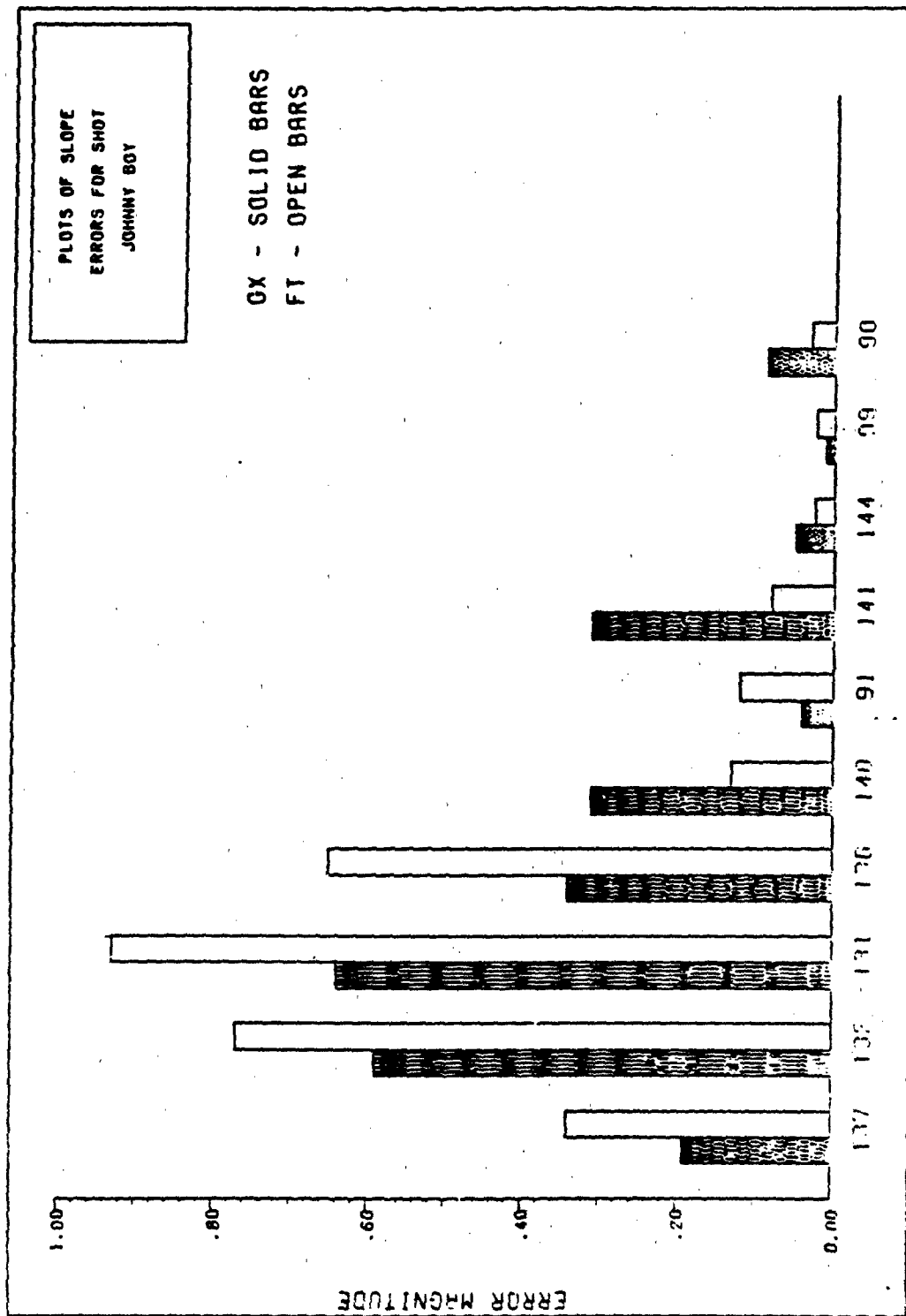


Figure 22. Fractionation Plot Slope Errors for Shot Johnny Boy:
Solid Bars are the G-X Model, Open Bars are the F-T Model

V. Conclusions and Recommendations

Conclusions

While the application of these models is restricted to ground surface bursts over silicate soils, they still have a wide range of applications. The assumptions made in developing the models are considered to be satisfactory in view of the many sources of error. As it is, the assumptions made here are somewhat less restrictive than those for the previous models, although there is still room for improvement. The success of the G-X Model for the two shots considered is very encouraging, however. While the S-V model (see Appendix A) shows promise for faster operational type codes, the G-X Model, because of the overall better performance, is the preferred one for work requiring more rigor, especially if concentrations of specific isotopes are required. The G-X Model certainly has the advantage of being based on physics rather than being an empirical fit as is the radial power model.

Recommendations

There are a number of areas which need further work in the fallout area. If one were intent on doing the problem correctly, all of the following things would need to be done:

- (1) The particle size distribution needs to be determined dynamically from early time in the fireball to include the partition

between solid, liquid, and gas. Emphasis should be placed on determining the extent and effect of agglomeration.

(2) The degree of mixing of the fission products with the soil carrier as a function of time and location in the hot toroid should be determined.

(3) Henry's Law constants and diffusion coefficients need to be measured for a variety of soil types.

(4) Interdiffusion coefficients for the diffusion of the fission product gases through the air to the surfaces of the soil particles should be determined.

(5) Surface attachment coefficients for each important compound need to be measured.

(6) An investigation of fall rates for different particle types needs to be done.

(7) Work on the effect of fractional condensation and compound formation by fission product oxides with the carrier material should be investigated.

(8) More information is needed on the thermal stability of the fission product oxides.

(9) And finally, work needs to be done on the influence of water on the reaction balances.

If, on the other hand, one is more concerned with improving the faster running, so-called "smear" codes, this can be accomplished by several techniques: One is to simply take the S-V Model of fractionation and determine decay rates for each of the components

(surface activity and volume activity). Alternatively, one could follow only those chains which make the largest contribution to the surface and volume components of the activity and distribute that activity using the S-V Model. Then the result could be normalized so that the combined total activity agrees with that which would be computed by the Way-Wigner formula. Either of these two techniques would allow for an explicit calculation of fractionation effects in a code such as the Air Force Institute of Technology model (Bridgman, 1982).

Finally, the G-X Model could be used in a parametric study of yield and fuel type (and perhaps other parameters) to determine a new set of activity size distributions for SEER, LASEER, PROFET, and KDFOC which are all derived from DELFIC calculations. These codes do not do explicit particle activity calculations but rather rely on fits of DELFIC calculations.

BIBLIOGRAPHY

- Adamson, A. W. A Textbook of Physical Chemistry. New York: Academic Press, July 1973.
- Batten, E. S., D. L. Iglehard, and R. R. Rapp. "Derivation of Two Simple Methods for the Computing of Radioactive Fallout." Santa Monica, California: The Rand Corporation, 18 February 1960. (RM 2460; AD 237 788).
- Benck, R. F. "The Mechanisms of Fallout Particle Formation: Annual Progress Report for Period ending June 1971." BRL-MR-2304. USA Ballistic Research Labs, June 1973. (AD 763 196).
- Bevington, P. R. Data Reduction and Data Analysis for the Physical Sciences. New York: McGraw Hill Book Co., 1969.
- Bridgman, C. J., and W. S. Bigelow. "A New Fallout Prediction Model," Health Physics, 43:205-218, 1982.
- Carslaw, H. S., and J. C. Jaeger. Conduction of Heat in Solids (Second Edition). Oxford: Clarendon Press, 1959.
- Cassidy, S. H. "Sensitivity Analysis of the Radial Distribution Model. Sensitivity to Carrier Material, Yield, and Type of Fission." USNRDL-TR-67-70. San Francisco: U.S. Naval Radiological Defense Laboratory, 22 May 1967. (AD-658-327).
- Chan, H. K. "Activity-size Relationship of Fallout particles from Two Shots, Operation Redwing." USNRDL-TR-314. San Francisco: U.S. Naval Radiological Defense Laboratory, 19 February 1959. (AD-233-607)
- Clark, R. S. "Time Interval Between Nuclear Detonation and Formation of Single Fallout Particles," Journal of Geophysical Research, 72:1793-1796, 15 March 1967.
- Crank, J. The Mathematics of Diffusion. Oxford: Clarendon Press, 1975.
- Crocker, G. R. "Estimates of Fission Product Yields of a Thermonuclear Explosion." USNRDL-TR-642. San Francisco: U.S. Naval Radiological Defense Laboratory, 4 April 1963.
- , et al. "Physical and Radiochemical Properties of Fallout Particles." USNRDL-TR-899. San Francisco: U.S. Naval Radiological Defense Laboratory, 15 June 1965. (AD 623-485).

- , F. K. Kawahara, E. C. Freiling. "Radiochemical Data Correlations on Debris from Silicate Bursts," Radioactive Fallout from Nuclear Weapons Tests, Proceedings of the Second Conference, Germantown, Maryland, November 1965. (CONF-765).
- Drinkwater, R. B. "Gamma Radiation from Fission Products." Unpublished MS thesis. Air Force Institute of Technology, Wright-Patterson AFB, Ohio, March 1979. (AD 777 842).
- Dunn, C. D. "Operation Roller Coaster, Project Officer's Report - Project 2.6c: Special Particulate Characteristics," FOR-2508 (WT-2508). Richmond, California: Tracerlab, 17 September 1965. (AD 470 140).
- Freiling, E. C. "Radionuclide Fractionation in Bomb Debris," Science, 133:1991-1998 (June 1961).
- , "Fractionation II. On Defining the Surface Density of Contamination." USNRDL-TR-631. San Francisco: U.S. Naval Radiological Defense Laboratory, 13 March 1963. (AD 402 293).
- , "Fractionation III. Estimation of Degree of Fractionation and Radionuclide Partition for Nuclear Debris." USNRDL-TR-680. San Francisco: U.S. Naval Radiological Defense Laboratory, 12 September 1963 b. (AD 423 725).
- , et al. "Fractionation IV. Illustrative Calculations of the Effect of Radionuclide Fractionation on Exposure-dose Rate from Local Fallout." USNRDL-TR-715. San Francisco: U.S. Naval Radiological Defense Laboratory, 6 January 1964.
- and M. A. Kay. "Radionuclide Fractionation in Air-Burst Debris." USNRDL-TR-933. San Francisco: U.S. Naval Radiological Defense Laboratory, 20 September 1965. (AD 626 608).
- , G. R. Crocker, and C. E. Adams. "Nuclear Debris Formation," Radioactive Fallout from Nuclear Weapons Tests, U.S. Atomic Energy Commission/Division of Technical Information, November 1965 b. (CONF-765).
- , "A Comparison of the Fallout Mass-Size Distributions Calculated by Lognormal and Power-Law Models." USNRDL-TR-1105. San Francisco: U.S. Naval Radiological Defense Laboratory, 14 November 1966. (AD 646 019).
- and G. R. Crocker. "Radiochemical Data Correlations for Small Boy. I. Selection, Adjustment and Condensation of Data." NRDL-TR-68-140. San Francisco: U.S. Naval Radiological Defense Laboratory, 28 June 1968. (AD 848 228).

- , "Mass-Transfer Mechanisms in Source-Term Definition," Radionuclides in the Environment, Advances in Chemistry Series No. 93. Washington, D.C.: American Chemical Society, 1970.
- , Naval Surface Weapons Center. Private communication, September 1981.
- Glasstone, S. and P. J. Dolan, Eds. The Effects of Nuclear Weapons (Third Edition). Washington, D.C.: United State Department of Defense and the United States Department of Energy, U.S. Government Printing Office, 1977.
- Hawthorne, H. A. "Compilation of Local Fallout Data from Test Detonations 1945-1962 Extracted from DASA 1251-1-EX. Washington, D.C.: Defense Nuclear Agency 1 May 1979. (AD A079 309).
- , "Compilation of Local Fallout Data from Test Detonations 1945-1962 Extracted from DASA 1251, Volume II - Oceanic U.S. Tests." DNA-1251-2-EX. Washington, D.C.: Defense Nuclear Agency 1 May 1979. (AD A079 310).
- Heft, R. E. "The Characterization of Radioactive Particles From Nuclear Weapons Tests." Radionuclides in the Environment, Advances in Chemistry, Series No. 93. Washington, D.C.: American Chemical Society, 1970.
- Hicks, H. G. "Calculation of the Concentration of Any Radionuclide Deposited on the Ground by Offsite Fallout from a Nuclear Detonation." UCRL-86177. Livermore, California: Lawrence Livermore National Laboratory, June 1981.
- , Lawrence Livermore National Laboratory. Private communication, March 1982.
- Holmberg, B. and S. Andersson. "Fractionation Phenomena in the Explosion Cloud." FOA 4 Report C 4351-28. Sweden, April 1968. (AD 853 745).
- Izrael, Yu. A. "Formation of Radioactive Particles During Nuclear Bursts in the Troposphere." Radioaktivnye Vypadeniya ot Yademykh Vzryvov. Moskow: "Mir.", 1968.
- , "Calculation of Fractionation Effects in Atmospheric Nuclear Bursts," Obrazovanie Radioaktivnykh Chastits Pri Yadernykh v Tropofere. Moskow: "Mir.", 1968 b.
- Kawahara, F. K., et al. "Fallout From Nuclear Cratering Shot Danny Boy, I. Radiochemical Analysis and Some Physical Observations

- on Selected Samples," USNRDL-TR-67-90. San Francisco: U.S. Naval Radiological Defense Laboratory, 3 July 1967. (AD 820 627).
- Klement, A. W., Jr., Ed. Radioactive Fallout from Nuclear Weapons Tests, Proceedings of the Second Conference, Germantown, Maryland. Oak Ridge: USAEC Division of Technical Information, November 1965. (CONF-765).
- Korts, R. F., and J. H. Norman. "A Computational Model for Condensed State Diffusion Controlled Fission Product Absorption During Fallout Formation." GA-7598. San Diego, California: General Atomic, 10 January 1967. (AD 651 755).
- Lai, J. R., and E. C. Freiling. "Interdiffusion Constants of Vapor Species of Fission Products and Uranium and their Oxides in Air: Preliminary Estimations at 500 Degrees to 2500 Degrees Kelvin." NRDL-TR-69-45. San Francisco: U.S. Naval Radiological Defense Laboratory, 10 June 1969. (AD 854 727).
- Lane, W. B. "Project Sedan: Some Radiochemical and Physical Measurements of Debris from an Underground Nuclear Detonation." PNE-299F. San Francisco: U.S. Naval Radiological Defense Laboratory, 6 July 1962. (AD 690 483).
- Layson, W. M. Science Applications Incorporated, McLean, Virginia, private communication to J. McGahan (also with SAI).
- Lee, H., P. W. Wong, and S. L. Brown. "Simplified Fallout Computational Systems for Damage Assessment." DASA-2690. Menlo Park, California: Stanford Research Institute, July 1971. (AD 727 636).
- Lederer, C. M., et al. Table of Isotopes. New York: John Wiley and Sons, Inc., 1967.
- Levine, J. D., and E. P. Gyftopoulos. "Adsorption Physics of Metals Partially Covered by Metallic Particles. II. Desorption Rates of Atoms and Ions," Surface Science, 1:225-241 (1964).
- Mackin, J. L., et al. "Radiochemical Analysis of Individual Fallout Particles." USNRDL-TR-386. San Francisco: U.S. Naval Radiological Defense Laboratory, 17 September 1958. (AD 232 901).
- and S. Z. Mikhail. "A Discussion of the State of the Art in Fallout Research." OCD Project No. 3100. San Francisco: U.S. Naval Radiological Defense Laboratory, 7 December 1965. (AD 484 959).

- Malonel, J., Ballistic Research Laboratories, U.S. Army, Aberdeen Research and Development Center, Aberdeen, Maryland, private communication to J. McGahan of Science Applications, Inc., McLean, Virginia, 1974.
- Mamuro, T., et al. "Radionuclide Fractionation in Fallout Particles from a Land Surface Burst," Journal of Geophysical Research, 74:1374-1387 (15 March 1969).
- McDonald, J. W., and J. B. Reid. "Crater, Ejecta and Ground Motion Calculations for Johnnie Boy." DNA-3168T. Sherman Oaks, California: Whittaker Corporation, 22 January 1974. (AD 529 116).
- McGahan, J. T. "Sensitivity of Fallout Predictions to Initial Conditions and Model Assumptions." SAI-74-548-WA. McLean, Virginia: Science Applications, Inc., December 1974. (AD A002 464).
- Meek, M. E., and B. F. Rider. "Compilation of Fission Product Yields." NEDO-12154-1. Pleasanton, California: Vallecitos Nuclear Center, 26 January 1974.
- Miller, C. F. "A Theory of Formation of Fallout from Land Surface Nuclear Detonations and Decay of the Fission Products." USNRDL-TR-425. San Francisco: U.S. Naval Radiological Defense Laboratory, 27 May 1960. (AD 241 240).
- "Fallout and Radiological Counter-Measures." SRI Project No. IM-4021. Menlo Park, California: Stanford Research Institute, January 1963. (AD 410 522).
- "Biological and Radiological Effects of Fallout from Nuclear Explosions." SRI Project No. IMU-4536 (OCD Subtask No. 3110A). Menlo Park, California: Stanford Research Institute, March 1964. (AD 476 572).
- and O. S. Yu. "The Mass Contour Ratio for Fallout and Fallout Specific Activity for Shot Small Boy." TRC-68-15. Menlo Park, California: Stanford Research Institute, December 1967. (OCD Work Unit 3119A, AD 677 403).
- "Some Properties of Radioactive Fallout: Tower Detonations Diablo and Shasta." URS 757-3, August 1969. (AD 699 420).
- Nathans, M. W. "The Specific Activity of Nuclear Debris from Ground Surface Bursts as a Function of Particle Size," Radionuclides in the Environment, Advances in Chemistry Series No. 93. Washington, D.C.: American Chemical Society, 1970.

- Nethaway, D. R., and G. W. Barton. "A Compilation of Fission Product Yields in Use at the Lawrence Livermore National Laboratory." UCRL-51458. Livermore, California: Lawrence Livermore National Laboratory, 3 October 1973.
- Norman, J., and P. Winchell. "Cloud Chemistry of Fallout Formation." Proceedings/Part I, Fallout Phenomena Symposium, April 12-14, 1966. USNRDL-R&L-177. San Francisco: U.S. Naval Radiological Defense Laboratory, 9 June 1966. (AD 488 164).
- "Henry's Law Constants for Dissolution of Fission Products in a Silicate Fallout Particle Matrix." GA-7058 (OCD Work Unit 3111A). San Diego, California: General Atomic, 29 December 1966 b. (AD 645 943).
- and P. Winchell. "Cloud Chemistry of Fallout Formation, Final Report." GA-7597 (OCD Work Unit 3111A). San Diego, California: 13 January 1967. (AD 814 721).
- and H. G. Staley. "Cloud Chemistry of Fallout Formation, Final Report." GA-8472 (OCD Work No. 3111A). San Diego, California: Gulf General Atomic, 31 January 1968. (AD 832 727).
- et al. "Cloud Chemistry of Fallout Formation, Final Report." GA-9180 (OCD Work No. 3111A T.O. No. 3110(68)). San Diego, California: Gulf General Atomic, 15 January 1970. (AD 707 427).
- et al. "Spheres: Diffusion-Controlled Fission Product Release and Absorption," Radionuclides in the Environment, Advances in Chemistry Series No. 93. Washington, D.C., American Chemical Society, 1970.
- , P. Pinchell, and S. J. Black. "Chemical Phenomena of Fallout Formation, Final Report." Gulf-GA-A10761 (Work Unit 3111C). San Diego, California: Gulf General Atomic, 5 November 1971. (AD 734 369).
- Gulf General Atomic. Private communication, July 1982.
- Norment, H. G. "Department of Defense Land Fallout Prediction System, Volume I. System Description." TO-B 66-40. Bedford, Massachusetts: Technical Operations Research 27 June 1966. (AD 483 897, DASA 1800-1).
- et al. "Department of Defense Land Fallout Prediction System. Volume II - Initial Conditions." Bedford, Massachusetts: Technical Operations Research, 30 September 1966 b. (AD 803 144).

----- DELFIC: Department of Defense Fallout Prediction System, Volume II - User's Manual." DNA5159F-2. Bedford, Massachusetts: Atmospheric Science Associates, 31 December 1979 b. (AD A088 512).

Pascual, J. N. "Bias in Fallout Data from Nuclear Surface Shot Small Boy: An Evaluation of Sample Perturbation by Sieve Sizing." USNRDL-TR-67-88. San Francisco: U.S. Naval Radiological Defense Laboratory, 26 June 1967. (AD 820 147).

----- and E. C. Freiling. "Fractionation Versus Particle Type in Nuclear Surface Shot Small Boy. Differences in Radiochemical Composition Between Fritter and Spheroidal Particles." USNRDL-TR-67-116. San Francisco: U.S. Naval Radiological Defense Laboratory, 2 July 1967. (AD 660 655).

Pavlotskaya, F. I., et al. "State of Strontium-90, Cesium-137, and Cerium-144 in Radioactive Fallout," Radioaktivnye Vypadeniya ot Yademykh Vzryvov. Moscow: "Mir.", 1968.

Proceedings, Part 1: Fallout Phenomena Symposium. Monterey, California: Naval Postgraduate School, April 1966. (AD 488 164).

Project Rand: Close-in Fallout. R-309. Santa Monica, California: The Rand Corporation, 30 September 1957. (AD 150 662).

Pugh, G. E., and R. J. Galiano. "An Analytic Model of Close-In Deposition of Fallout for Use in Operational-Type Studies." Washington, D.C.: Weapon System Evaluation Group, 15 October 1959. (WSEG-RM-10).

Radionuclides in the Environment, Advances in Chemistry Series - No. 93. Washington, D.C.: American Chemical Society, 1970.

Sherwood, R. D. "Operation Roller Coaster, Project Officer's Report - Project 2.6b: Special Particulate Analysis." POR-2507 (WT-2507). Richmond, California: Tracerlab, 26 May 1966. (AD 486 477).

Silker, W. B., and C. N. Thomas. "Fractionation of Radionuclides During Nuclear Testing." BNWL-1051 Pt-2 (UC-48), 1968.

Tompkins, R. C. "Department of Defense Land Fallout Prediction System, Volume V - Particle Activity." NDL-TR-102. Edgewood Arsenal, Maryland: U.S. Army Nuclear Defense Laboratory, February 1968. (DASA 1800-V).

- , I. J. Russell, and M. W. Nathans. "A Comparison Between Cloud Samples and Close-In Ground Fallout Samples from Nuclear Ground Bursts," Radionuclides in the Environment, Advances in Chemistry Series No. 93, Washington, D.C.: American Chemical Society, 1970.
- Trullo, J. G. "Calculations of Device-Air-Ground Interaction in a Scaled Smallboy Burst. DNA-3405F. Washington, D.C.: Defense Nuclear Agency 17 December 1974. (AD C000 933).
- Weast, R. C., Ed. Handbook of Chemistry and Physics. Cleveland: CRC Press, The Chemical Rubber Company, 55th Edition, 1974.
- Winchell, P., and J. H. Norman. "A Study of the Diffusion of Radioactive Nuclides in Molten Silicates at High Temperatures," High Temperature Technology, Proceedings of the Third International Symposium, Asilomar, California, 1967.
- Winegardner, D. K. "Department of Defense Land Fallout Prediction System, Volume VII - Operator's Manual." DASA 1800-VII, NDL-TR-104, April 1968. (AD 836 871L).
- , "PROFET: A Rapid Method for Generating Fallout Predictions from Field Data." NDL-TR-124. Edgewood Arsenal, Maryland: U.S. Army Nuclear Defense Laboratory May 1969. (AD 852 969).

Appendix A

The S-V Model

Introduction

Because of the ease and speed with which a model developed by the Air Force Institute of Technology (Bridgman, 1982) can be used, and because the Air Force Institute of Technology (AFIT) model has the potential for accounting for fractionation in an explicit manner, the first model developed as part of this research was one which would allow direct adaptation for use with the AFIT model. The new model described here will be termed the S-V model because it separates the activity size distribution into surface and volume distributed components.

Model Description

The S-V model is a modification of Miller's method. The method is implemented by first computing the time at which the cloud would reach the soil solidification temperature. The fission product inventory is then calculated at the time of soil solidification using rigorous computations with the Bateman equations. After that, the amount of soil in the active region of the cloud is computed along with cloud volume. Next, the amount of material which will dissolve into a bulk liquid soil at that temperature is computed using Henry's Law (these calculations are discussed in the next sub-section). This

portion of the fission product inventory is then saved temporarily in a large array. Those fission products which remained in the gas phase are also saved in another array. The Bateman equations are solved again to compute the decay of the solid phase fission products in the first array to the time of interest, taken here to be $H + 1$ hour. Those decay products, regardless of their volatility, are assumed to be locked into a solid matrix and are distributed uniformly throughout the volume of the fallout particles.

Next the second array, representing the gas phase at soil solidification, is allowed to decay to $H + 1$. These fission products are then distributed according to the distribution of surface area for the fallout particles. The assumption here is that the particles are now solid and will not absorb any more fission products but may adsorb them. A further assumption is that no particles leave the cloud until all fission products have been absorbed. A refinement of the method allows the last assumption to be relaxed and is discussed in the recommendations.

Discussion

The model, while it is very simplistic, does account in a direct way for the major processes involved in particle formation. Its major drawbacks are that it does not account for the presence of crystalline particles nor for the fact that larger particles will leave the active region of the cloud earlier due to centrifugal or gravitational forces. But because the model divides the fission product inventory

into a surface distributed component and a volume distributed component, it can be used to develop a number of composite activity size distributions for the AFIT model. More specifically, if $S(d)$ is the distribution of activity on the surfaces of the particles and $V(d)$ is the distribution of activity inside of the particles, and if the particle size distribution $N(d)$ is taken to be lognormal, then the total activity size distribution takes on a very powerful form because of the properties of the lognormal distribution. Surface area is distributed as the second moment of the particle size distribution and volume is distributed as the third moment of the particle size distribution. Thus the total activity size distribution becomes

$$A(d) = A_s S(d) + A_v V(d) \quad (A-1)$$

or

$$A(d) = A_s \text{LN}(\alpha_2, \beta) + A_v \text{LN}(\alpha_3, \beta) \quad (A-2)$$

where

A_s = the surface distributed activity

A_v = the volume distributed activity

$\text{LN}(\alpha_j, \beta)$ = the lognormal distribution with median α_j and standard deviation β

and

$$a_n = a_0 + nb^2 \quad (A-3)$$

is the median for the n-th moment of the particle size distribution. Since the two parts of the distribution have their activity computed separately, this allows for two K-factor constants (these are used to convert from activity to dose rate) to be computed at the time of interest. The effect of this is to allow for differences in the average energy of emission for the two groups. In addition, the decay is usually computed with the Way-Wigner formula which is approximately correct for fission products taken as a whole, but when the debris is fractionated, this method is no longer applicable. Freiling has shown that at late time there is considerable difference between the rates of decay for the two groups (Freiling, 1964: 7-10). This formulation allows for separate approximate rates of decay (perhaps curve fits from a parametric study) to be used for each group.

Appendix B

$R_{i,j}$ Plots for Small Boy

This appendix includes fractionation plots for all chains for which data is available in the literature (Crocker, 1965: 72-81). The nuclides used for radiochemical analysis are as follows:

137	Cs
89	Sr
132	Te
106	Ru
131	I
136	Cs
140	Ba
103	Ru
91	Y
141	Ce
144	Ce
99	Mo
95	Zr
90	Sr

Least squares fits to the test data are shown on the plots as the solid straight lines. Mass chains 89 and 95 are reference chains.

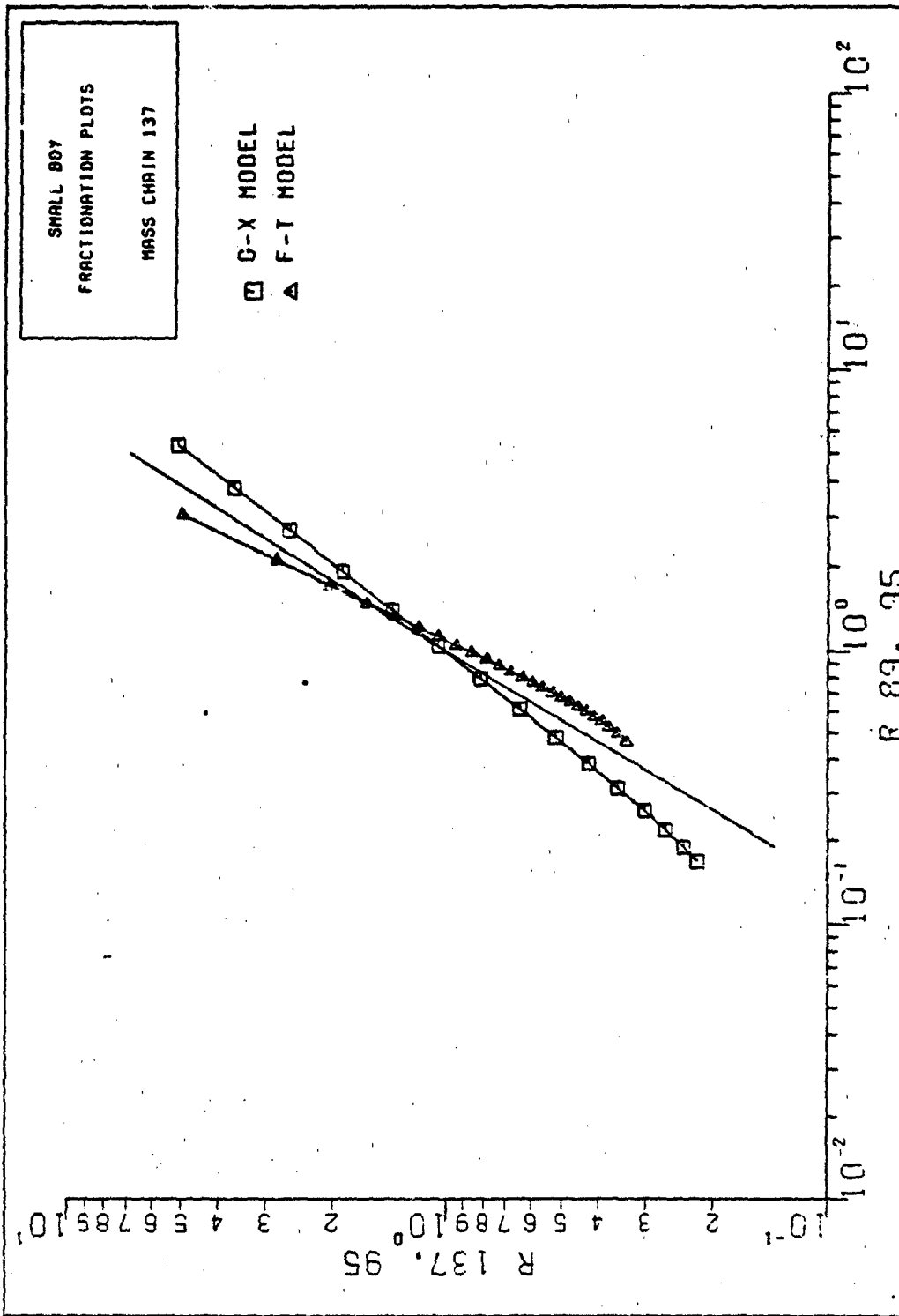


Figure 23. Small Boy Fractionation Plots: Mass Chain 137

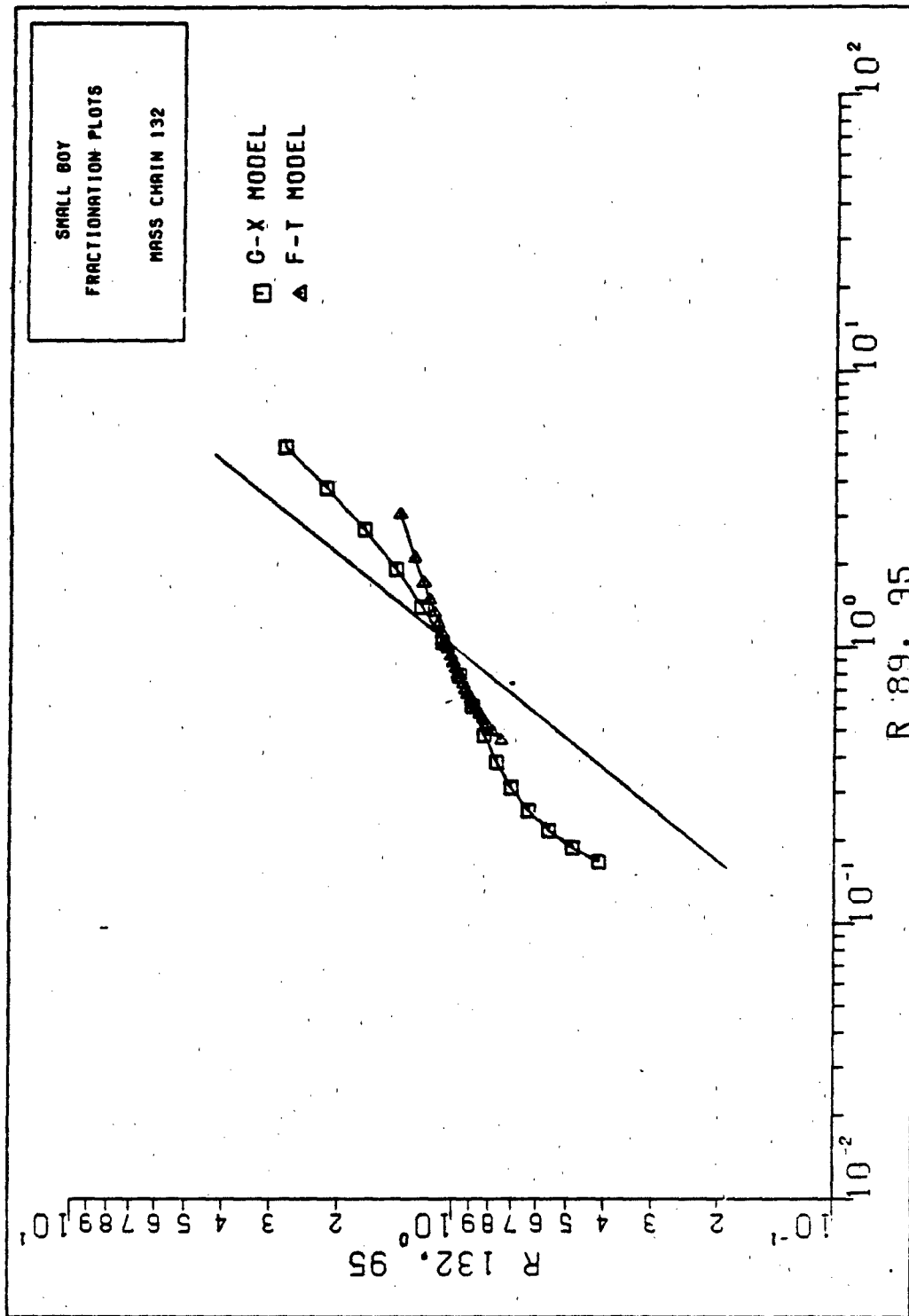


Figure 24. Small Boy Fractionation Plots: Mass Chain 132

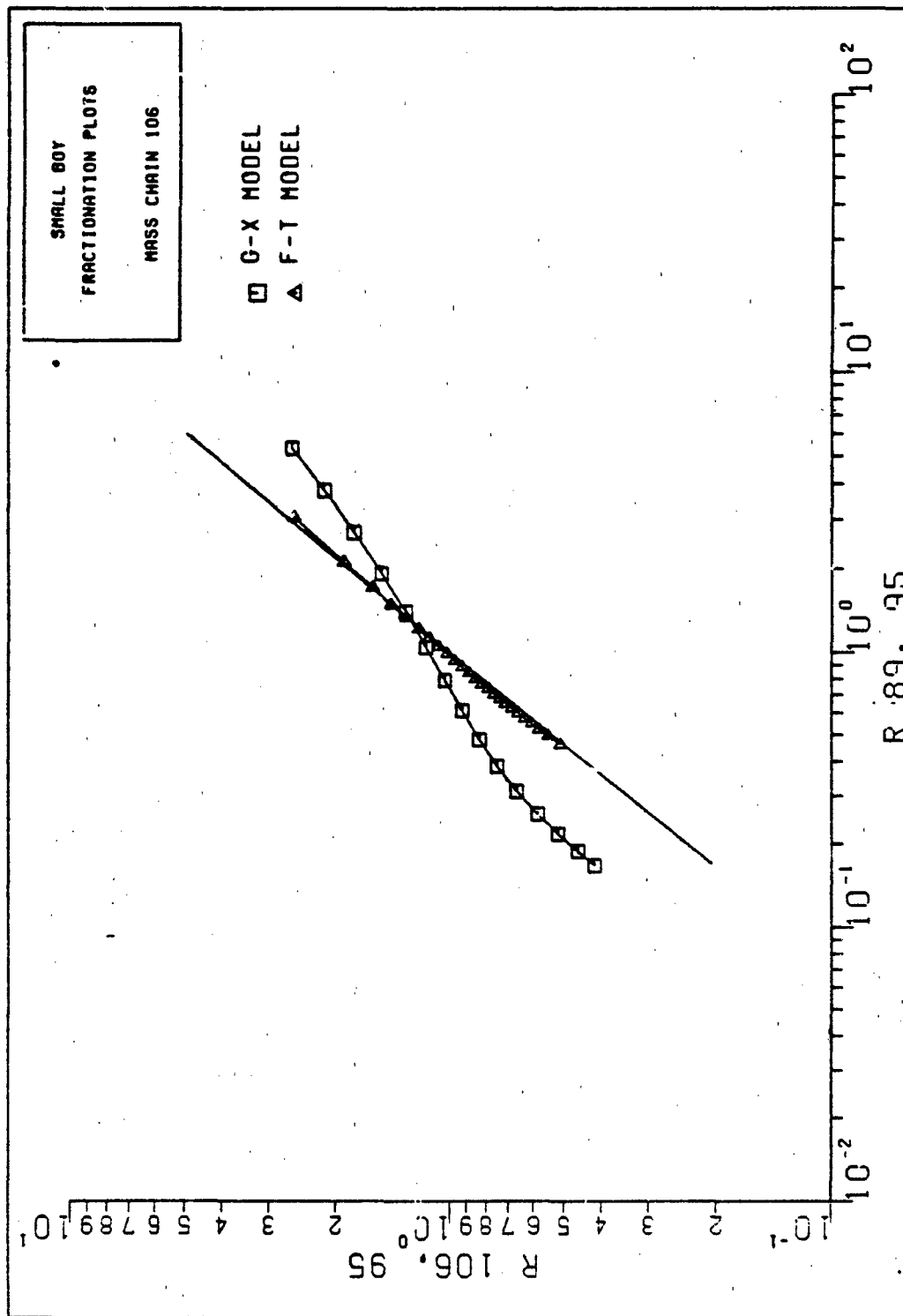


Figure 25. Small Boy Fractionation Plots: Mass Chain 106

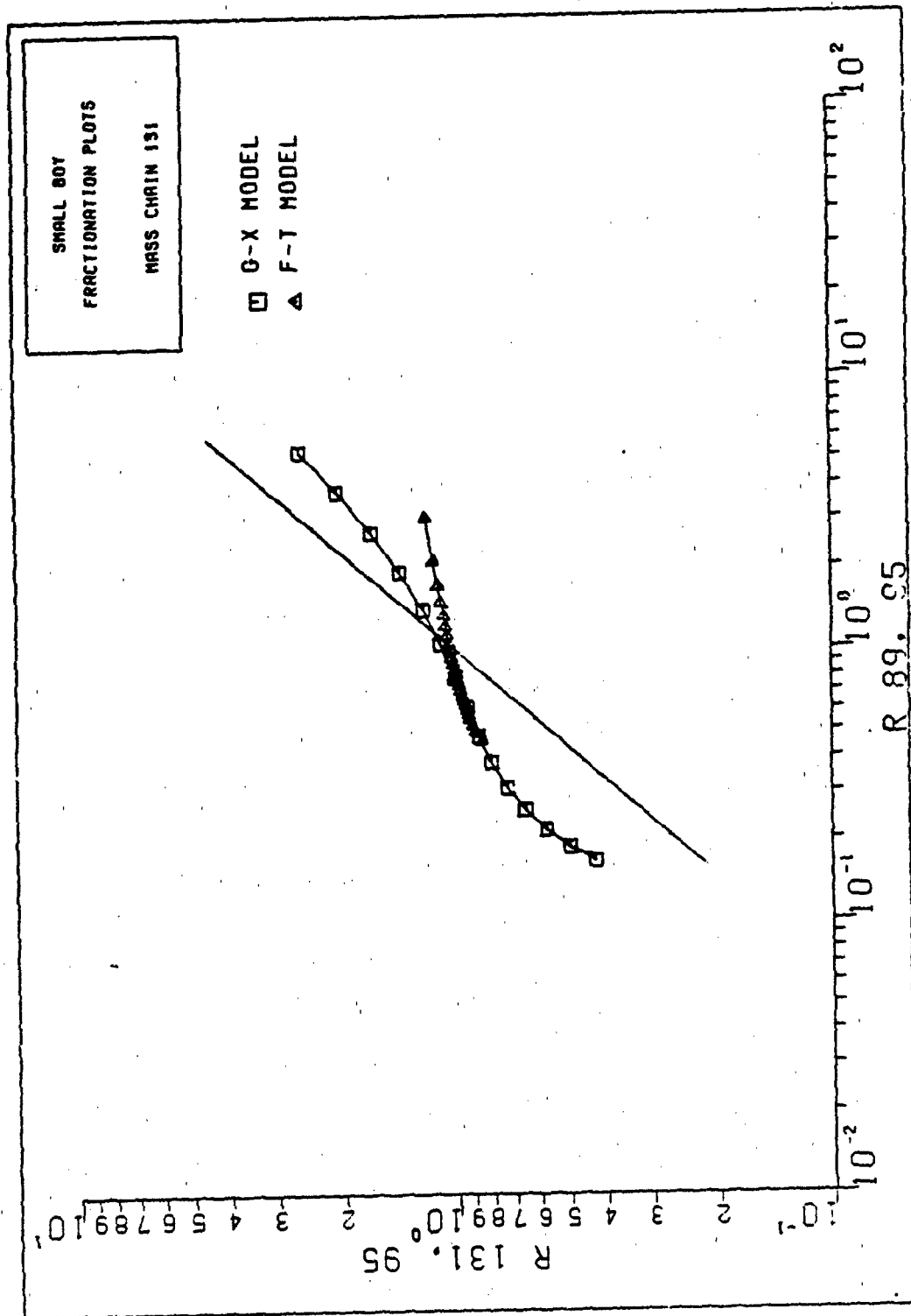


Figure 26. Small Boy Fractionation Plots: Mass Chain 131

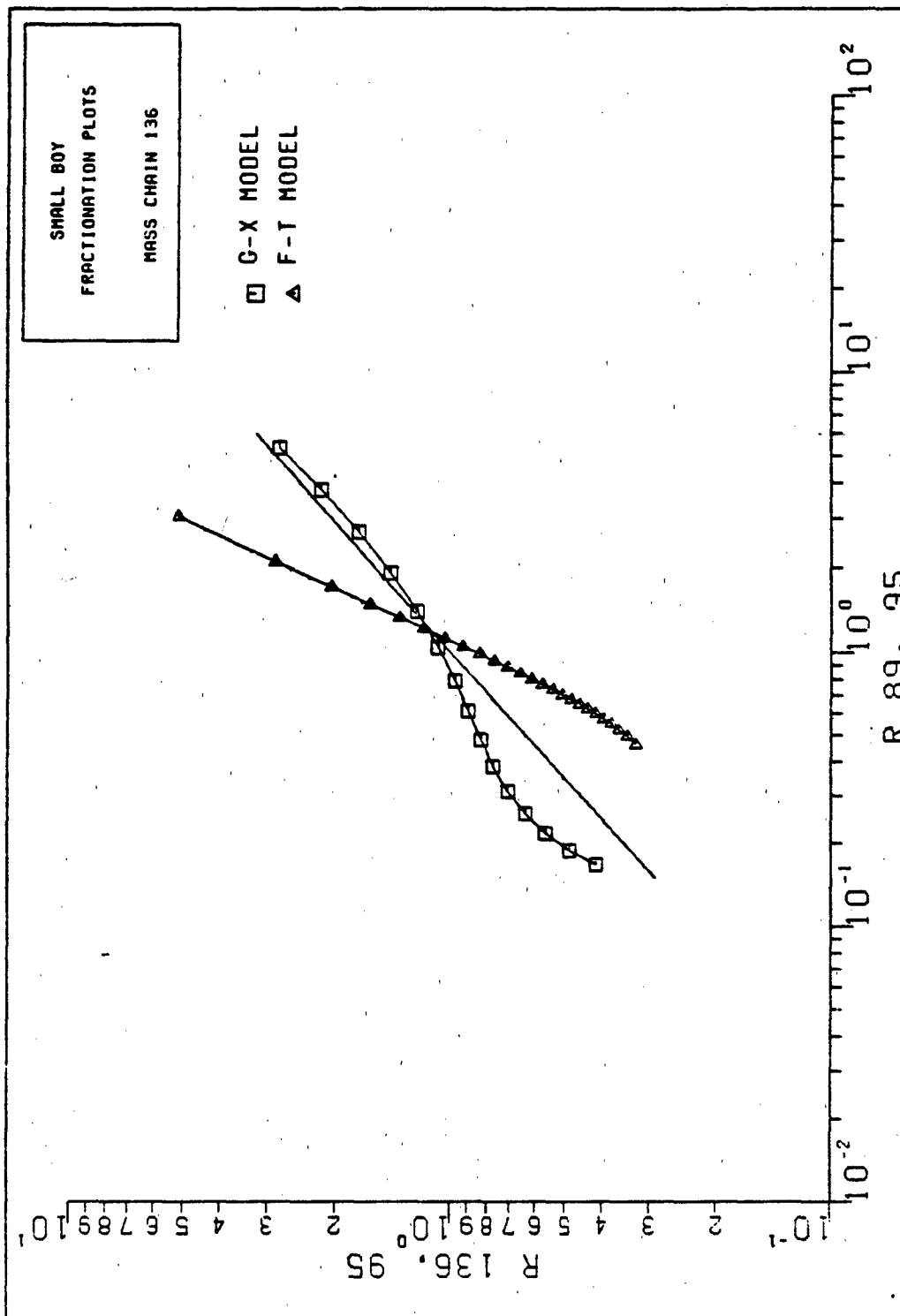


Figure 27. Small Boy Fractionation Plots: Mass Chain 136

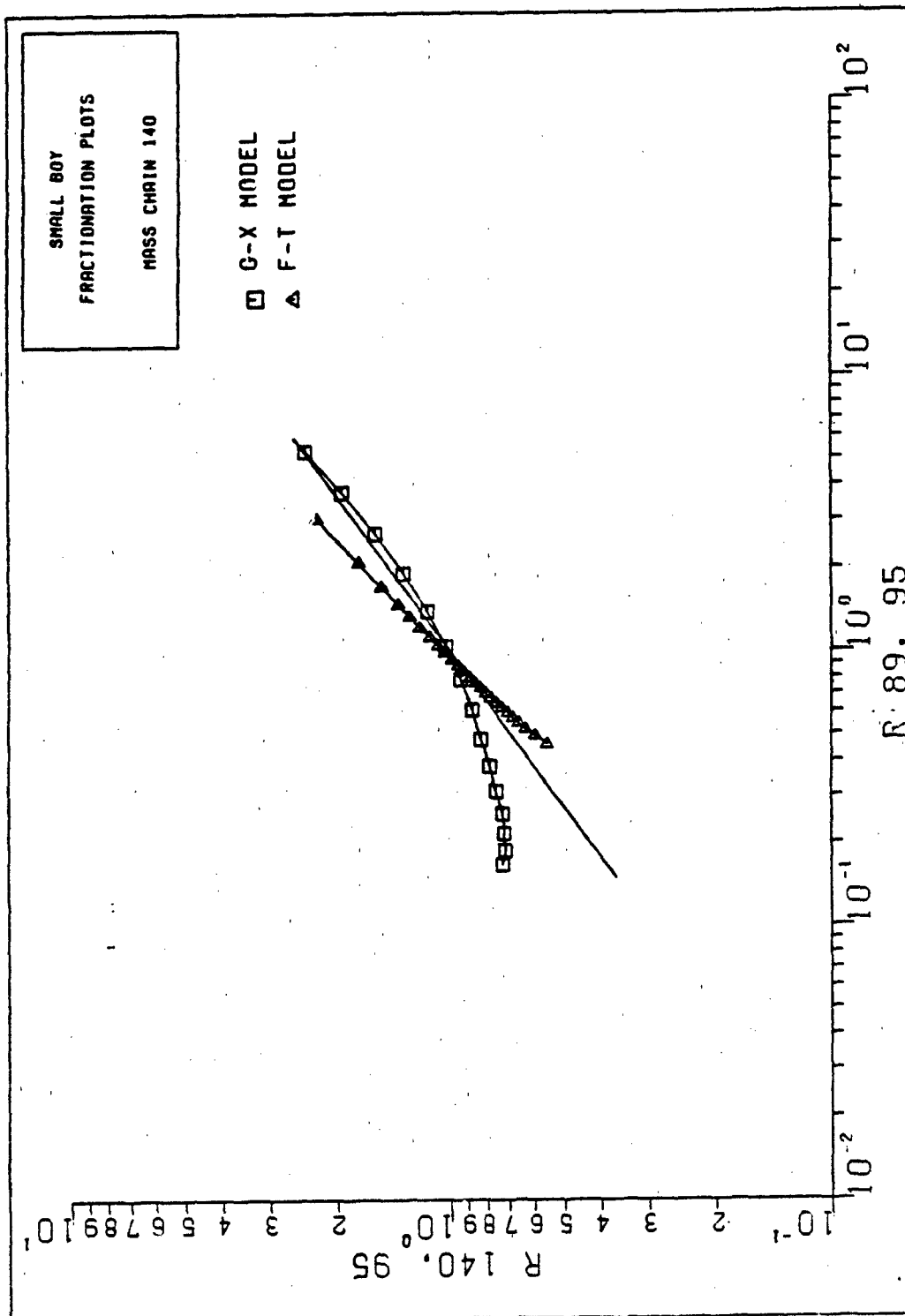


Figure 28. Small Boy Fractionation Plots: Mass Chain 140

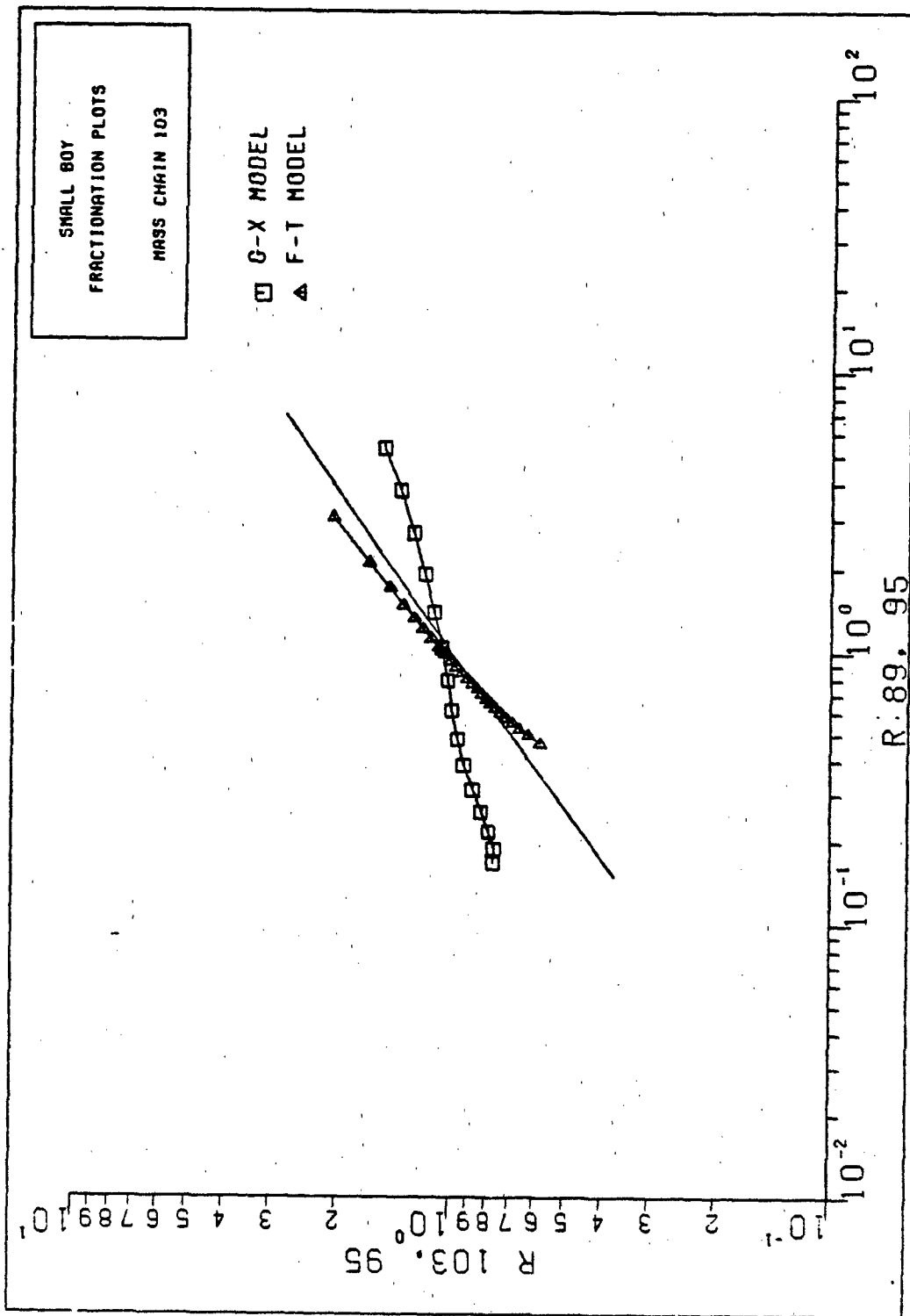


Figure 29. Small Boy Fractionation Plots: Mass Chain 103

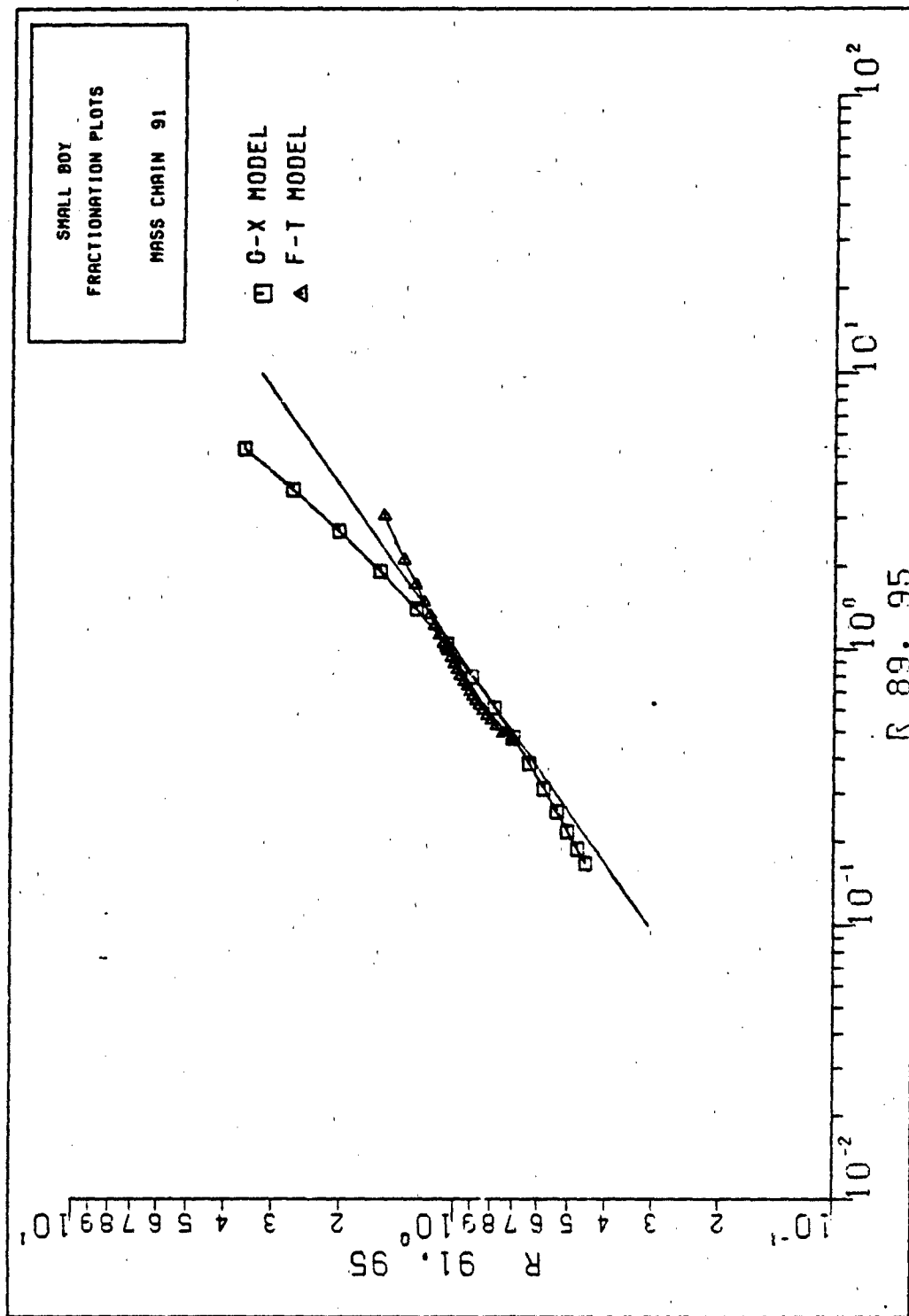


Figure 30. Small Boy Fractionation Plots: Mass Chain 91

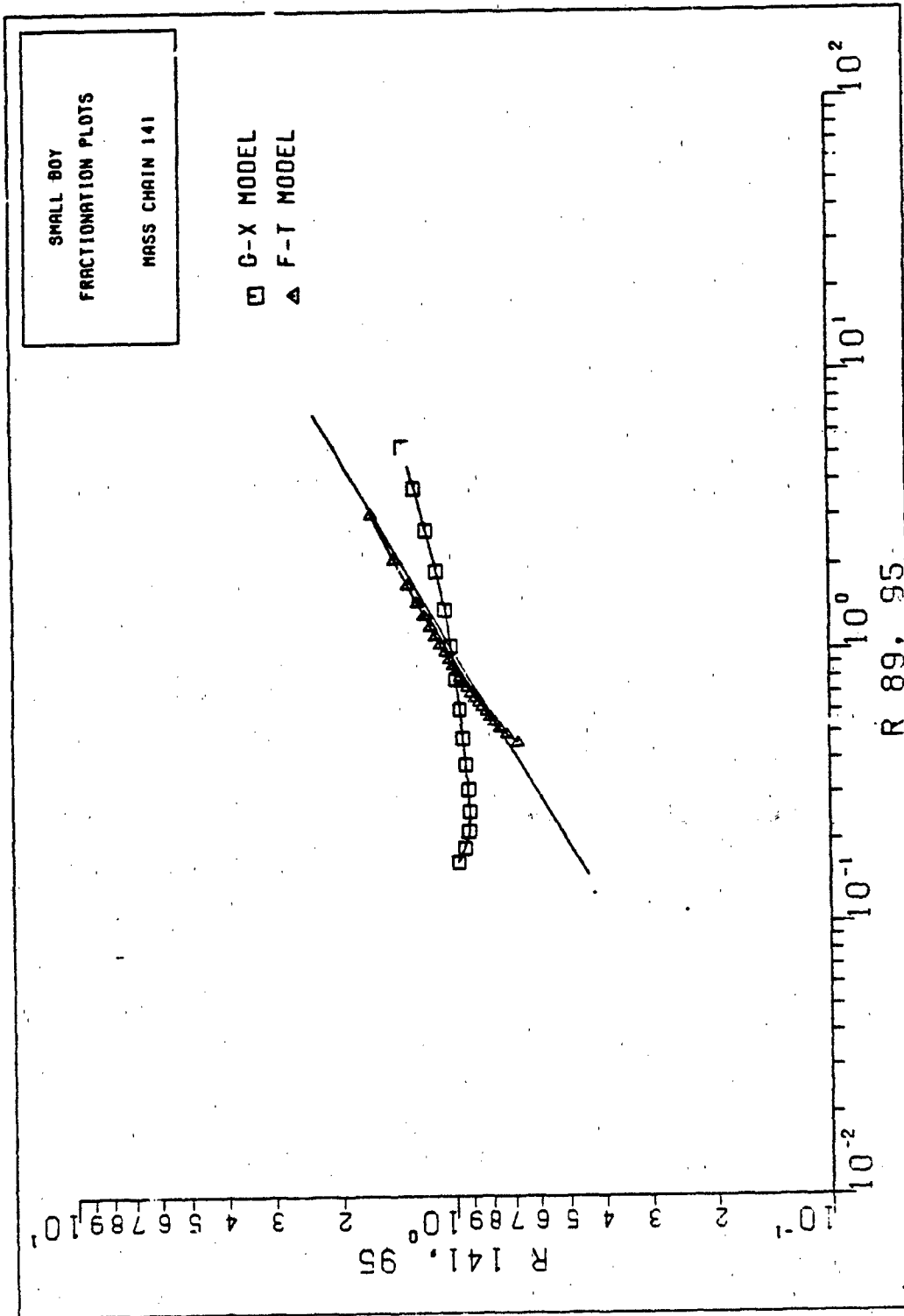


Figure 31. Small Boy Fractionation Plots: Mass Chain 141

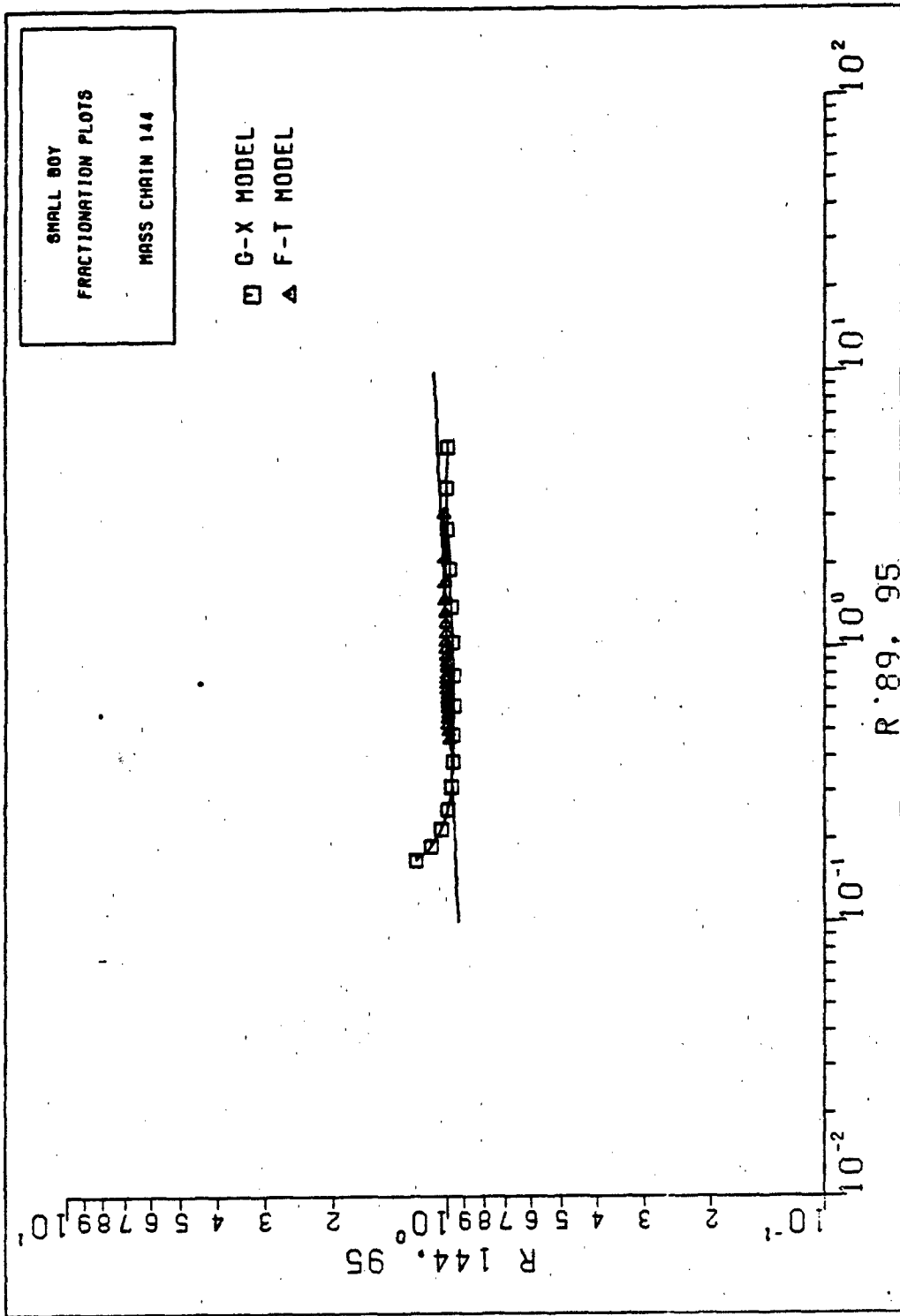


Figure 32. Small Boy Fractionation Plots: Mass Chain 144

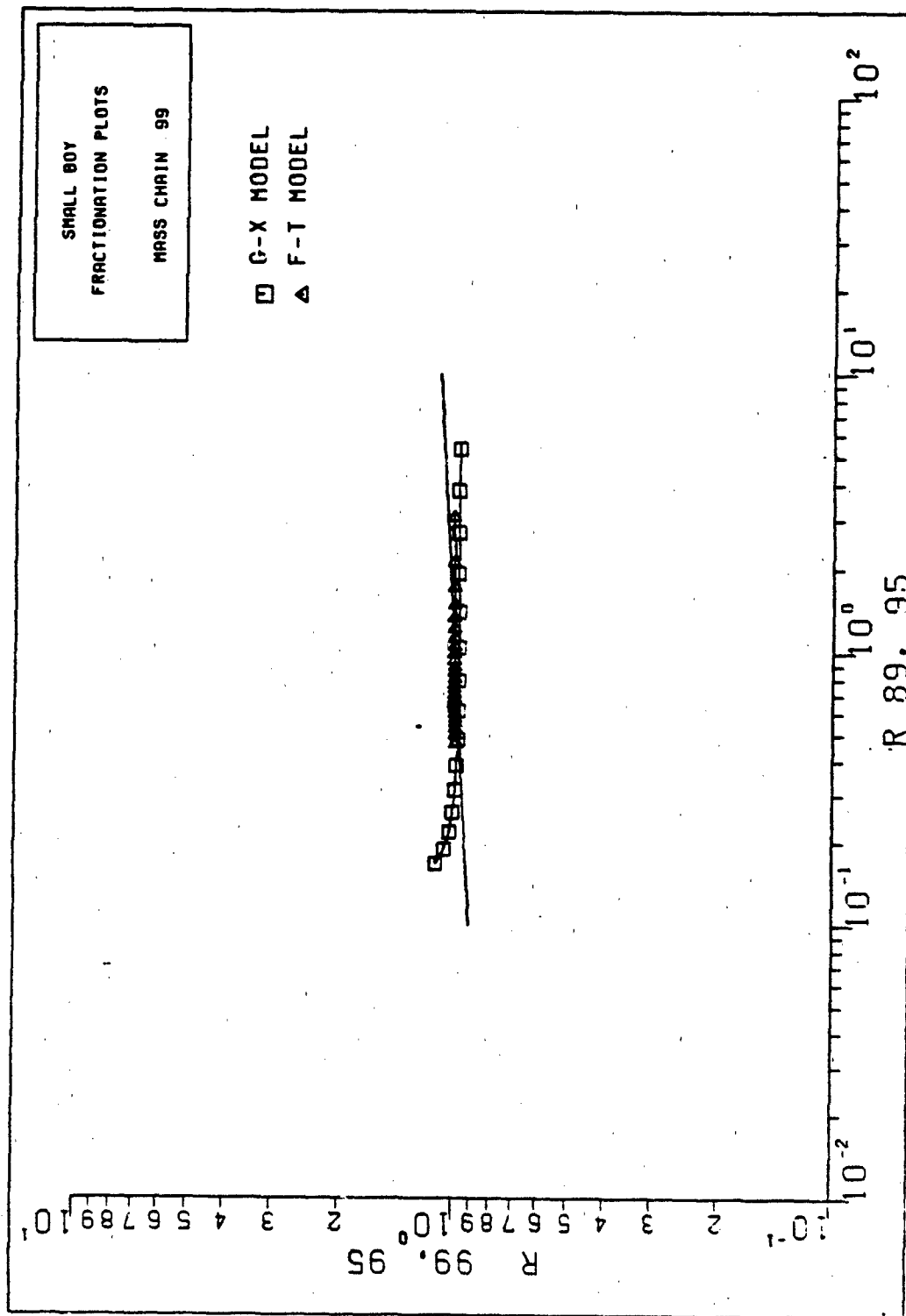


Figure 33. Small Boy Fractionation Plots: Mass Chain 99

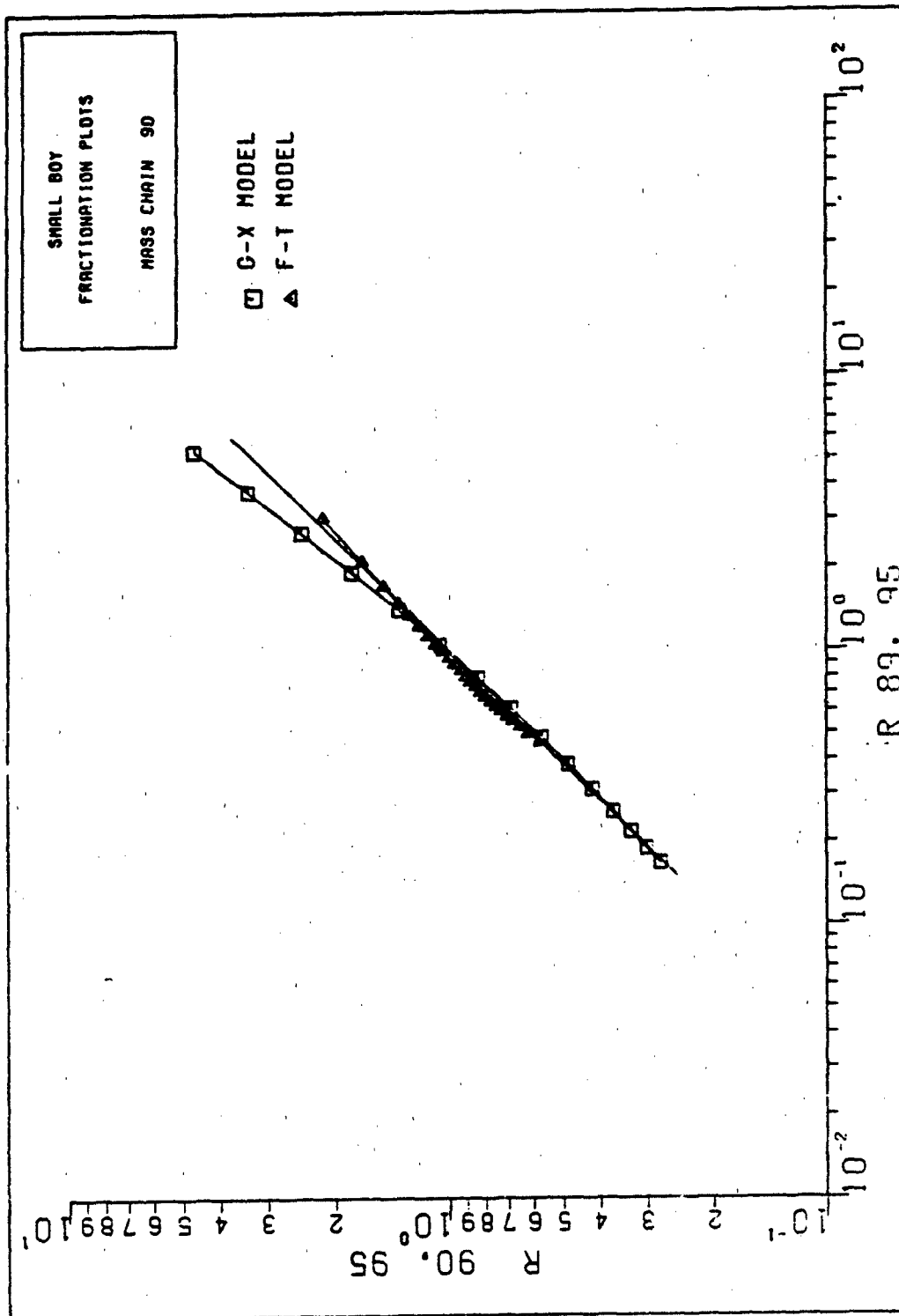


Figure 34. Small Boy Fractionation Plots: Mass Chain 90

Appendix C

$R_{f,j}$ Plots for Johnny Boy

This appendix includes fractionation plots for all chains for which data is available in the literature (Crocker, 1965: 72-81). The nuclides used for radiochemical analysis are as follows:

137	Cs
89	Sr
132	Te
131	I
90	Sr
136	Cs
140	Ba
91	Y
141	Ce
144	Ce
99	Mo
95	Zr

Least squares fits to the test data are shown on the plots as solid straight lines. Mass chains 89 and 95 are reference chains.

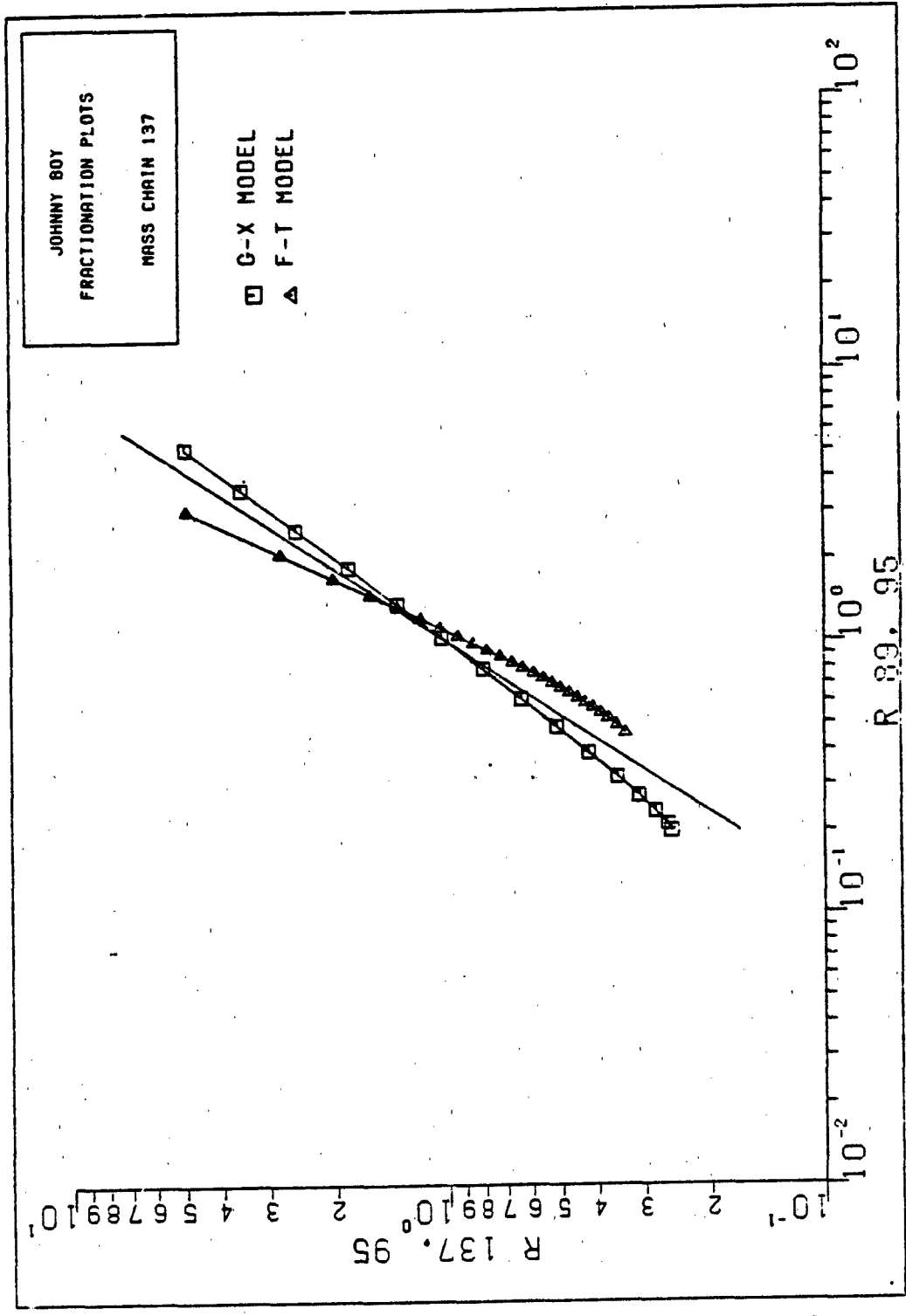


Figure 35. Johnny Boy Fractionation Plots: Mass Chain 137

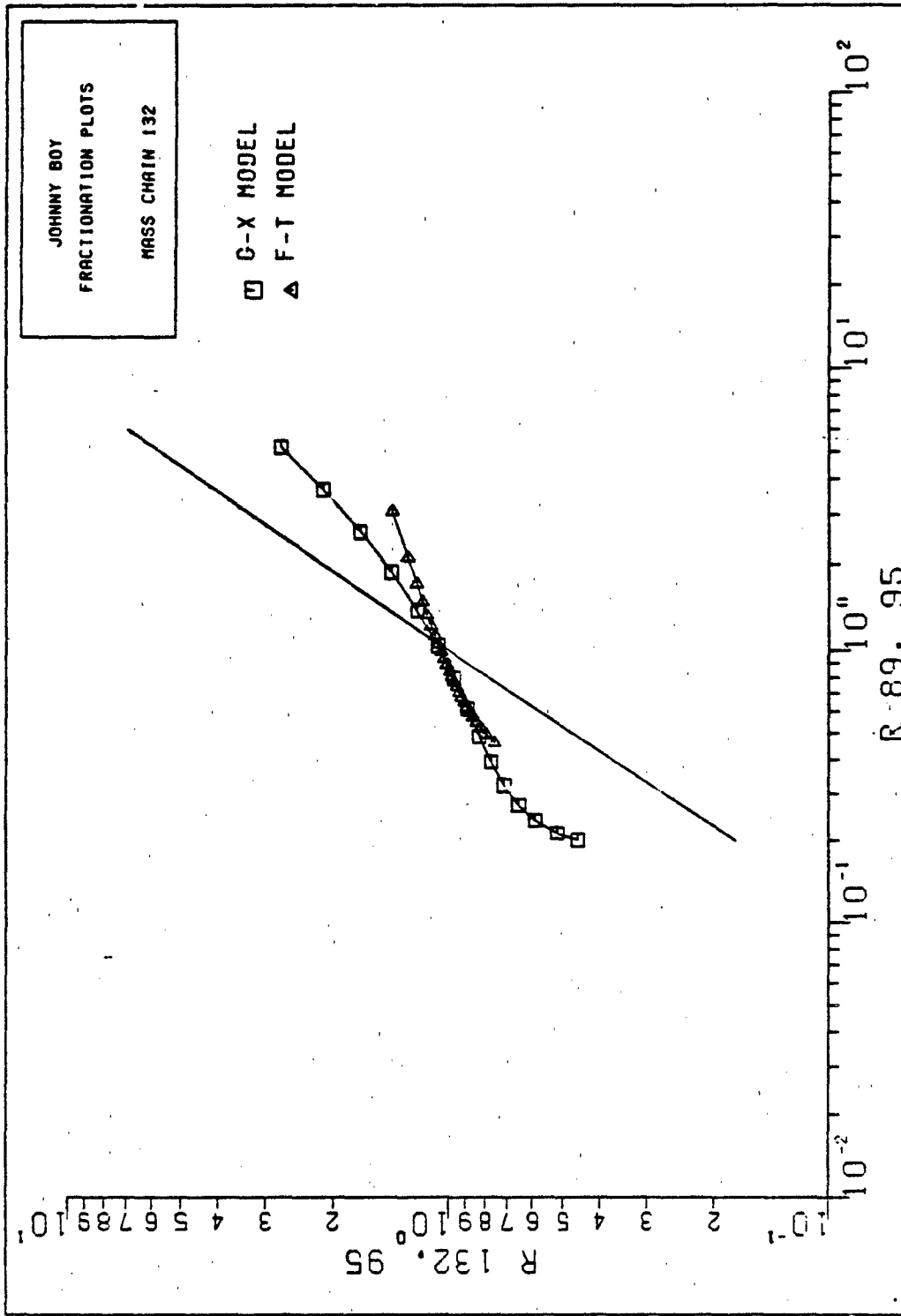


Figure 36. Johnny Boy Fractionation Plots: Mass Chain 132

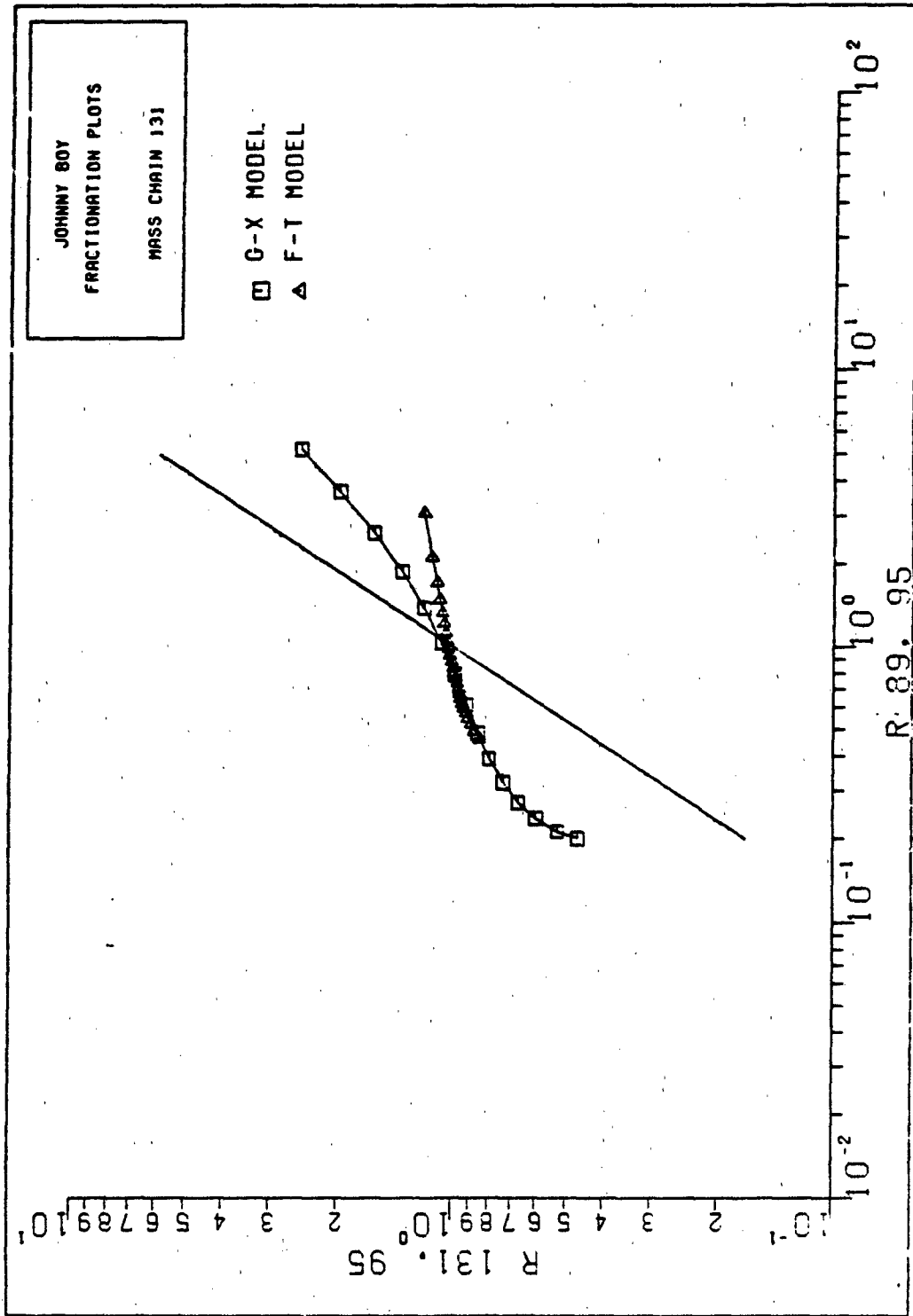


Figure 37. Johnny Boy Fractionation Plots: Mass Chain 131

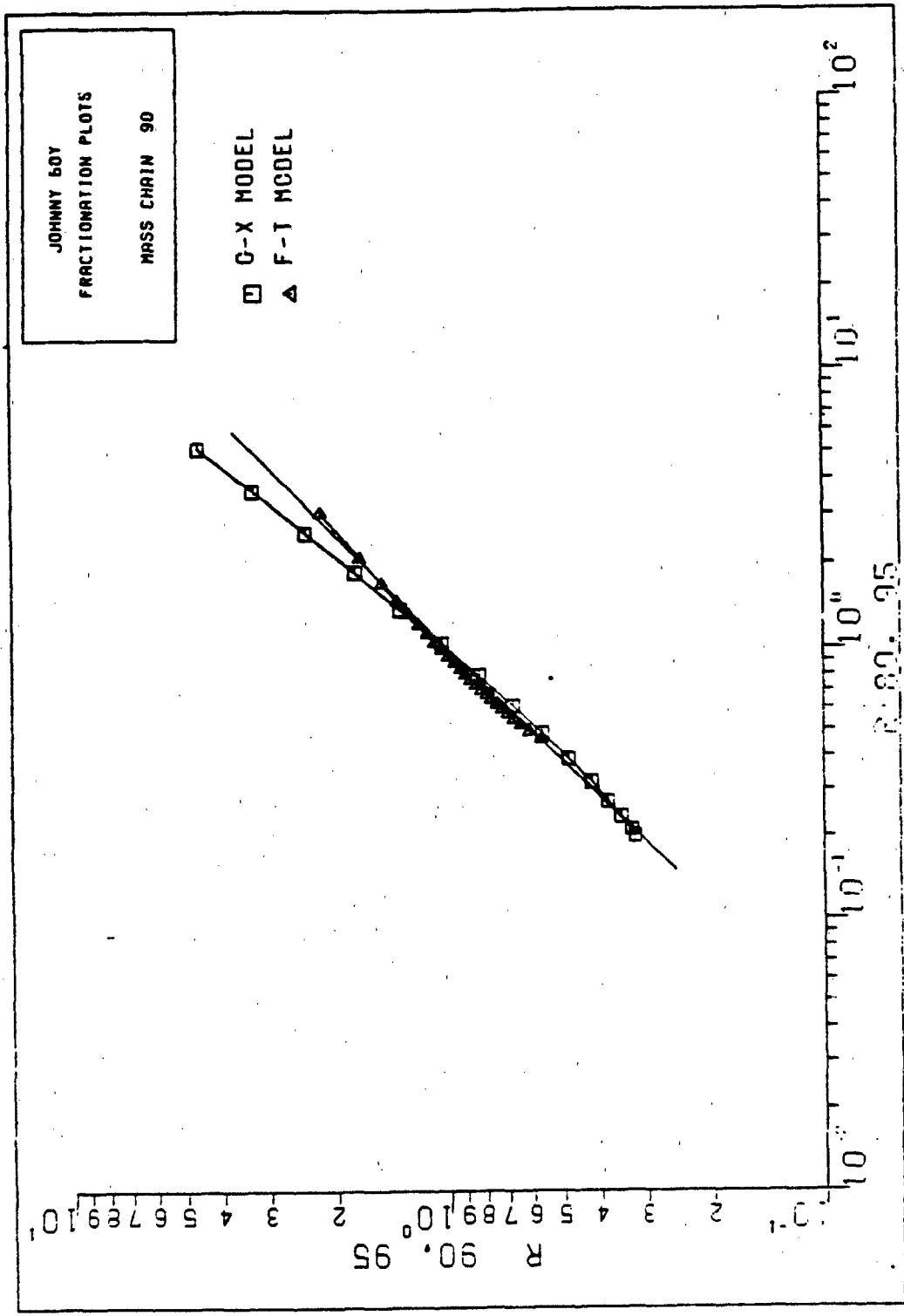


Figure 38. Johnny Boy Fractionation Plots: Mass Chain 90

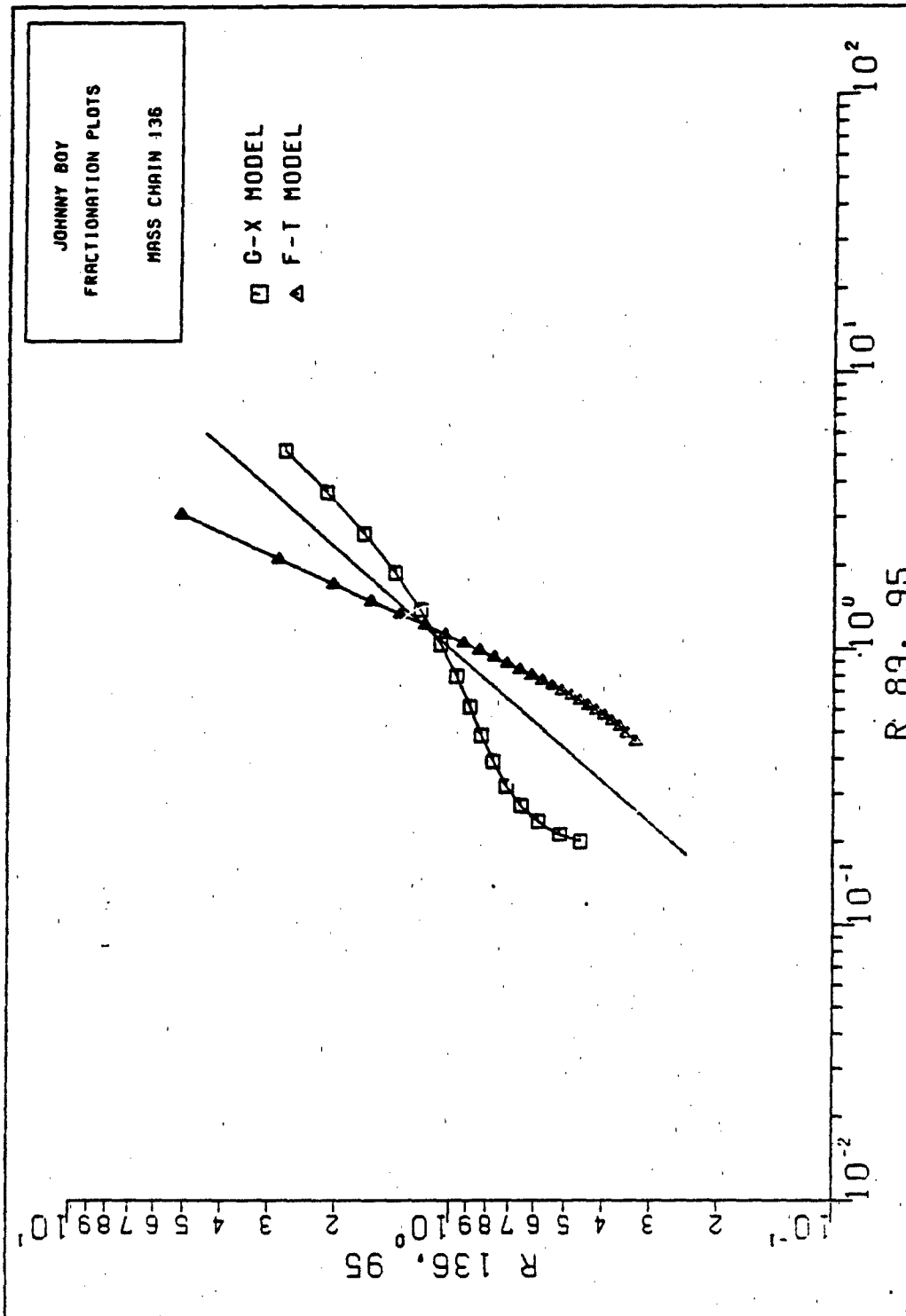


Figure 39. Johnny Boy Fractionation Plots: Mass Chain 136

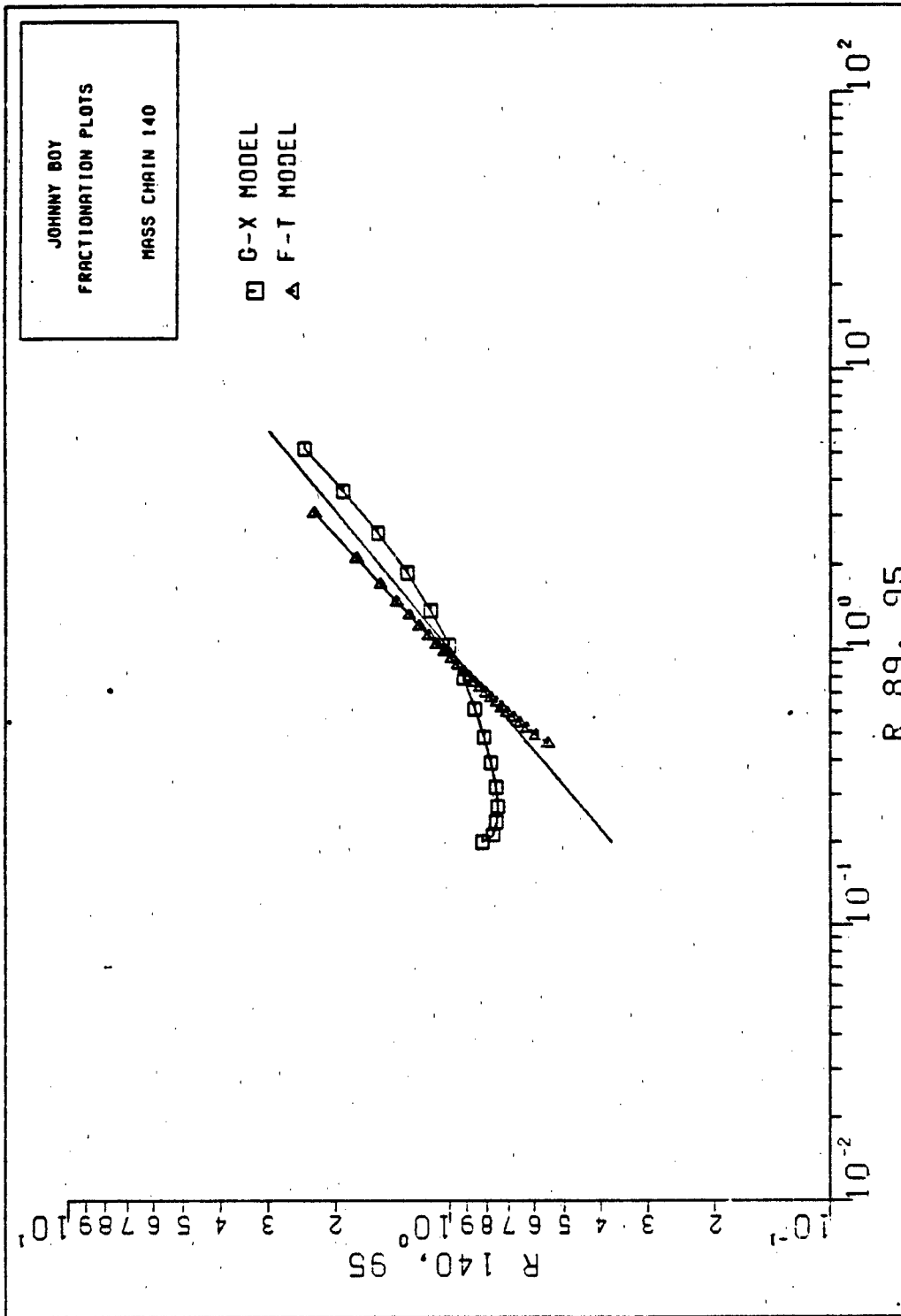


Figure 40. Johnny Boy Fractionation Plots: Mass Chain 140

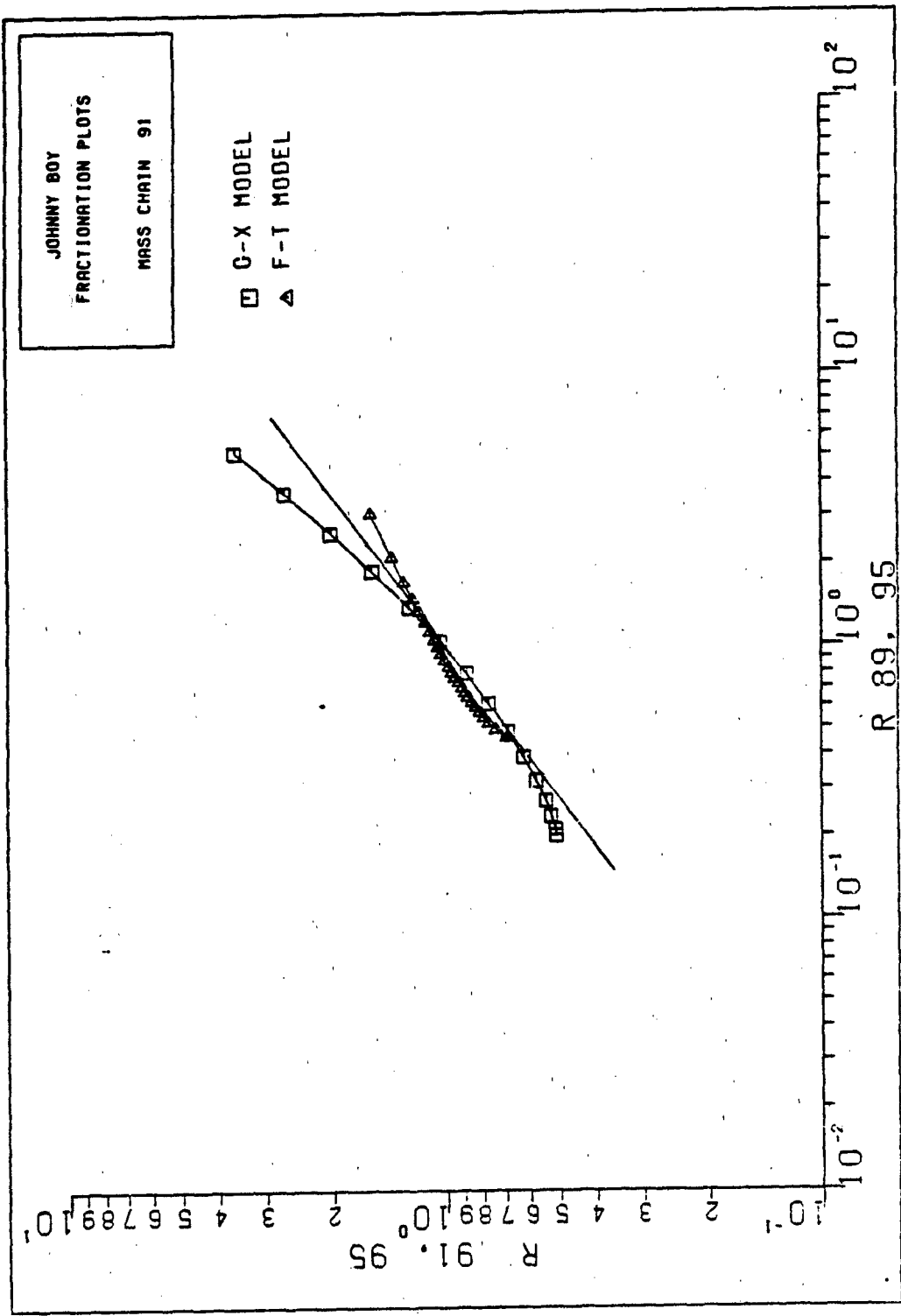


Figure 41. Johnny Boy Fractionation Plots: Mass Chain 91

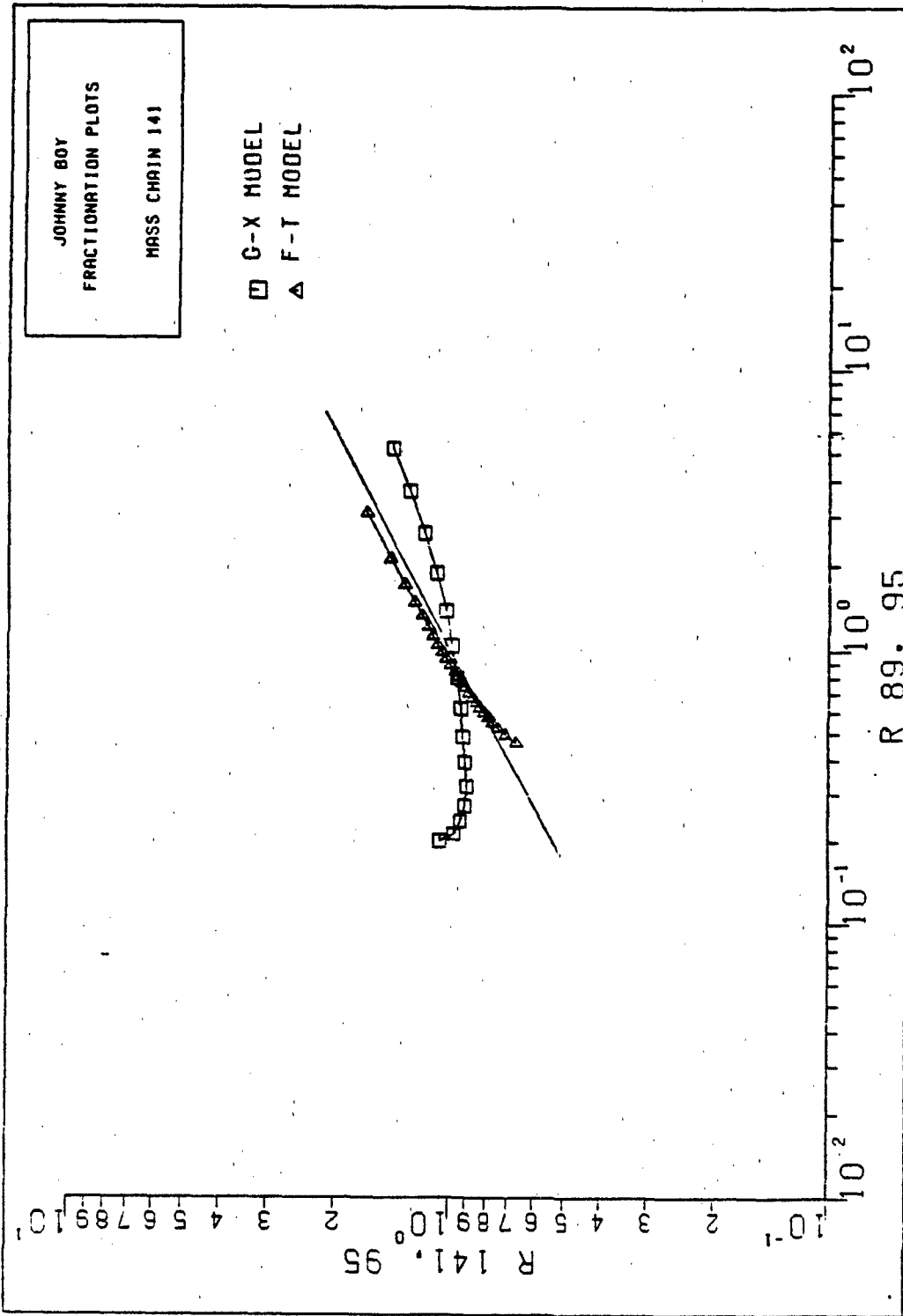


Figure 42. Johnny Boy Fractionation Plots: Mass Chain 141

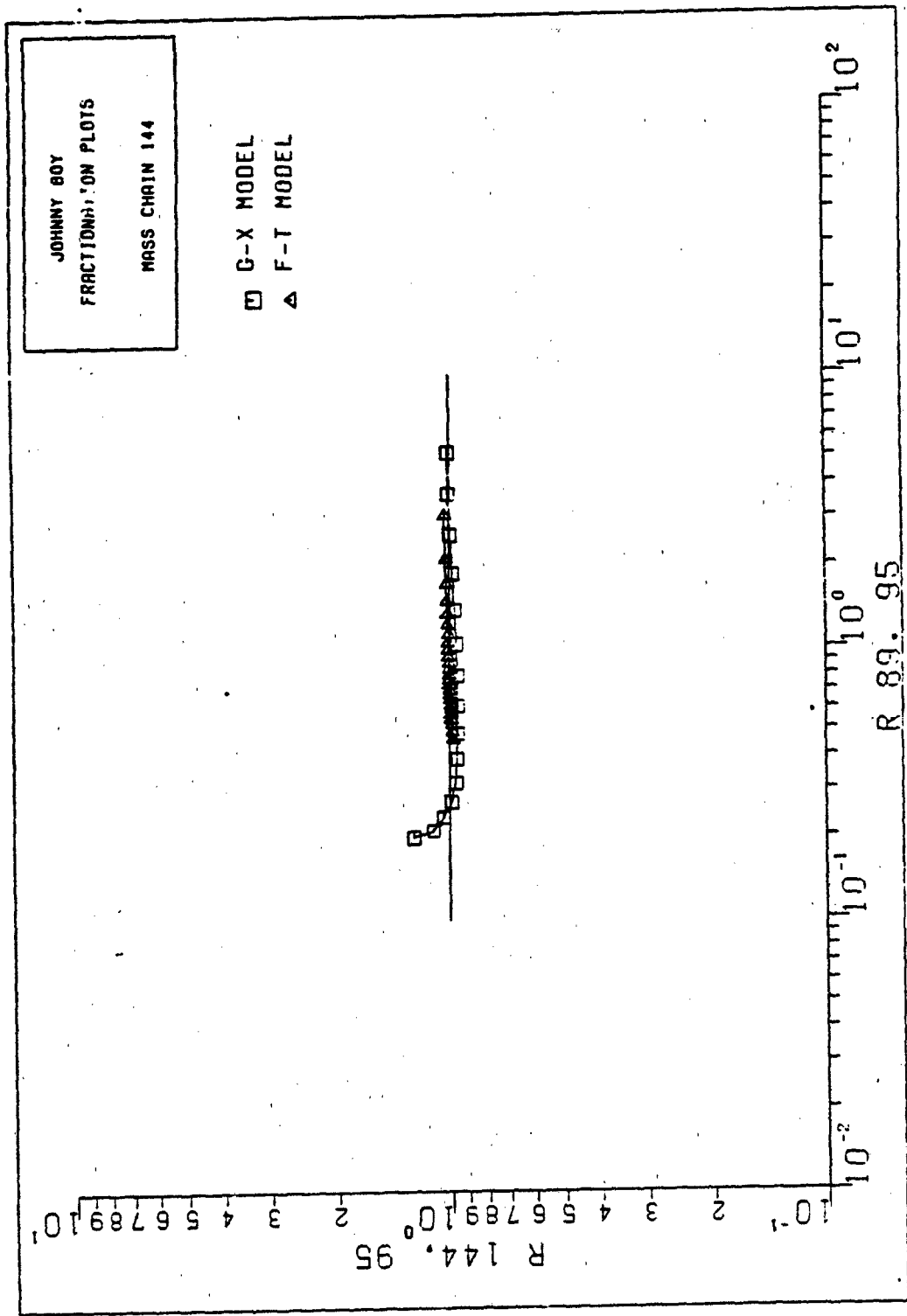


Figure 43. Johnny Boy Fractionation Plots: Mass Chain 144

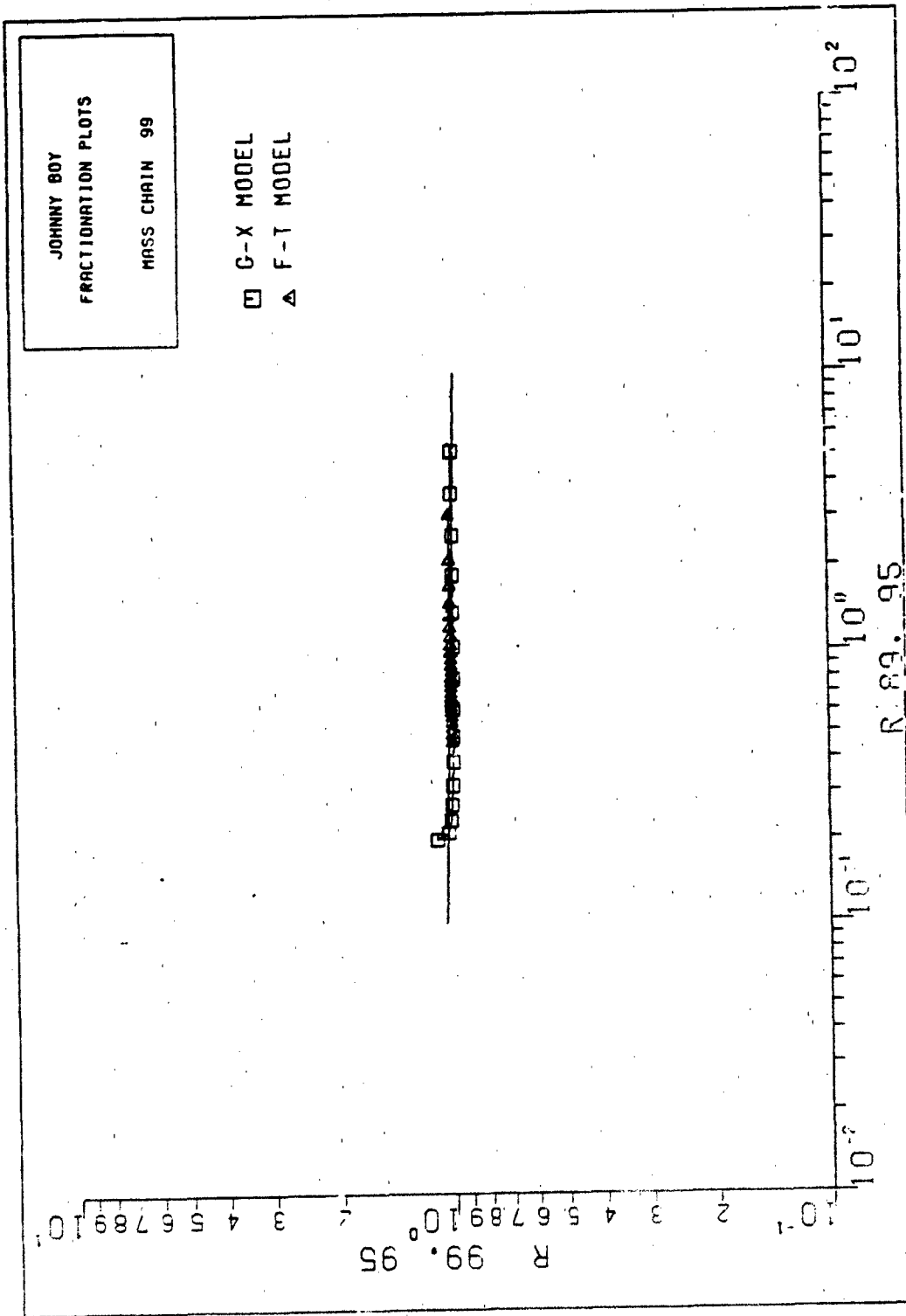


Figure 44. Johnny Boy Fractionation Plots: Mass Chain 99

Appendix D

Specific Activity Plots for Small Boy

This appendix includes plots of the specific activity for all chains of general interest. Mass chains which are volume distributed will have constant specific activity curves. Mass chains which are surface distributed will show a marked decrease in specific activity as particle size increases. Chains which have mixed behavior will exhibit a combination of these.

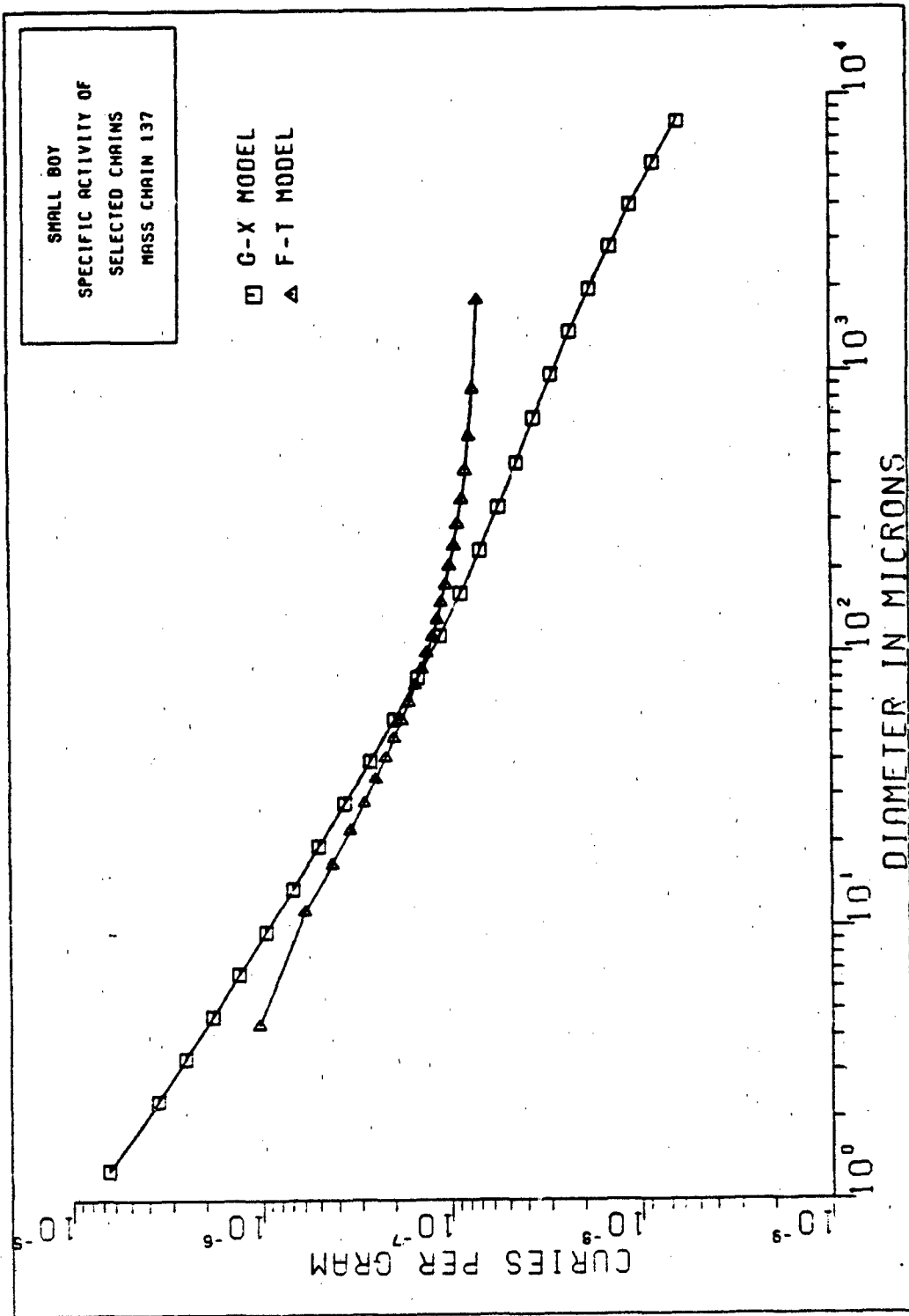


Figure 45. Small Boy Specific Activity for Mass Chain 137

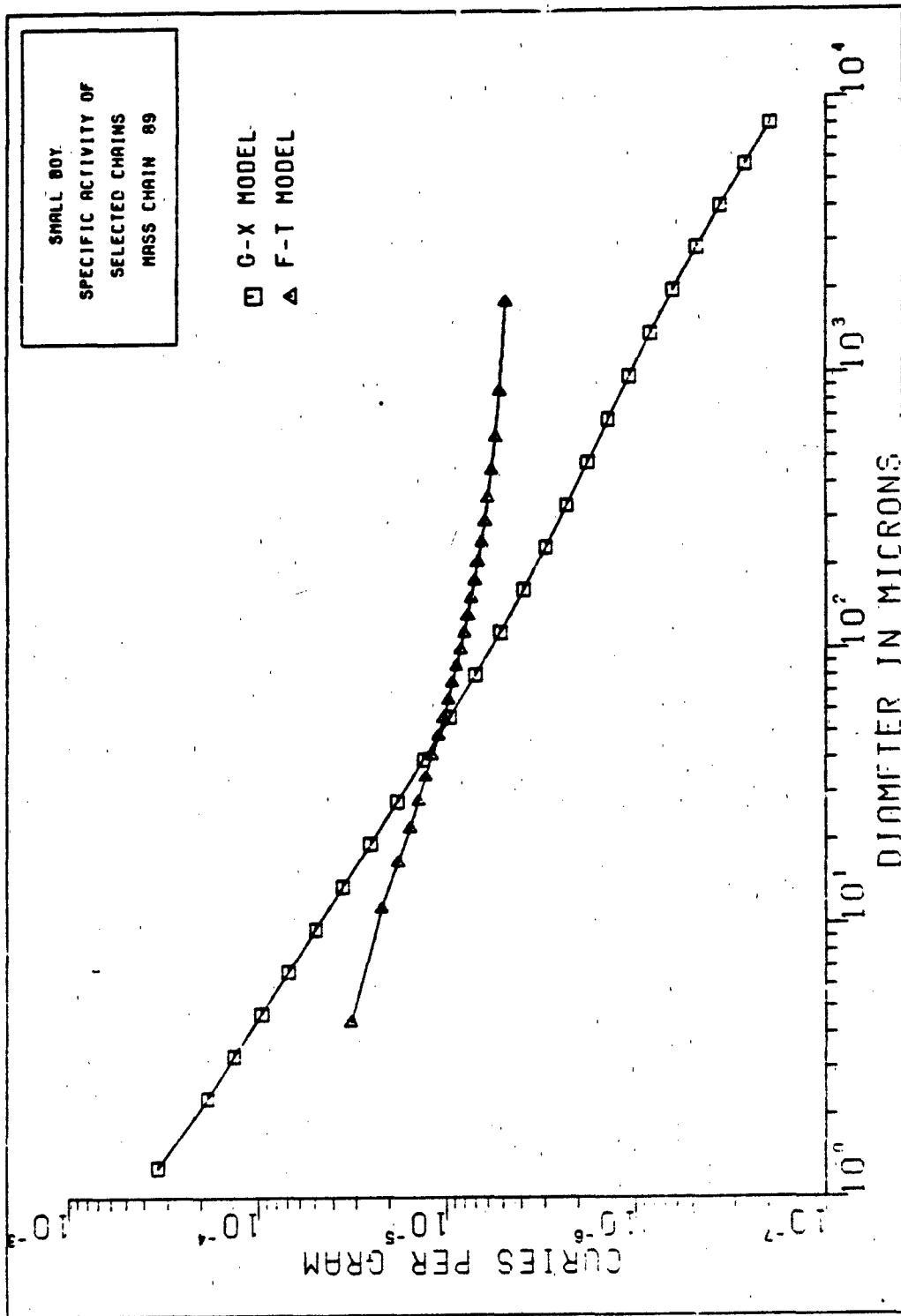


Figure 46. Small Boy Specific Activity for Mass Chain 89

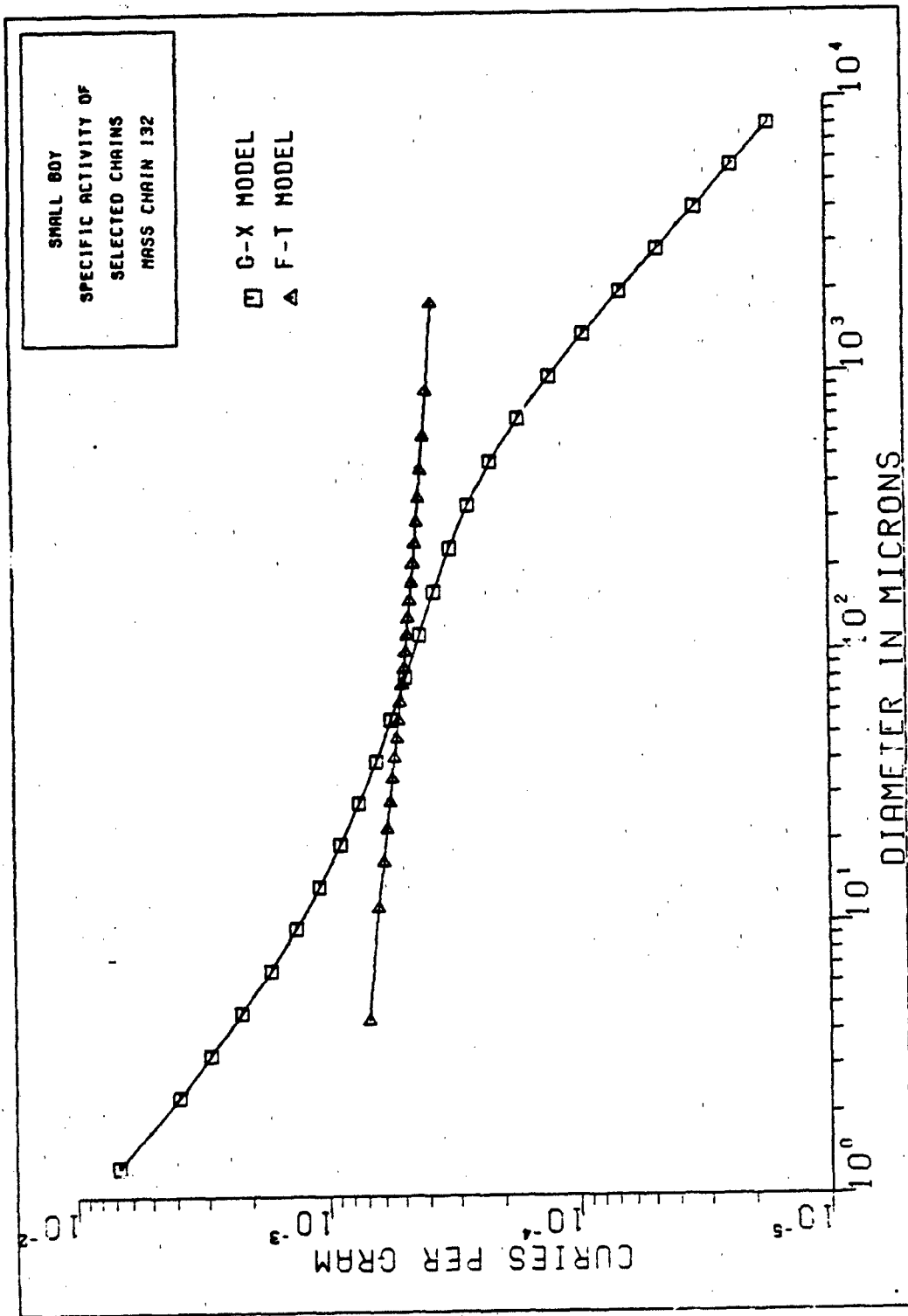


Figure 47. Small Boy Specific Activity for Mass Chain 132

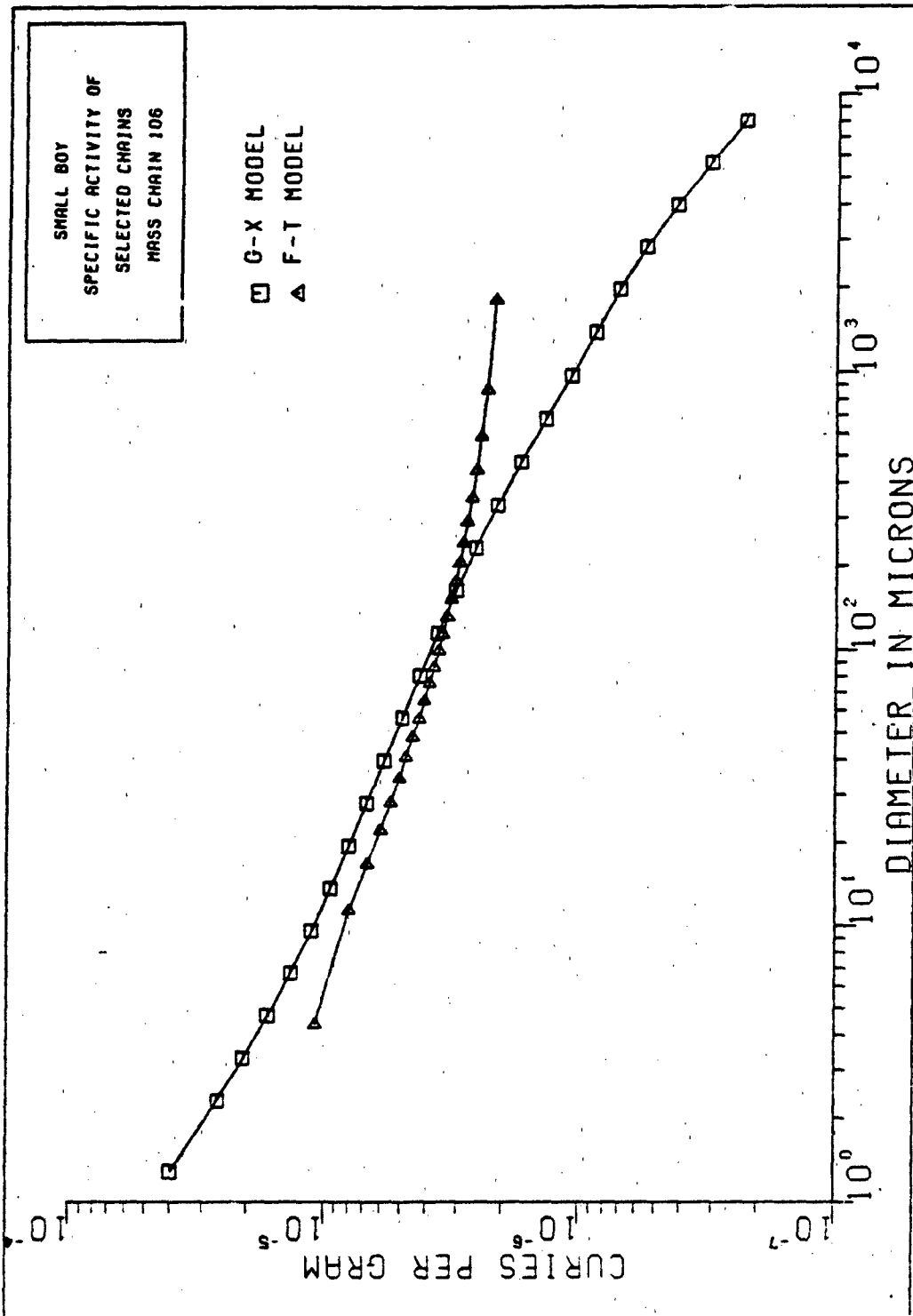


Figure 48. Small Boy Specific Activity for Mass Chain 106

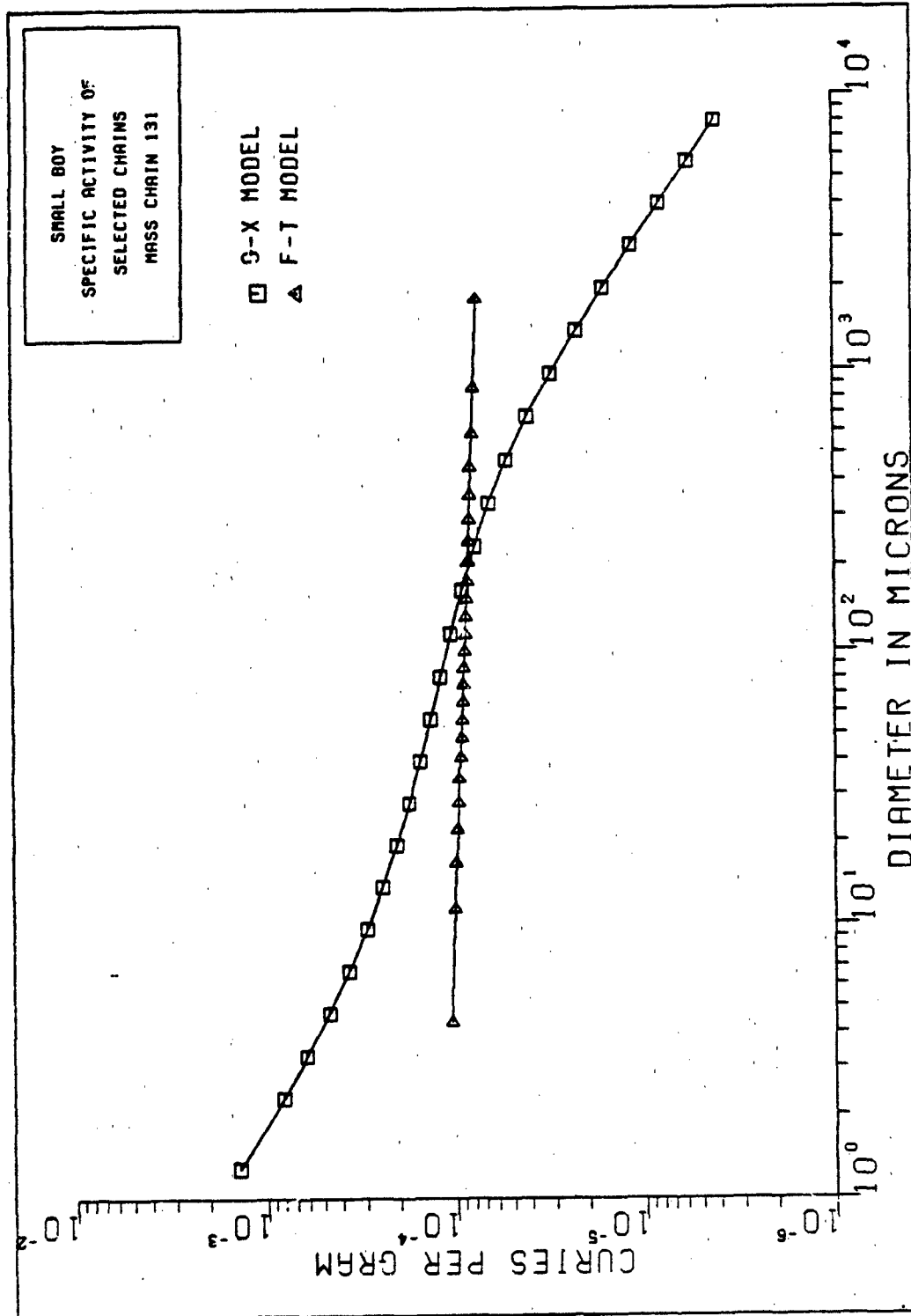


Figure 49. Small Boy Specific Activity for Mass Chain 131

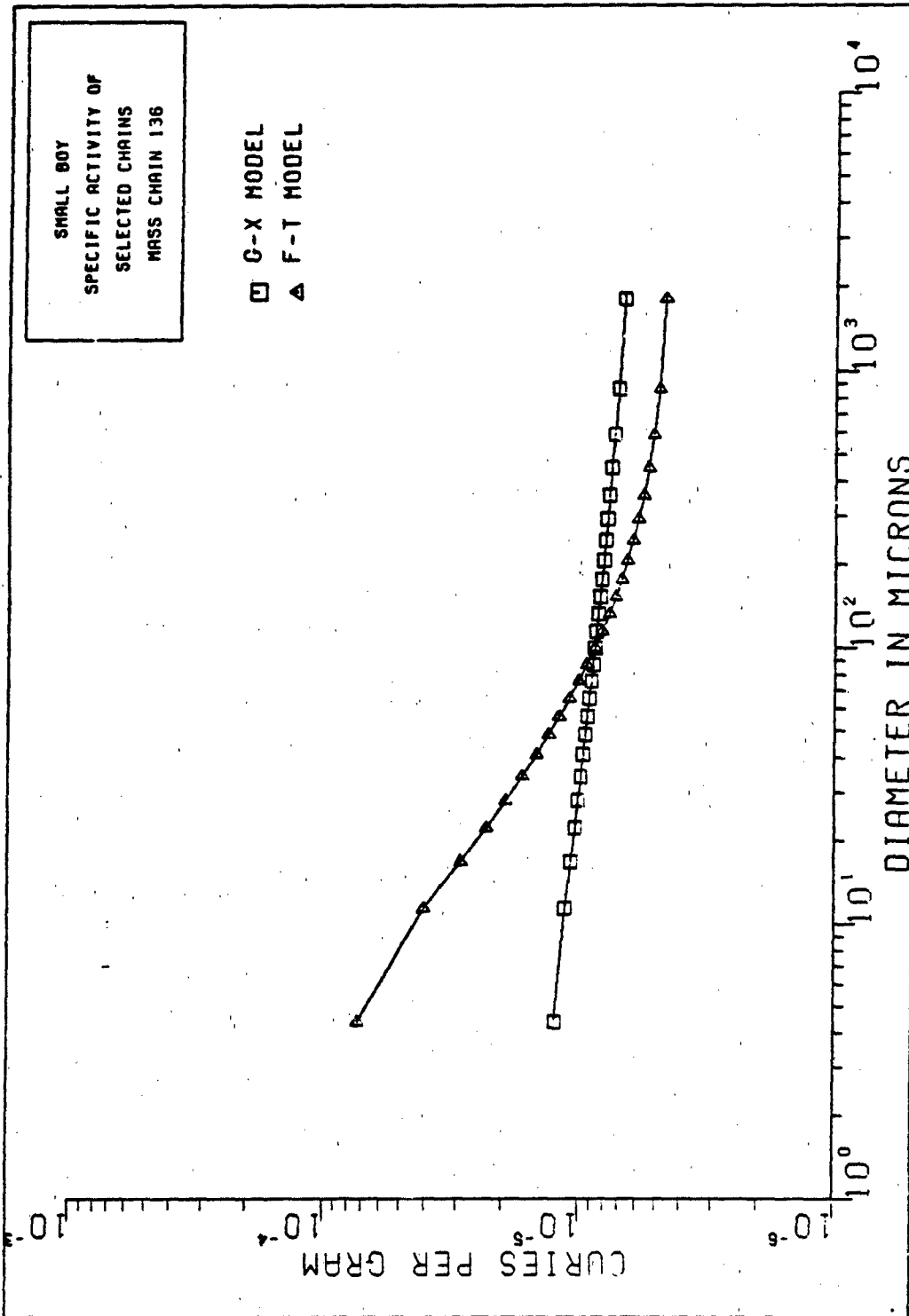


Figure 50. Small Boy Specific Activity for Mass Chain 136

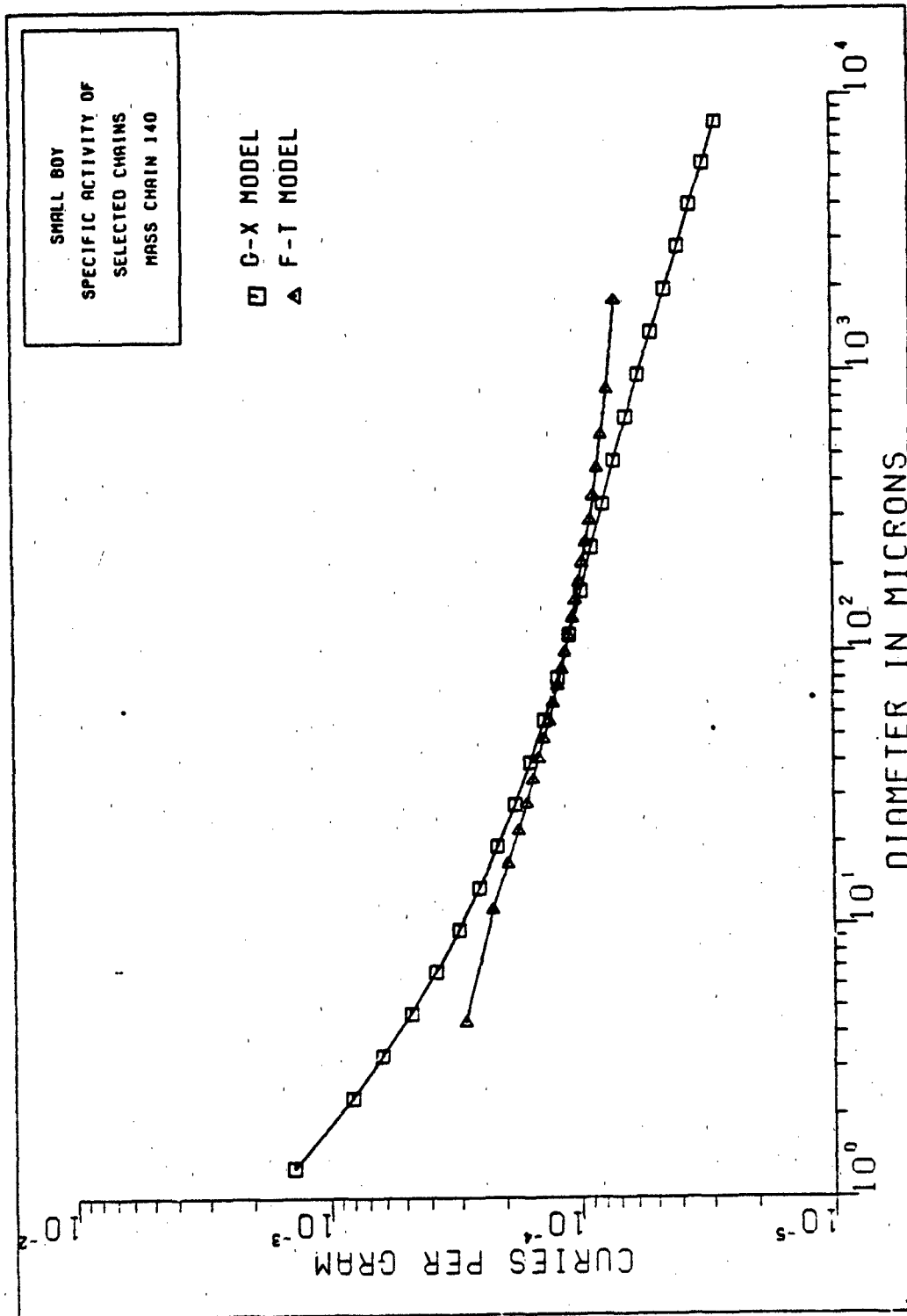


Figure 51. Small Boy Specific Activity for Mass Chain 140

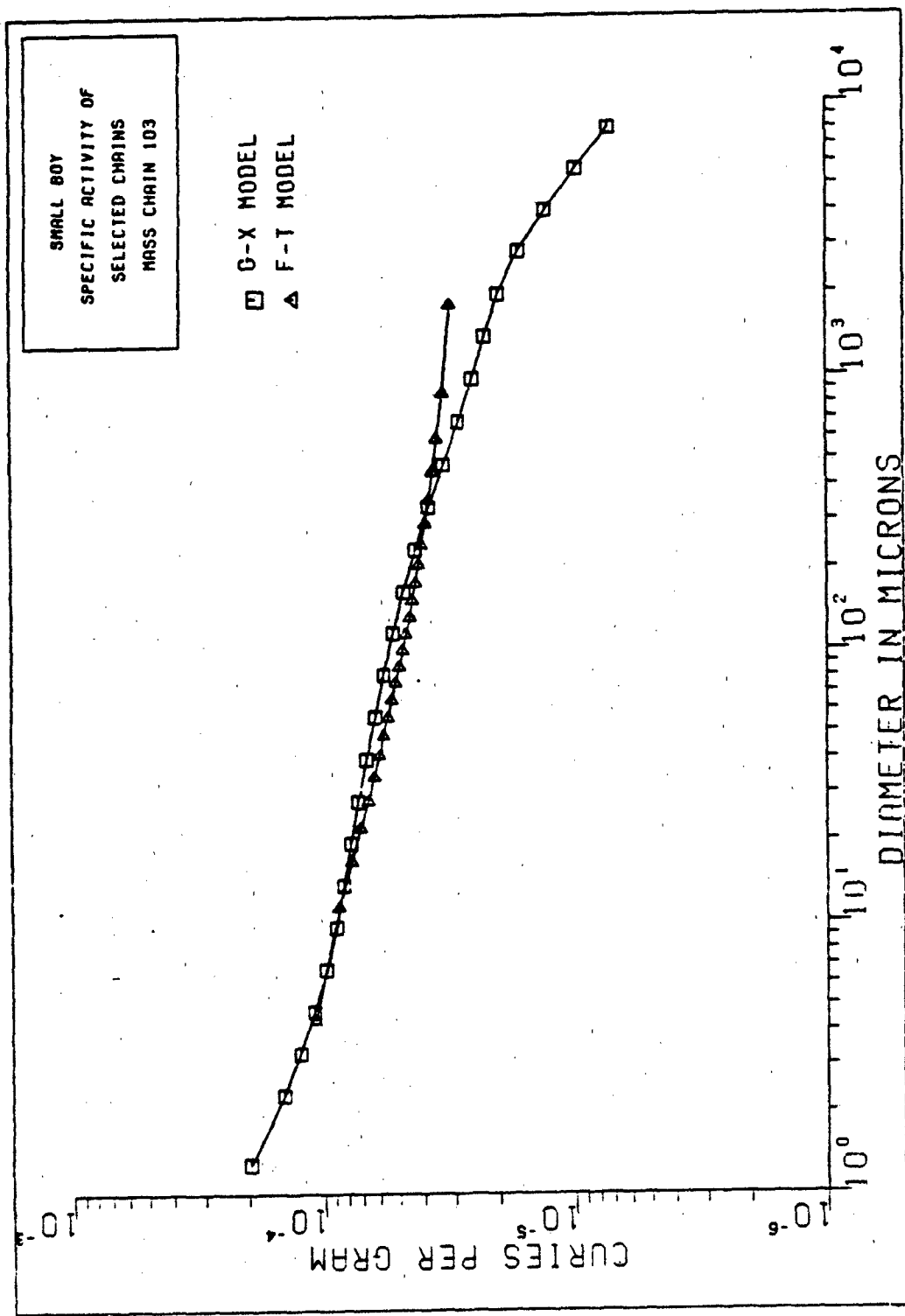


Figure 52. Small Boy Specific Activity for Mass Chain 103

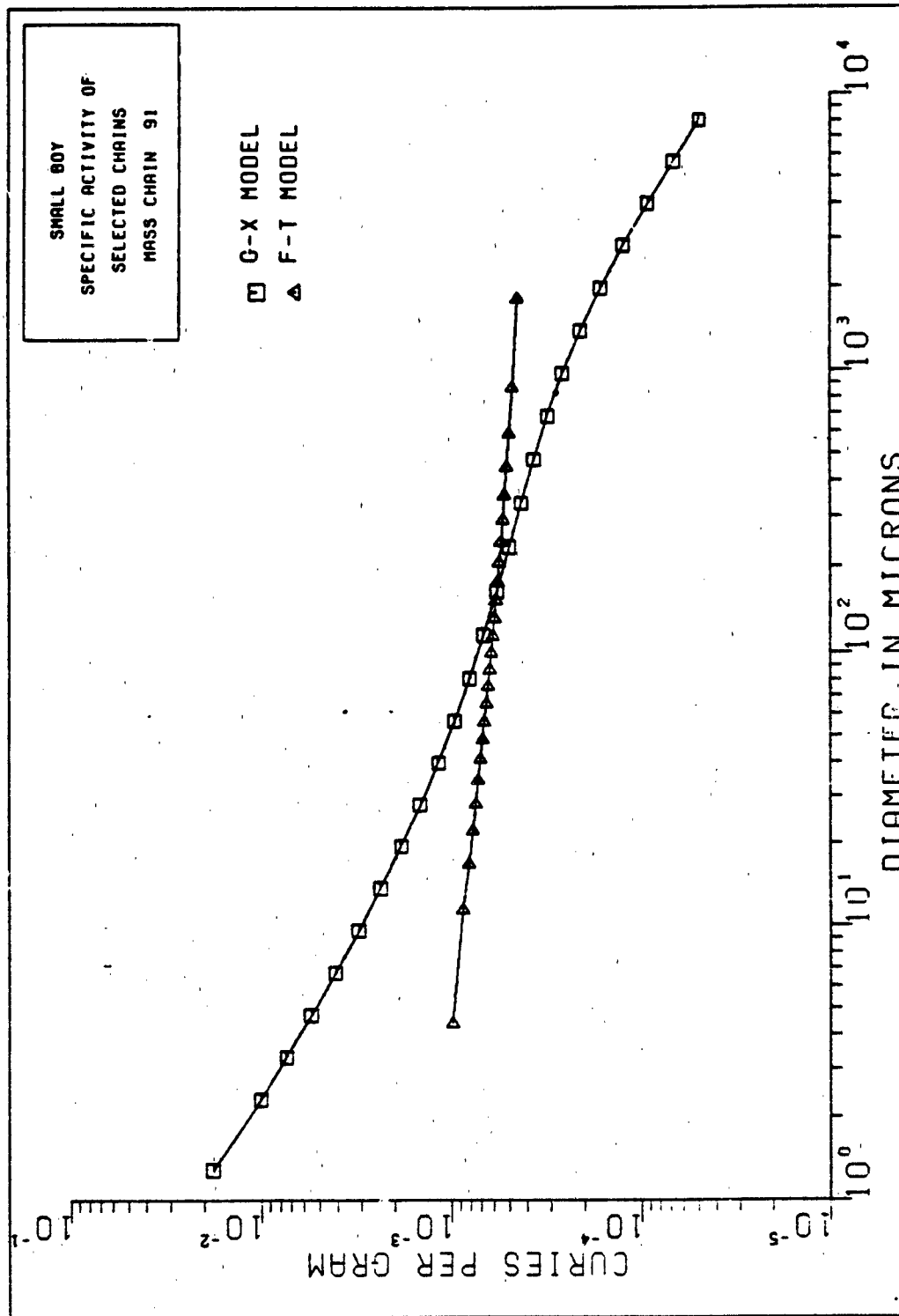


Figure 53. Small Boy Specific Activity for Mass Chain 91.

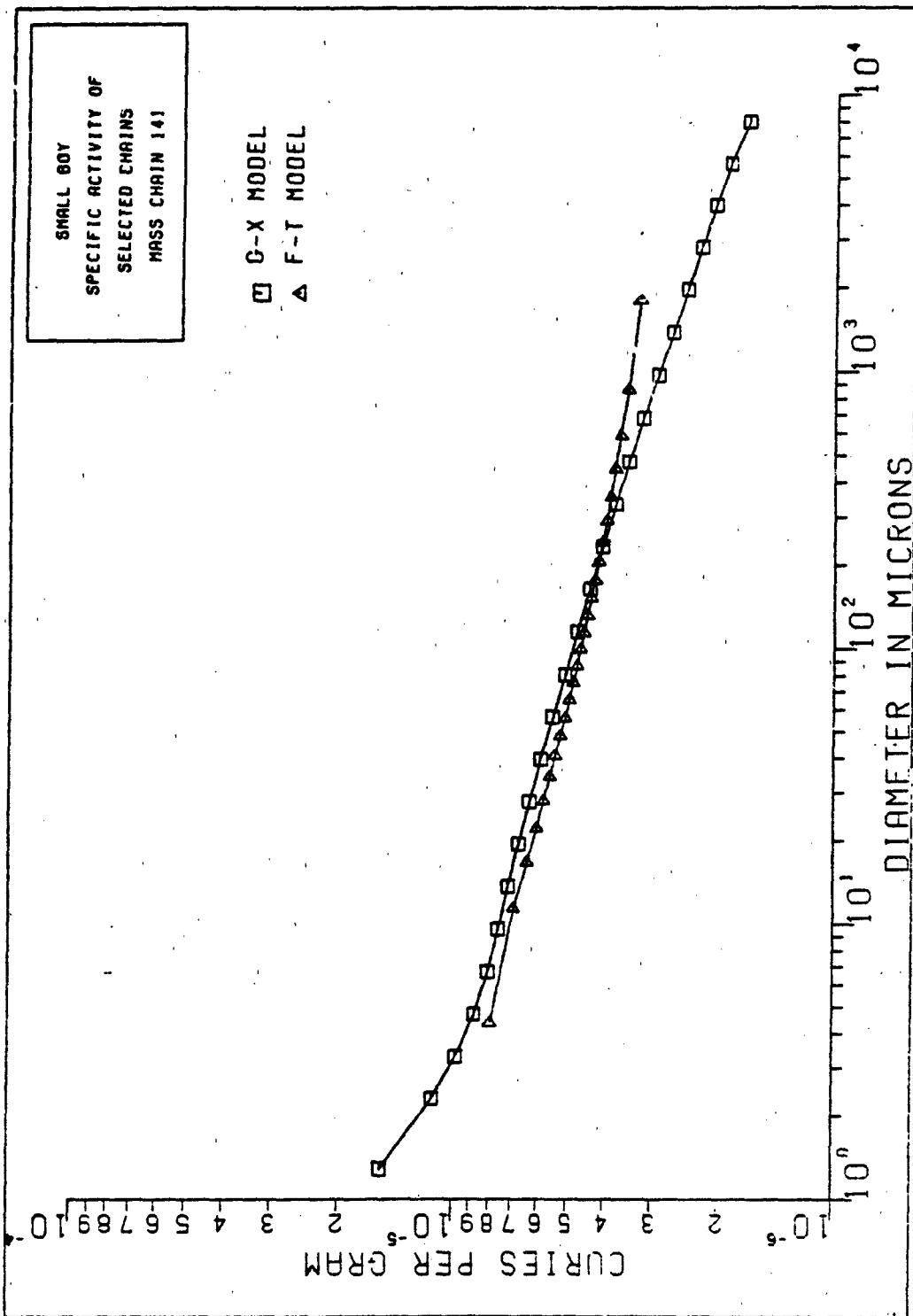


Figure 5d. Small Boy Specific Activity for Mass Chain 141

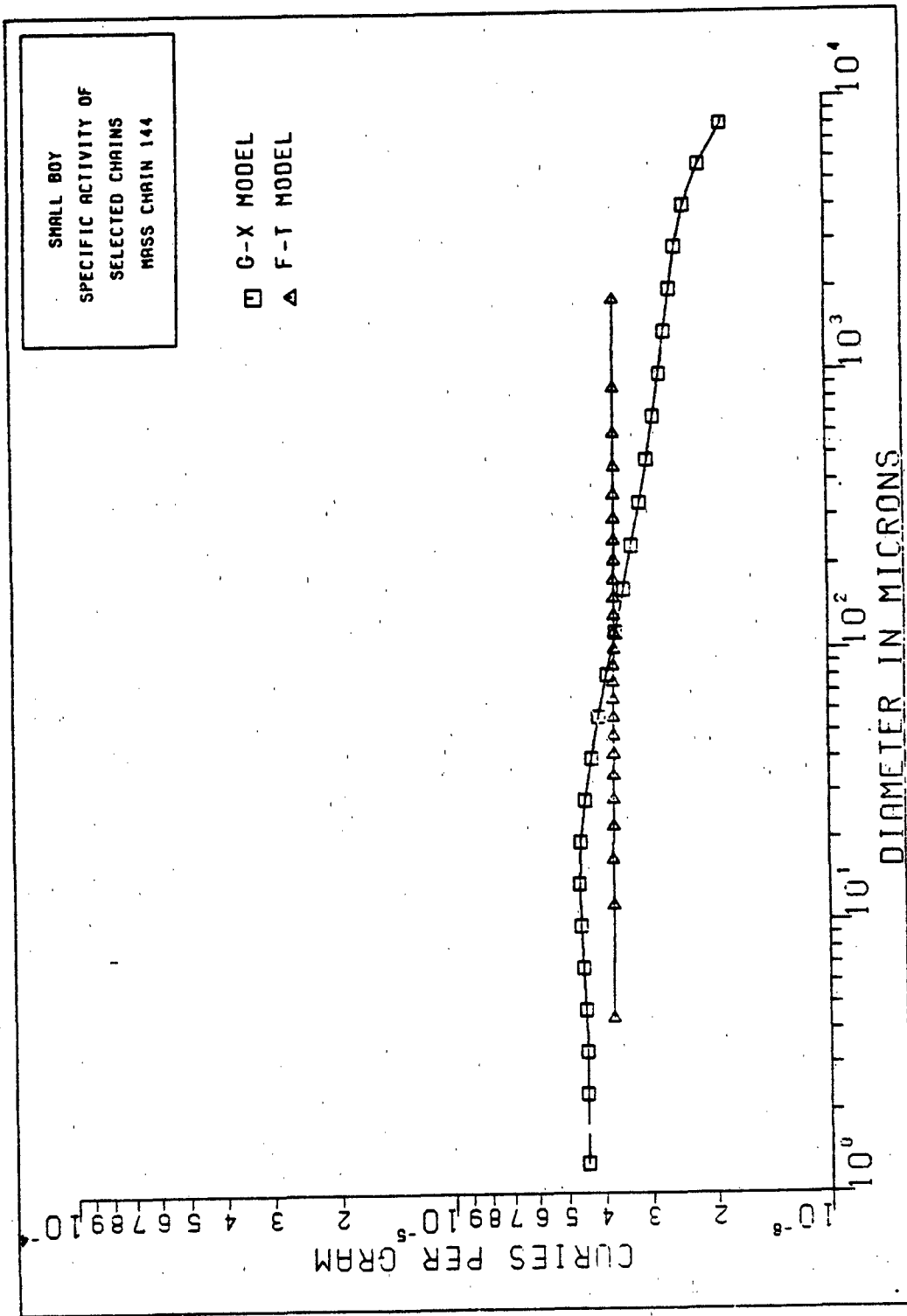


Figure 55. Small Boy Specific Activity for Mass Chain 144

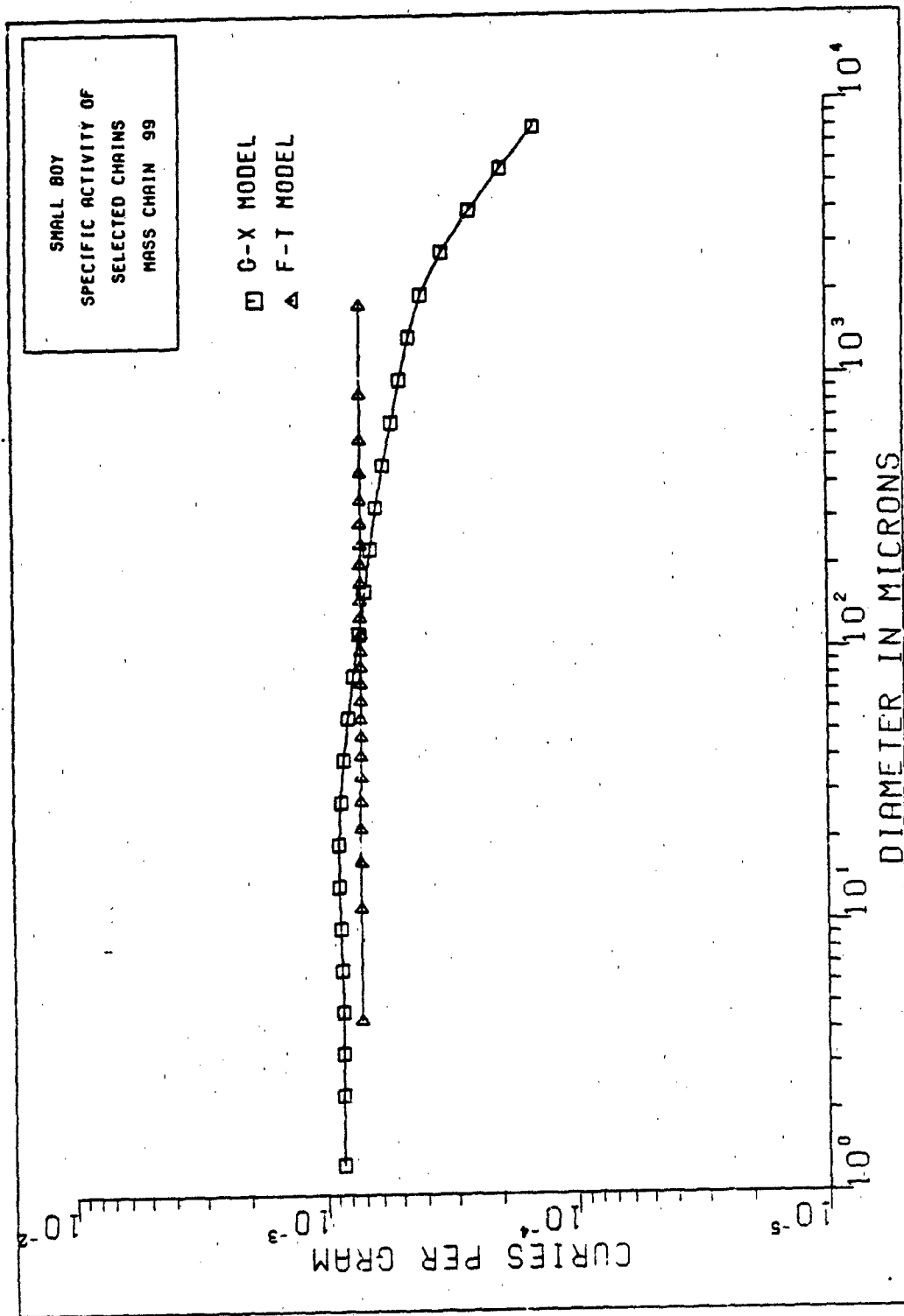


Figure 56. Small Boy Specific Activity for Mass Chain 99

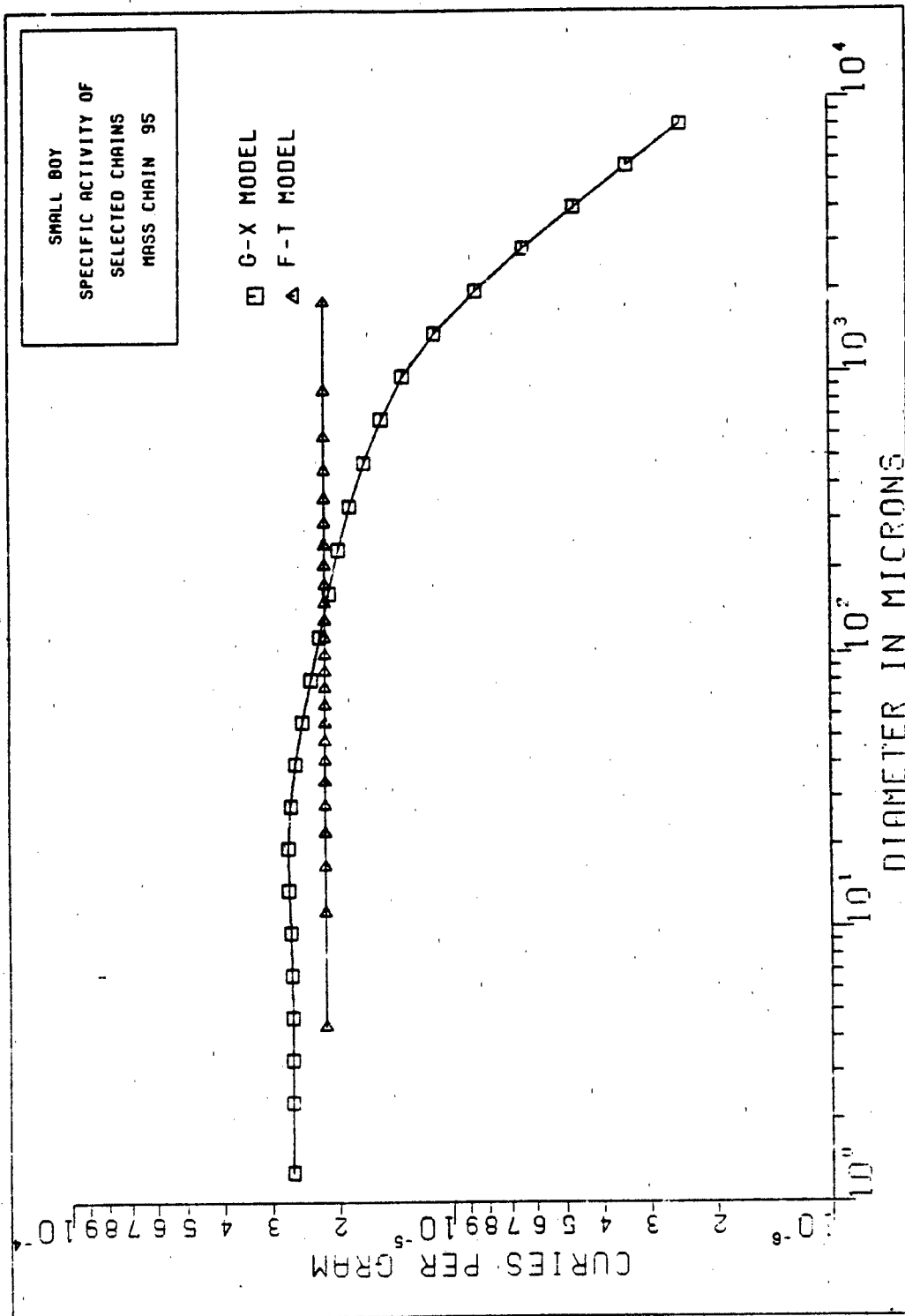


Figure 57. Small Boy Specific Activity for Mass Chain 95

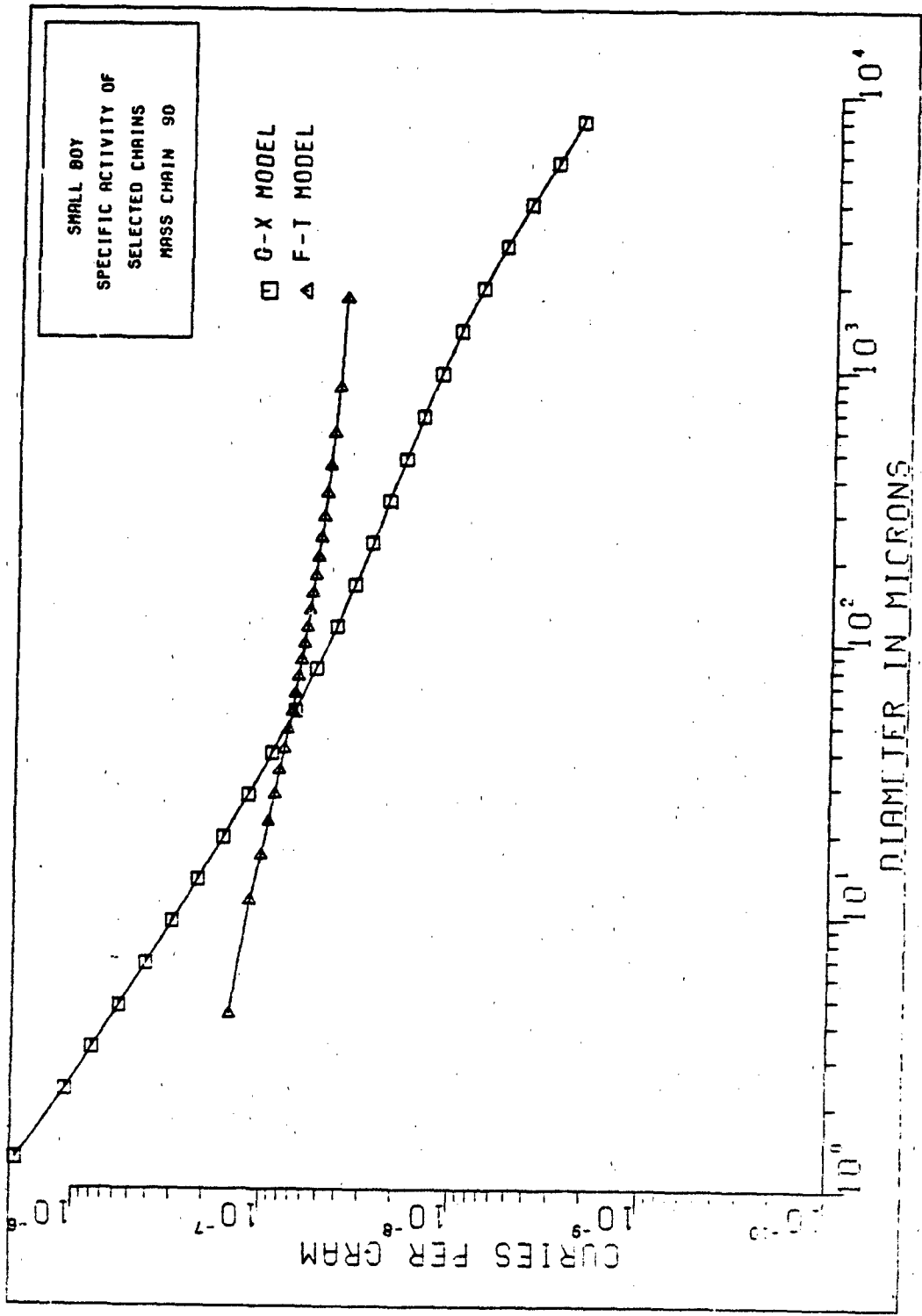


Figure 58. Small Boy Specific Activity for Mass Chain 90

Vita

Charles R. Martin was born on 25 September 1950 in Wiesbaden, Germany, the son of Clyde J. Martin and Lillian R. Martin. Upon completion of high school at Watauga High School, Boone, North Carolina, in 1968, he entered North Carolina State University at Raleigh, North Carolina, where he was enrolled in a cooperative education program in Nuclear Engineering. His cooperative work was performed with the Nuclear Division of Duke Power Company, Charlotte, North Carolina. In May 1973, he was graduated with honors as a Bachelor of Science in Nuclear Engineering. Concurrently, he completed the Reserve Officer Training Corps program and was awarded the designation of Distinguished Graduate. In November 1973, he completed Missile Combat Crew Operational Readiness Training at Vandenburg AFB, California, as a Distinguished Graduate. For the next three years, he served as a Deputy Missile Combat Crew Commander and Missile Launch Procedures Instructor at Malmstrom AFB, Montana. In March 1978, he was graduated with distinction with a Master of Science in Nuclear Engineering by the Air Force Institute of Technology, Wright-Patterson AFB, Ohio. He then served for two years as an instructor of mathematics at the Air Force Academy. In June 1980, he was sponsored by the Academy to return to the Air Force Institute of Technology to pursue the degree of Doctor of Philosophy.

Permanent Address: 8717 Hood Road

Charlotte, North Carolina